ABSTRACT

SAMPLE, CHRISTOPHER JAMES. Identification and Characterization of Novel Type I Interferons in *Pteropus vampyrus* Bats. (Under the direction Dr. Elizabeth Ramsburg.)

Pteropid bats are the asymptomatic reservoir hosts of Nipah virus, Ebola virus, and severe acute respiratory syndrome coronavirus (SARS-CoV); viruses that are considerably more pathogenic in humans than in bats. The extreme variation in pathogenicity of these viruses between humans and bats has driven an increased interest to understand mechanisms behind the differences in pathogenicity. Little information, however, is known about the bat immune system even at the very basic antiviral level. This raises the question of whether viral factors, host factors, or a combination of the two are responsible for the difference in pathogenicity between species. The Nipah virus and Ebola virus strains isolated from bats and those isolated from humans are highly homologous in nucleotide sequence. In addition the cellular receptors that Nipah virus and Ebola virus respectively bind in both species are highly homologous. Taken together, these facts suggest that host factors, not viral factors, are responsible for the differences between species. Type I interferons are key cytokines in the rapid response to infection by a multitude of pathogens, including viruses. We used a statistical gene assembler to infer possible interferon gene sequences from the genome traces of a megachiropteran bat, *Pteropus vampyrus*, and identify the type I interferons encoded by the *P. vampyrus* genome. The validity of the inferred sequences was then confirmed by direct cloning and sequencing from *P. vampyrus* genomic DNA. Interferon-β is considered a major initiator and component of the interferon induced antiviral pathway. From our *P. vampyrus* IFN-β gene sequence, we produced recombinant *P. vampyrus* IFN-β protein to test its antiviral activity. We also report on the development of a bioassay to measure the

biological activity of Pteropid interferons. We used Illumina-based RNA-Seq transcriptome deep sequencing to qualitatively and quantitatively compare the response of *P. vampyrus* and human peripheral blood mononuclear cells to VSV infection. This study provides comparative data about the initial antiviral immune response of bats and humans to VSV infection in order to better understand the factors involved in the differences in pathogenicity between bats and humans.

Identification and Characterization of Novel Type I Interferons in *Pteropus vampyrus* Bats

by
Christopher James Sample

A thesis submitted to the Graduate Faculty of
North Carolina State University
in partial fulfillment of the
requirements for the Degree of
Master of Science

Immunology

Raleigh, North Carolina

2011

APPROVED BY:

_____	_____
Matthew D. Koci, Ph.D.	Barbara Sherry, Ph.D.
_____	_____
Susan L. Tonkonogy, Ph.D. Co-Chair of Advisory Committee	Elizabeth A. Ramsburg, Ph.D. Co-Chair of Advisory Committee

DEDICATION

To my 4th grade teacher, Mrs. Barb Westendorf, at Cline Elementary School in Centerville, Ohio, Without her guidance and help, this path in life would never have been an option. She recognized my problems and guided my family to get the help for my learning disability. That help transformed a C student into an A student. I still have the spider plant you gave me over 20 years ago and yes it's still alive. Thank you for everything!

BIOGRAPHY

Christopher James Burek Sample was born on February 13, 1982 in Washington, DC to James Lawrence Sample and Denise Ann Burek Sample. As FBI brats, Chris and his little brother Gregory Charles Sample grew up in many places east of the Mississippi River but Centerville, Ohio holds a special place in Chris' heart where he lived for 9 years. He attended Centerville High School for three years until he moved to Alpharetta, Georgia. Chris graduated from Centennial High School where he was the state wrestling champion. He attended Duke University, Durham, North Carolina for undergraduate studies in Biomedical Engineering. After completing his Bachelors of Science in Engineering in 2004, he married his wife Laura, a fellow Duke graduate, that September. After graduation, he accepted a position as a research technician with Dr. Yehia Daaka in the Department of Surgery at Duke University School of Medicine, Durham, North Carolina studying the role of G-coupled protein receptors in prostate cancer cells. He transitioned to a new position in late 2005 with the Duke Human Vaccine Institute where he still continues to work as the lab manager for Dr. Elizabeth Ramsburg. While continuing to conduct his research, Chris enrolled as a graduate student at North Carolina State University in the Immunology Program in 2008. Upon the completion of his Master's degree, Chris will continue with his current research at Duke University.

ACKNOWLEDGEMENTS

I would like to thank my primary advisor and employer, Dr. Elizabeth A. Ramsburg, and my committee members, Dr. Susan L. Tonkonogy, Dr. Barbara Sherry, and Dr. Matthew D. Koci, for their guidance throughout this project and my time at North Carolina State University. Also thank you to all the faculty, staff, and fellow students in the Immunology Program and throughout the school. Thank you to Immunology Journal club and all the staff that shared their vast knowledge and insights, and thank you to those who grilled me and pushed me to critically read journal articles at a level I could not have achieved alone.

Thank you specifically to Dr. Thomas Kepler of the Department of Bioinformatics and Biostatistics at Duke University for all the work, help, and collaboration on this project. Your statistical gene assembler, acquisition of funding for deep sequencing, and RNA-seq mapper were crucial to this project. Thank you also to Al Haines, formerly of Dr. Kepler's lab, for the qRT-PCR work and teaching me how to purify RNA and run qRT-PCR.

Thank you to past and present members of the Ramsburg Lab: Brice Barefoot, Kathryn Hudak, Lizzy Do, Kathleen Athearn, Jay Tourigney, and James Clark. A special thank you to Brice Barefoot, my peer in the lab from the beginning and fellow graduate student at NCSU. Thank you to Brice Barefoot, Lizzy Do, and especially Kathryn Hudak for their work with the PCR and sequencing of many bat interferon clones. Jason Tourigney was responsible for the initial work with poly(I:C) and interferon treatment on BHK cells.

I also want to acknowledge the Duke Proteomics Core facility. Thank you to Meredith Turner and Erik Soderblom for their work and analysis of my samples. I also want to thank Dr. Will Thompson for his guidance through sample preparation, selection of services, and taking the time to review and explain the results and assays in depth.

Thank you to Scott Soderling for all of his knowledge, help, and donated resources on the production and purification of my recombinant protein. I would also like to thank Feng Yuan, Fred Jaeger, and Dr. Munir Alam for their help and suggestions to troubleshoot the protein purification.

Thank you to Michelle Baker and her laboratory at Commonwealth Scientific and Industrial Research Organisation (CSIRO) Livestock Industries in Australia for kindly providing the *Pteropus alecto* cell lines.

A special thank you to Allyson Walsh of the Lubee Bat Conservancy and, of course, the bats: Snook, Arthur, Lucifer, Sovann, Murray, Ozzy, Colosus, Munny, Joshua, and Crimson.

Thank you to my mother, my father, and my brother for all their support and strange sense of humor. Thank you to my wonderful wife Laura, for teaching me PivotTables and Excel intricacies, for thesis editing, and for learning how to cook when I was writing every night. And of course, thank you so much for your unending encouragement, support and love.

TABLE OF CONTENTS

LIST OF TABLES

LIST OF FIGURES

LIST OF ABBREVIATIONS

6xHT:	6x-Histidine Tag
ACE2:	angiotensin-converting enzyme 2
AP:	Alkaline phosphatase
BHK:	baby hamster kidney
bp:	basepair
CD:	cluster of differentiation
cDNA:	complementary DNA
CDR:	complementarity determining region
CNS:	central nervous system
cpe:	cytopathic effect
CSIRO:	Commonwealth Scientific and Industrial Research Organisation
C-terminal:	carboxy terminals
DC:	dendritic cells
DHMRI:	David H. Murdock Research Institute
DHVI:	Duke Human Vaccine Institute
DMEM:	Dulbecco's modified eagle medium
DNA:	deoxyribonucleic acid
dsRNA:	double-stranded RNA
E. coli:	*Escherichia coli*
EBOV:	Ebola virus

EDTA: Ethylenediaminetetraacetic acid

EGFP: enhanced GFP

EGTA: ethylene glycol tetraacetic acid

eIF2α: eukaryotic translation initiation factor 2α

ELISA: enzyme-linked immunosorbent assay

ER: endoplasmic reticulum

FPLC: fast protein liquid chromatography

gDNA: genomic DNA

GDP: guanidine di-phosphate

GFP: green fluorescent protein

GP: glycoprotein

GST: glutathione S-transferase

HeV: Hendra virus

HI-FBS: heat inactivated fetal bovine serum

HPLC: high performance liquid chromatography

IACUC: Institutional Animal Care and Use Committee

IF: immunofluorescence

IFN: interferon

IFNAR: interferon-α/β receptor

Ig: immunoglobulin

IgC: immunoglobulin constant domain

ICC:	immunocytochemistry
IKKε:	inhibitor of NF-κB kinase subunit epsilon
IL:	Interleukin
IMAC:	immobilized metal ion affinity chromatography
IRF:	interferon regulator factor
ISG:	interferon stimulated gene
ISGF-3:	interferon stimulated gene factor 3
ISRE:	interferon stimulation response element
JAK:	Janus kinase
kb:	kilobase
kDa:	kiloDalton
LAL:	Limulus amebocyte lysate
LC-MS/MS:	liquid chromatography and tandem mass spectrometry
MALDI:	matrix-assisted laser desorption/ionization
MDA5:	melanoma differentiation-associated gene-5
MHC:	major histocompatibility complex
mRNA:	messenger ribonucleic acid
MS:	mass spectrometry
Mx GTPases:	Mx guanosine triphophatases
MOI:	multiplicity of infection
MWCO:	molecular weight cut-off

NF-κB:	nuclear factor kappa-light-chain-enhancer of activated B cells
NiV:	Nipah virus
NS1A:	influenza A non-structural 1
NS1B:	influenza B non-structural 1
nsp:	nonstructural protein
nt:	nucleotide
N-terminal:	amino terminal
OAS:	oligoadenlyate synthetases
ORF:	open reading frames
PaLuSD8:	*P. alecto* lung clonal cells
PAMP:	pathogen-associated molecular pattern
PBMC:	peripheral blood mononuclear cells
PBS:	phosphate buffered saline
PCR:	polymerase chain reaction
PFA:	paraformaldehyde
pfu:	plaque forming units
PIAS1:	protein inhibitor of activated STAT1
PKR:	protein kinase R
PRR:	pattern recognition receptor
qRT-PCR	quantitative real-time RT-PCR
RBC:	red blood cell

rEK:	recombinant enterokinase
RIG-I:	retinoic acid inducible gene I
RNA:	ribonucleic acid
RNase L:	ribonuclease L
RT:	room temperature
RT-PCR:	reverse transcriptase polymerase chain reaction
SARS:	severe acute respiratory syndrome
SARS-CoV:	severe acute respiratory syndrome coronavirus
SF9:	*Spodoptera fugiperda* insect cells
sGP:	soluble glycoprotein
SL-CoV:	SARS-like coronavirus
ssRNA:	single stranded ribonucleic acid
STAT:	signal transducer and activator of transcription
SUMO:	small ubiquitin-like modifier
SV40:	simian virus 40
TANK:	TRAF family member-associated NF-κB activator
TBK:	TANK-binding kinase
TC:	tissue culture
TLR:	toll-like receptor
TNF:	tumor-necrosis factor
TRAF:	TNF-receptor-associated factors

U:	unit
Ubc9:	ubiquitin carrier protein 9
USA:	United States of America
UV:	Ultraviolet
VH:	variable heavy
VP:	virion protein
VSV:	vesicular stomatitis virus
WNV:	West Nile virus

1. INTRODUCTION

1.1. Bats are mammals of the Order Chiroptera

As the only flying mammals, bats are incredibly unique and interesting animals for many ecological and physiological reasons. Furthermore, bats are hosts to many diseases that are highly pathogenic in humans and are therefore an important species for study. Chiroptera is the second largest order of mammals and includes approximately 20% of all species in the class Mammalia [1-3]. Despite the large percentage of species of bats in Mammalia, bats remain a disproportionately low percent of the species that have been studied scientifically [2]. Phylogenetically, there is much discussion as to whether bats are more closely related to horses, dogs, or primates, but most phylogenetic trees have placed bats farther from rodents than even humans (Figure 1) [4-7]. Bats also have very unique life histories when compared to other small mammals. Unlike many small mammals, bats have a long lifespan averaging around 20 years although some bats have been reported to live for up to 41 years in the wild [2, 8]. In addition bats are slow to develop and reproduce, and typically bear only one offspring [2].

Several unique anatomical features distinguish bats from other mammals, for example the wings, heart, and female reproductive tract. The wings of bats are formed by a collapsible broad membrane that extends out from the length of the body from rear to the neck that is supported by the arm, hand, and lengthy finger bones [9]. Bat wings are not feathered like those of birds, and there are many morphological specializations of the first carpel or "thumb" that can be used for gripping, climbing, and roosting [9, 10]. Relative to

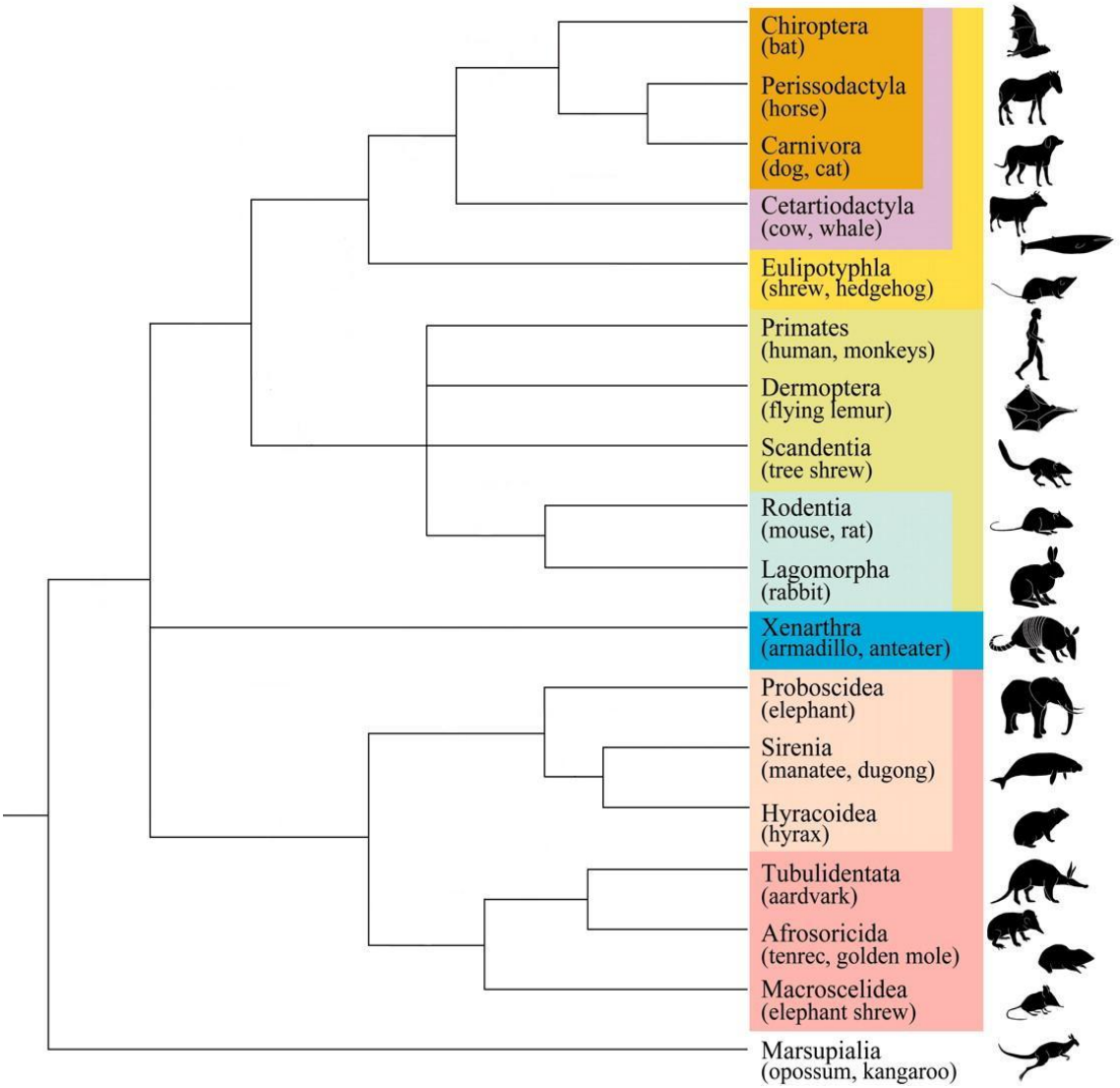

Figure 1. Bats are not rats! Interordinal mammalian phylogenetic tree demonstrating relationship between bats and other mammals. Figure adapted from Nishihara, H *et al*. 2006 [11]. © 2006 National Academy of Sciences, USA.

body size, bats have the largest and most muscular heart of any mammal, and the increased cardiac capacity likely evolved due to the body's oxygen demand during flight [9]. Another likely evolution to accommodate flight by conserving body mass, one ovary and one uterine horn are reduced and nonfunctional in the female reproductive tract of most bat species [2]. Anatomical characteristics can be significant factors in infection and disease transmission, thus it is important understand some of the unique anatomy of bats.

Bats have important roles in ecosystem maintenance, and the diversity of bats allows many species of bats to live in the same geographical locale [12]. Bats can be insectivorous, carnivorous, or frugivorous, and only a few species are sanguivorous. Many ecosystems depend heavily on bats for insect control, pollination, and seed dispersion. As different bats emerge at various times of the day, certain flowers have evolved specifically to attract bats by a variety of methods such as colors, shapes, and the time of the day blooms are accessible to maximize likelihood of multiple flower visitation and successful pollination [9, 12-15]. Insectivorous bats have large roles in insect and pest control that impact ecosystems and agriculture [16]. These bats consume large numbers of insects each night [17] and, for a region of cotton production in Texas, a study estimated the value of pest suppression by bats of up to 1.73 million dollars per year [18]. The importance of bats in ecosystem maintenance and agriculture is becoming more evident, therefore it is important to understand disease transmission among bats so that we can better protect them.

The roosting behavior of bats is important to note as a likely contributor to disease spread and perseverance. Bats roost in caves, manmade structures, tree limbs, tree cavities,

or self-created tents. Some species of bats are very social and roost with thousands of conspecifics, while others are solitary animals or live in small groups [10]. Bats in North America hibernate in groups of thousands, but an emerging fungal disease is spreading, causing collapse in bat colonies. The fungus easily spreads when bats are hibernating in close contact, causing alteration in arousal patterns during hibernation and premature depletion of energy reserves, that results in bats emerging prior to spring and when food is available [19].

The order Chiroptera is divided into 2 suborders: megachiroptera and microchiroptera. As the name suggests, microchiropteran bats are mainly small-bodied with the majority weighing less than 20g. Microchiropteran bats can be found around the world mainly in tropical regions with only a few species living in more temperate regions [20].

Megachiropteran bats (commonly known as flying foxes) are mostly large-bodied bats with a mean body mass of greater than 200g and wingspans up to 1.7m [1, 9, 20]. Pteropodidae is the only family within the suborder and consists of at least 188 species [20]. Megachiropterans are found only in the Old World tropics which span Africa, the eastern Mediterranean, southern Asia, the South Pacific, and Australia [12]. Megachiropteran bats utilize vision and smell as the dominant senses in orientation and food selection because their diet consists almost solely of fruit and vegetation [12, 13]. Many Pteropus species occupy large home ranges and have been known to fly 50 kilometers a night and hundreds of kilometers over the course of a week in order to forage [21-23]. The ability of bats to

migrate over large areas and diet of fruit shared by bats as well as humans and other animals contributes to the capacity of pteropid bats to spread disease.

1.2. Many emerging infectious agents are zoonoses

The World Health Organization estimated that over 12 million or >20% of deaths in 2008 were due to infectious diseases, many of which were caused by new or emerging infectious agents [24]. Emerging infections are defined as previously unrecorded infections or previously known infections that are new to geographic regions or species [25, 26]. An estimate of deaths due to emerging infections for one particular year does not accurately represent the impact of emerging infections because some emerge suddenly while others cause more gradual and widespread infections [27]. For example, the 1918 influenza pandemic killed over 50 million people in two years [28] while human immunodeficiency virus has had a more gradual impact and global spread [29].

Zoonoses are defined as "infectious diseases that are naturally transmitted between vertebrate animals and humans" [30] and account for over 60% of emerging infectious diseases; over 70% of these zoonoses originate in wildlife [31]. Zoonotic disease events are concentrated in tropical/equatorial developing nations in common with the distribution pattern of species richness. In addition, socioeconomic factors in developing nations such as population density and agricultural encroachment into the natural environment can increase the risk of novel and/or repeated zoonotic encounters [31, 32].

Almost all of the zoonotic emerging viral infections in humans in the past 30 years have been caused by RNA viruses [29, 33]. It has been proposed that the propensity of zoonotic viruses to have RNA genomes can be largely, but not solely, attributed to the error prone replication and rapid evolution of RNA viruses. The greater mutation or evolution rate increases the chances that a particular mutation increases the fitness for the progeny virus to infect and replicate a new host. Other factors that facilitate the transmission of zoonoses are mode of transmission, post-transfer adaptation, receptor binding, and host immune evasion and regulation [27, 32, 34].

1.3. Bats are a reservoir for emerging viruses with high pathogenicity in humans

A reservoir host is defined as a population or an ecologically and epidemiologically connected system in which an infectious agent can survive indefinitely [35-37]. At least 11 families of viruses known to infect vertebrates have been associated with bats: one family of DNA viruses (Herpesviridae) and 10 families of RNA viruses [38, 39]. Three highly pathogenic viruses in humans have been implicated as originating in bats from the Old World tropics: severe acute respiratory syndrome coronavirus (SARS-CoV), Ebola virus (EBOV), and Nipah virus (NiV) [39]. These viruses are considerably more pathogenic in humans than they are in bats. This raises the question of whether viral factors, host factors or a combination of the two are responsible for the difference in pathogenicity between species. In the next sections, I will discuss the three examples of bat-vectored viruses, and compare and contrast what we know about them and how it relates to the difference in pathogenicity

between bats and humans. Then I will discuss what we know about the immune system of bats followed by their interferon pathway, a major antiviral immune response, and how these viruses attempt to thwart interferon to promote infection. Our central hypothesis is that the interferon system of the host is largely responsible for the differences in pathogenicity between bats and humans for SARS-CoV, EBOV, and NiV.

1.3.1. SARS

1.3.1.i. Epidemiology of SARS

An emerging infection can have a substantial impact on global society and economics without a concomitantly sizeable death toll. Severe acute respiratory syndrome (SARS) first gained global attention in early 2003 with outbreaks in Vietnam, Hong Kong, and the Guangdong province in China with the first cases occurring in November 2002 [40, 41]. Patients exhibited influenza-like symptoms that progressed to a more severe form of pneumonia and, in many cases, death [40]. Due in large part to the ease of global travel and the slow onset of disease and hospital admission (~6 days and ~10 days respectively) [42], the virus spread to 29 countries and infected over 8000 individuals causing 774 deaths over the course of 9 months [43]. In many instances, hospital admission coincided with peak viral load and peak of transmissibility and as a result, many healthcare workers were infected (constituting 20% of the total infected) [43, 44]. Although the outbreak ended by July 2003, and the health impact ultimately was much less than initially feared, the global economic

impact was quite substantial, with the cost of the SARS epidemic estimated at over 10 billion US dollars [45, 46].

1.3.1.ii. Virology and genetics of the SARS virus

Our ultimate goal is to understand why viruses of high pathogenicity enter the human population from the bat reservoir. To begin to reach that goal, it is important to determine whether the viruses emerging from bats have molecular features in common. SARS was caused by a novel coronavirus, the SARS-CoV [47, 48]: an enveloped virus with a positive-sense single stranded RNA (ssRNA) genome in the family *Coronaviridae* [49]. The SARS-CoV genome is ~30,000 nucleotides (nt) and is organized 5'-replicase-spike (SARS-CoV S)-envelope-membrane glycoprotein (SARS-CoV M)-nucleocapsid (SARS-CoV N)-3' consistent with other coronaviruses. However the SARS-CoV does not closely resemble any of the other three groups of coronaviruses phylogenetically [49, 50]. Two strains of SARS-CoV were identified during the outbreak: one strain isolated from humans and animals during the early phase of the outbreak, and a second strain isolated from humans during most of the outbreak. In the second strain, a 29 nt sequence was deleted upstream from the SARS-CoV N gene and the timeline of isolation suggests that the deletion event occurred during adaptation of the early phase SARS-CoV from animals to the new human host [51]. The replicase gene comprises approximately two-thirds of the genome [49] and encodes 2 large polypeptides that undergo proteolytic cleavage to form 16 nonstructural proteins (nsp) and enzymes some of which form the replicase complex [52]. Alternate open reading frames

(ORFs) between the spike and envelope genes and between the membrane glycoprotein and nucleocapsid genes encode proteins 3a, 3b; and proteins 6, 7a, 7b, 8a, and 8b, respectively. SARS-CoV 9b is encoded from an alternate ORF within the SARS-CoV N gene (with the nucleocapsid considered SARS-CoV 9a) [52]. As will be discussed later, viral pathogenicity in different species can be attributed to the ability of the virus to overcome the interferon antiviral pathway and the SARS-CoV proteins have multiple functions such as inhibition of host cell translation, messenger RNA (mRNA) degradation, and suppression of the cellular antiviral response [52].

1.3.1.iii. SARS entry and replication

To enter the host cell, SARS-CoV spike glycoprotein binds cell surface angiotensin I converting enzyme (ACE2) [53] and is endocytosed. Cathepsin L cleaves SARS-CoV S and activates fusion of the viral envelope with the endosomal membrane [54]. Tightly bound to SARS-CoV N, viral RNA is released into the cytoplasm. The viral genome is then translated and resultant proteins are cleaved into the individual components that form the replicase complex. This replicase complex transcribes the positive sense genomic RNA into negative sense antigenomes that serve as templates for positive sense progeny genomes. In addition, the replicase complex transcribes negative sense subgenomic RNAs of the individual genes that serve as templates to produce mRNAs for the translation of individual viral proteins. During virus production, replicase proteins localize in double membrane vesicles that are induced during replication and these membranes act as the sites of replication likely to

sequester RNA species from antiviral sensing proteins [54, 55]. Structural proteins localize to the endoplasmic reticulum (ER)/Golgi intermediate compartment where virus assembly and budding occur. Mature virions are then secreted using the cell secretory apparatus [54].

1.3.1.iv. Pteropid bats are a reservoir for SARS coronaviruses

The SARS outbreaks were caused by two strains of SARS-CoV that have not been found circulating in any animal population and which likely arose through mutation and amplification in an intermediate host, the palm civet [51]. Palm civets were identified as carriers of multiple strains of SARS-CoV that spread to other animals in the markets, although the SARS-CoVs were not endemic in the populations from which the civets were taken [51, 56]. Experimentally, palm civets are highly susceptible to infection and disease by both human strains [57], and wide distribution of palm civets in public markets has supported their role as the likely amplification intermediate host [51, 58]. This leaves the question of how the virus was acquired by palm civets.

Although SARS coronavirus has not been directly isolated from bats, a family of "SARS-like coronaviruses (SL-CoVs)" has been recovered from bats, and these viruses are presumed to be the progenitors of SARS-CoV. SL-CoVs isolated from horseshoe bats were ~90% identical to the strains found in palm civets and humans and contained the 29-nt sequence present in the early phase isolate of SARS-CoV [51, 59, 60]. Further studies found SL-CoVs in both microchiropteran and megachiropteran bats around the world [61-63] and some bats harbored multiple distinct strains simultaneously [63, 64]. In addition, pteropid

bats were asymptomatic, without histopathological signs of infection, and viral RNA was amplified and detected in the bats after experimental inoculation with SL-CoVs [65]. The ability of bats to control multiple coronaviruses and the conditions for which a bat coronavirus can spillover into unrelated species need to be examined further, although this evidence strongly supports bats as reservoir hosts of the progenitor strains that lead to development of SARS-CoV.

1.3.1.v. Alterations in SARS attachment protein facilitate cross-species transmission

Molecular reasons for spillover of SL-CoVs and SARS-CoV into new hosts may be due either to host factors and/or mutations in the virus progeny. ACE2 was identified as the cellular receptor used by SARS-CoV S protein [53, 66, 67]. The S proteins from the two SARS-CoVs and the S protein from a SARS-CoV isolated from palm civets were all able to efficiently utilize palm civet ACE2, however, the SARS-CoV S protein isolated from early phase of outbreak and the palm civet S proteins utilized human ACE2 less efficiently [67]. SL-CoV S protein was unable to utilize human, palm civet, or bat ACE2 as a receptor, nor were SARS-CoV S proteins from human or civet able to use bat ACE2 [68]. The evidence that SL-CoVs do not use ACE2 receptor [68], the varying efficiencies of different SARS-CoVs for binding ACE2 from different animals [67, 68], the numerous different species in close contact in markets [51, 56, 58], and the molecular diversity of SL-CoVs found in bats [63, 64] together reasonably suggest the evolution and mutation of SL-CoV to utilize a

completely different host receptor through one or more intermediate and amplification hosts including the palm civet prior to SARS-CoV jumping to the human population [51, 68].

1.3.2. Ebola virus

1.3.2.i. Epidemiology of Ebola virus

Unlike SARS, Ebola virus (EBOV) has never caused a worldwide epidemic, likely due to a combination of the following factors: onset of serious disease is rapid and patients are usually isolated as soon as they become symptomatic, EBOV is transmitted from person-to-person almost exclusively through direct contact of mucosa or non-intact skin with infected patients/animals and their body fluids rather than via the respiratory route, and outbreaks are often in remote areas with limited travel capabilities [69, 70]. The first human Ebola cases were reported in 1976 when two outbreaks in Sudan and Zaire resulted in more than 500 individuals infected with mortality rates of 53% and 88% respectively [71]. Ebola strains have emerged in humans sporadically in Africa since 1976, though cases are becoming more frequent as environmental encroachment and zoonotic encounters with bats and infected non-human primates rise [69, 71]. Most outbreaks throughout Ebola's reported history are within African countries although there have been a few asymptomatic human cases of Ebola Reston, a strain not associated with human disease but with disease in monkeys and pigs, in the Philippines, the United States of America (USA), and Italy from monkey import/export facilities and a pig farm/slaughterhouse, as well as one laboratory-

acquired infection of Ebola Sudan in England [71, 72]. There have been eleven outbreaks since the year 2000; six involved >50 cases and most with case/fatality rates of over >50% [69, 71]. Disease onset is usually sudden after an incubation period of 2-21 days. Clinical signs include myalgia, hemorrhaging, gastrointestinal bleeding and diarrhea, and neurological problems such as cephalgia and obnubilation [69]. While the typical natural mode of transmission is direct contact, aerosol transmission is still a possibility as Ebola Zaire is highly lethal in orally infected macaques and virus titers are high in infected organs [69, 73, 74]. The import/export of infected animals, possible aerosol transmission, and the high case-fatality rate make Ebola an important public health concern and possible bioterrorist threat.

1.3.2.ii. Virology and genetics of Ebola virus

Ebola viruses are enveloped viruses with negative-sense RNA genomes in the family *Filoviridae*. There are currently five known strains of Ebola: Zaire, Sudan, Ivory Coast (or Taï Forest), Reston, and Bundibugyo [75]. The Ebola genome is ~19,000 nt long and is organized 3'-leader-nucleoprotein-virion protein (VP) 35-VP40-glycoprotein (GP)-VP30-VP24-polymerase protein (EBOV L)-trailer-5'. Intergenic regions between VP35 and VP40, glycoprotein and VP30, and VP24 and L genes overlap slightly to conserve transcriptional signaling [76, 77]. The glycoprotein gene is comprised of two ORFs to produce a small soluble glycoprotein (sGP) and transcriptional insertion of a single adenosine and translational frame shifting produces the full-length membrane-anchored virion GP [76, 77].

The sGP has been proposed to mediate anti-inflammatory cytokines, act as neutralizing antibody decoy, and regulate immune cell function. Additionally, sGP is the major gene product translated from GP transcripts (~80%) and GP has been shown to be cytotoxic, thus production of sGP may represent a mechanism to control GP-induced cytotoxicity during infection [76]. Nucleoprotein, VP35, and EBOV L are sufficient for replication, but viral transcription also depends on VP30. VP40 and VP24 function as viral matrix proteins [76]. VP24 and VP35 modulation of antiviral mechanisms will be described in detail in another section.

1.3.2.iii. Entry and replication of Ebola virus

The Ebola virus GP is a promiscuous viral receptor that binds a multitude of cell surface factors including a variety of C-Type lectins containing carbohydrate recognition domains, β1 integrin adhesion receptors, folate receptor-α, and receptor tyrosine kinases: Axl, Dtk, and Mer [76]. In addition, the Ebola virus uses different endocytotic pathways and phagocytosis to mediate entry into the cell after receptor binding. Acidic pH, proteolytic cleavage of GP, and an unknown trigger induce fusion of the viral and cellular membranes. Nucleoproteins, the VPs, EBOV L, and the negative sense viral genome are then released into the cytoplasm [76]. Viral mRNA is transcribed by the viral polymerase and then translated by the host cell machinery. Genome replication is dependent upon ample levels of nucleoprotein to encapsidate plus strand anti-genomes and subsequent negative strand progeny genomes. VP40 mediates transport of encapsidated progeny genomes and

endosomal GP to the cell surface where encapsidated genomes and viral proteins are packaged and virus buds from the cell surface [76].

1.3.2.iv. Pteropid bats are the likely reservoir for EBOV

A model of a non-pathogenic host-virus relationship in bats has been strongly suggested for Ebola but isolation of the etiologic agent from bats remains elusive. Bats were asymptomatic, without histopathological signs of infection, and virus was still able to replicate and be shed by the bats after experimental inoculation with Ebola [78]. An epidemiologic study identified contact with fruit bats after hunting the bats for food as the likely causative event of an Ebola outbreak in 2007 [79]. Serologic studies of bats in regions of outbreaks in eastern Africa identified anti-Ebola antibodies [80-83] and isolated Ebola virus RNA [81, 84] from fruit bat populations.

1.3.2.v. Increased pathogenicity of EBOV in humans cannot be attributed to viral factors

Unlike the genetic divergence of SARS-CoVs, differences in EBOV infection between bats and humans are likely due to host factors. Ebola viruses isolated from bats are highly homologous and matched phylogenetically with strains found in the human outbreaks [81, 84]. Many host cell surface molecules have been implicated in Ebola virus entry, as described above, but a common receptor has not been identified in humans and bats [85, 86]. However, Axl, Dtk, and Mer receptor tyrosine kinases are highly conserved among different species and are widely expressed in many cell types [76]. In agreement with our hypothesis,

the high homology of bat and human EBOV strains and the likely similar receptor usage strongly suggest that difference in pathology between bats and humans is due to host factors.

1.3.3. Nipah virus

1.3.3.i. Epidemiology of Nipah virus

Nipah virus (NiV) is one highly pathogenic species of two recently emergent viruses of the genus *Henipavirus*. An outbreak of viral encephalitis in Malaysia and Singapore in 1998 to mid-1999, mainly among pig farmers, was the first reported emergence of Nipah virus with more than 280 cases with 109 fatalities [87, 88]. The initial symptoms of Nipah infection are flu-like with rapid progression to neurological problems such as dizziness, headache, and loss of consciousness. Pathologically Nipah virus mainly causes acute encephalitis however the virus does spread to and damage other organs [88, 89]. In this outbreak, domestic pigs were also infected and were considered to be the primary mode of transmission to humans [90-92]. Since 1999, there have been several small outbreaks in Bangladesh and India caused by another Nipah virus strain with increased capacity for human-to-human transmission [93-95].

1.3.3.ii. Virology and genetics of Nipah virus

Nipah virus is an enveloped virus with an 18 kilobase (kb) single-stranded negative-sense RNA genome in the family *Paramyxoviridae*. The viral genome is organized 3'-nucleoprotein (NiV N)-phosphoprotein (Niv P)-matrix protein (NiV M)-fusion protein (NiV

F)-glycoprotein (NiV G)-large polymerase protein (NiV L)-5'. During transcription of the NiV P gene, the Nipah virus polymerase complex occasionally inserts one or two non-templated guanine nucleotides at a conserved editing site in the middle of the NiV P gene. These one or two nucleotide additions result in a frame shift during translation which produces two nonstructural proteins termed NiV V and NiV W, respectively, which share the same amino terminal (N-terminal) as NiV P but different carboxy terminals (C-terminals). In addition, alternate translational start and stop codons prior to the edit site in NiV P, V, and W mRNAs produce another nonstructural protein called the NiV C protein [92, 96]. NiV P protein is a cofactor for the NiV L protein to form the polymerase complex and has some antiviral antagonistic activity [97]. The nonstructural NiV V, W, and C proteins antagonize the cellular antiviral response and will be described in detail in another section [96].

1.3.3.iii. Entry and replication of Nipah virus

The NiV G protein binds to Ephrin B2 and B3 [98-100] on the host cell surface and this binding allows NiV F protein to mediate fusion of the viral envelope with the host cell plasma membrane at neutral pH [96]. NiV G differs from the attachment proteins of other paramyxoviruses in that NiV G has no hemagglutinating or neuraminidase activities [101]. After fusion, the virus uncoats in the cytoplasm and NiV P and NiV L associate to begin viral transcription and replication. Viral mRNAs are transcribed directly from the viral negative strand genome, monocistronic capped and polyadenylated, and translated by the host cell machinery. At the end of each gene, the polymerase complex reaches a stop signal that either

causes the polymerase to initiate transcription of the next gene or disengage and restart from the beginning of the genome. This reinitiation mechanism leads to gradient production of viral transcripts inversely proportional to the distance of a gene from the 3' terminus of the genome and is a form of transcriptional regulation. Accumulating NiV N protein encapsidates and stabilizes the positive strand and switches the polymerase from transcription to replication of full length antigenomes to act as templates for subsequent replication of negative strand progeny genomes in the presence of more NiV N protein [96, 101, 102]. The NiV G and F surface glycoproteins are translated at ER-associated ribosomes and are inserted in the ER membrane to be transported to the cell surface through the secretory pathway. The NiV F protein associates into trimers that must be cleaved into two disulfide linked subunits to become active prior to incorporation into new virions [102]. Nipah virus uses a cellular protease, cathepsin L [103], and a unique mechanism to cleave the NiV F proteins. Virion transport to the cell surface and subsequent clathrin-mediated endocytosis is followed by cathepsin L proteolysis in the early or recycling endosomal compartment [102-104]. Viral membrane associated proteins NiV G, F, and M assemble with the NiV N encapsidated progeny genomes at the cell surface where progeny virions bud from the cell surface and release [101].

1.3.3.iv. Pteropid bats are the reservoir for Nipah virus

After the initial outbreak of Nipah virus in Malaysia in 1999, studies suggested *Pteropus vampyrus* and *Pteropus hypomelanus* might be the reservoir host, because

neutralizing antibodies to Nipah virus were isolated from bats. Importantly, clinical signs of illness in bats were not observed [92, 105, 106] in the seropositive bats. Several species of animals including domestic dogs (*Canis lupus*), wild boar (*Sus scrofa*), and rats (*Rattus rattus*), and 14 species of bats were sampled for neutralizing antibodies. Of these only bats, 97 percent of which were megachiropteran, had neutralizing antibodies in sera [92, 105-107]. Virus was isolated from the urine of Pteropid bats and from swabs of partially eaten fruit and confirmed by sequencing of reverse transcriptase polymerase chain reaction (RT-PCR) products and immunofluorescence of infected Vero cells, which further supported the role of megachiropteran bats as the Nipah virus reservoir hosts and suggested viral transmission was from saliva and urine [106, 107].

1.3.3.v. Experimental infection of bats with Nipah virus

To date, only one study has examined experimental Nipah virus infection in Pteropid bats. In that study, seventeen *Pteropus poliocephalus* bats, along with guinea pigs, were inoculated with Nipah virus obtained from the central nervous system of a fatally infected human. The animals were observed for up to 23 days after challenge. Blood samples and conjunctival, nasal, tonsillar, and rectal swabs were collected every other day. In addition, bats were sacrificed on days 3, 5, 7, 10, 12, and 14 after challenge to check tissues for virus isolation and histological and immunohistochemical evaluation [108]. Unlike similar inoculation studies in pigs, cats [91], and guinea pigs in which infection causes febrile response and respiratory and neurological syndromes occasionally leading to death, NiV

infection in bats was completely subclinical with no recordable febrile responses [108]. Virus was only isolated from the experimentally infected bats in three instances: in the urine of one bat on days 12, 16, and 18 even in the presence of neutralizing antibody in the serum, from a kidney of a second bat on day 7, and from the uterus of a third bat on day 7. There were no gross abnormalities upon postmortem examination and mild lesions found in some organs were not attributed to NiV infection. All tissues in all bats were negative for NiV antigens as determined by immunohistochemical detection using a polyclonal antibody against partially purified whole virus [108]. This study outlines a completely different form of infection in Pteropid bats than the deadly inflammatory infection in other mammals and is consistent with the idea that megachiropteran bats are asymptomatic reservoir hosts of Nipah virus.

1.3.3.vi. Antibody recrudescence and seasonal infectious cycles maintain Nipah virus in the bat population

A trend of seasonal antibody recrudescence and viral presence is evident from serology studies and research that has followed Pteropid bats over time. In one study, seventeen *P. vampyrus* bats were captured, quarantined, and serum antibody titers were monitored for up to twelve months. In addition, virus shedding was monitored in urine and throat swabs. Thirteen of seventeen bats were seropositive for Nipah virus neutralizing antibodies at the start of the study indicating naturally acquired infection. The antibody titers of six bats maintained a steady level throughout the study. Antibody titers of six other bats

waned below detection during the course of the study. Interestingly, the antibody titers of three bats waned before increasing after nine months. Additionally, virus was only isolated from the urine of one bats when its antibody titer was rising. No febrile responses were detected throughout the study in any of the bats [107, 109]. Another study followed wild *P. lylei* in Thailand, a country with no known NiV outbreaks over the course of two years, and examined NiV RNA presence in urine. Both the Malaysian and Bangladesh strains were identified in urine of these bats. The Malaysian strain was detected from December to June whereas the Bangladesh strain was detected almost exclusively from April to June, with the peak recovery of NiV RNA occurring in May [110]. Single time point studies have only found low percentages of anti-NiV antibody seroprevalence and NiV RNA isolation around 10% [92, 105, 106, 111-117]. Even in experimental infection [108] or attempts at isolation of virus from wild bats [106], viral shedding in bats was a rare event. Recent research into the persistence of NiV under environmental conditions has shown that NiV can survive briefly in bat urine of pH 3-7 and for longer periods when kept around room temperature on fruits and in fruit juices of pH 4-7 [118]. Recorded bat urine pH falls well within these ranges [108, 118]. The seasonal aspect of the outbreaks from January to June correlates with seasonal availability of fruits and date palm sap collection during the colder months [88, 115, 118, 119]. All of these aspects, specifically the isolation of virus after a seropositive bat's antibody levels waned below detection levels, suggest a model in which viral circulation in bat populations relies on short seasonal infectious cycles and quickly waning antibody titers as opposed to long-term immunity to maintain a group of susceptible individuals within the

population without the acute infection and disease found in humans and other mammals [109].

1.3.3.vii. Transmission of Nipah virus from bats to humans

As evidenced above, bats maintain a unique asymptomatic relationship with Nipah virus as opposed to the pathogenic relationship of humans and pigs with Nipah virus. The transmission cycle (Figure 2) from bats to pig (secondary host) and ultimately humans was associated with different pathology in each host [91, 120, 121]. Pigs developed clinical and subclinical infection and excrete virus from the oropharynx as early as 4 days post-infection. Naïve pigs in contact with inoculated pigs excreted virus identically several days after viral excretion was recorded in the inoculated pigs [91]. Transmission from pig-to-pig and pig-to-human is likely through contact with infected oropharyngeal and nasal secretions, and clinical disease was often associated with a loud cough [91, 92]. Experimental and natural infection in pigs was characterized by systemic vasculitis, lesions in the trachea and lungs, aveolitis, and meningitis, rarely leading to encephalitis [91, 122]. Although infection and inflammation was systemic, infection rarely resulted in death [92]. In contrast to bats and pigs, Nipah virus infection in humans is highly pathogenic with a high case-fatality rate and presents itself mainly through fever, neurological, and respiratory illness. Infection was characterized by extensive vasculitis and necrosis in many organs, mainly the lungs and brain. High mortality was associated with severe central nervous system and neuronal infection leading to encephalitis. Central nervous system (CNS) tropism was easily

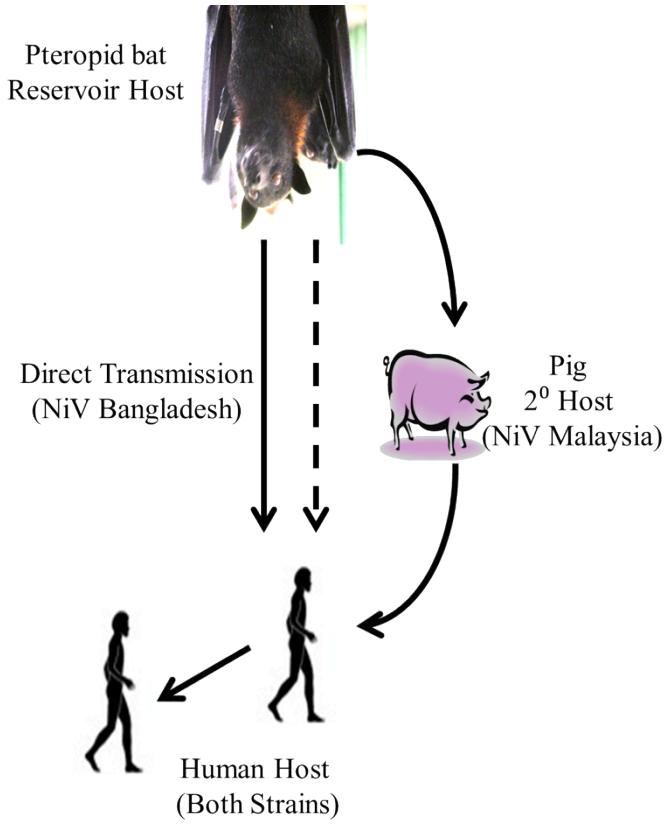

Figure 2. Transmission cycle of Nipah virus from bats to humans. Nipah Virus is asymptomatically maintained in the Pteropid bat reservoir. In the outbreak of NiV Malaysia, pigs were identified as the secondary hosts. Pigs showed clinical symptoms but infection was not as lethal as in humans. Bat-to-human transmission was also likely for NiV Malaysia but was unreported and is indicated by the dashed line. NiV Bangladesh transmission has not been associated with a secondary host. NiV Bangladesh can directly infect humans from contact with bats or bat contaminated date palm sap [115, 119, 123, 124]. Once in the human host NiV can spread from person to person through contact with infected body fluids.

demonstrated, as the CNS was three to four times more likely to be positive for Nipah virus antigens [120-122, 125]. Experimental models of Nipah virus infection in ferrets, cats, dogs, hamsters, pigs, squirrel and African green monkeys all recapitulate various aspects of highly pathogenic infection associated with neurologic and/or respiratory disease [126], however only megachiropteran bats appear to maintain an asymptomatic non-pathogenic host relationship. As will be further discussed below, we hypothesize these differences in pathogenesis are due to host factors, in particular the interferon system, and not changes in the virus itself.

1.3.3.viii. Increased pathogenicity of NiV in humans cannot be attributed to viral factors

Unlike the genetic divergence of SARS-CoVs, differences in NiV infection between bats and humans are likely due to host factors. Based on the high homology of viral strains and high homology of the cellular receptor between bats and humans, the ability of NiV to infect both human and bat cells is not likely due to changes in the virus itself. NiVs isolated from bats and humans are highly homologous at ~96-99% amino acid sequence homology and 98-99% attachment protein homology [106, 107, 127, 128]. In addition, other possible Nipah virus strains have been identified in Thailand with >92% amino acid homology to the Bangladesh and Malaysia strains based on short 181-nt sequences of the Nipah virus nucleoproteins [116]. The Bangladesh strain was found to be most divergent from the Malaysia strain with amino acid homologies >92% and biologic effects of amino acid differences are under investigation [127]. Ephrin B2 and B3 ligands have been identified as

receptors for Nipah virus [98-100] and amino acid sequences are >95% homologous between human, horse, pig, cat, dog, *P. alecto*, *P. vampyrus*, and mouse [129]. Furthermore, NiV was capable of infecting cells expressing any ephrin ligands of the aforementioned species [129]. Unlike SARS-CoV that has diverged greatly from its ancestry to be able to infect humans, the high homology of Nipah viruses and host receptors and universal infectivity strongly suggests that other host factors are important in the control of Nipah virus pathogenicity post-infection.

1.3.4. A common viral strategy does not account for the differences in host pathogenicity for EBOV, SARS-CoV, and NiV

The three bat derived virus examples described above are highly pathogenic in humans but not in bats. Even though SARS-CoV, EBOV, and NiV are single stranded RNA viruses that originated in bats, they also demonstrate a great diversity in almost all other aspects. All three viruses bind different host cellular receptors. While SARS-CoV and EBOV require endocytosis for fusion and cell entry, NiV F can mediate fusion directly to the cell membrane after NiV G binds the cellular receptor. All three viruses utilize different replication and transcription strategies. As a large positive sense RNA virus, SARS-CoV replicase proteins are translated directly from the genome as a single polypeptide and then enzymatically processed. The SARS-CoV also transcribes negative sense subgenomic RNAs of individual genes that serve as templates for mRNAs for translation of individual viral proteins. Multiple alternate ORFs within the genes and intergenic regions encode for

nonstructural genes and replication mainly occurs within specialized double membrane vesicles. In contrast, individual EBOV mRNAs are transcribed from the negative sense genome without alternate ORFs. Only the EBOV glycoprotein is transcriptionally modified by adenosine insertion to produce a soluble nonstructural product or the full length glycoprotein. NiV utilizes a similar replication strategy as that of EBOV to create positive sense antigenome templates for negative sense genomic progeny strands through the accumulation of N protein to stabilize the antigenomes and progeny genomes. Unlike EBOV, NiV transcribes nonstructural proteins, NiV V and NiV W, from the NIV P ORF by transcriptional insertion of one or two non-templated guanine nucleotides; NiV C is completely encoded from an alternate ORF within NiV P mRNA. SARS-CoV progeny are released through the host cell secretory pathway while EBOV and NiV progeny bud from the cell surface. While the SARS-CoV S protein mutated greatly to be able to jump to the human host, much of the rest of the virus maintained similar nucleotide homology with SL-CoVs. Additionally, EBOV and NiV strains are almost identical in bats and humans. As will be discussed later, these three viruses target similar aspects of the interferon pathway through different molecular actions. None of the evidence above supports the idea that the increased pathogenesis in humans than bats is the result of a common viral strategy or molecular feature shared by SARS-CoV, EBOV, and NiV. Rather, the evidence above supports the hypothesis that a host factor or factors are responsible for the differences in pathology between the species. In the following sections I will describe what is known about the megachiropteran immune system followed by interferon and the antiviral state.

1.4. Megachiropteran bat immunophysiology

While megachiropteran bats have been identified as likely hosts to many highly pathogenic viruses as described above, very little is known about the bats' immune systems and ability to control these infectious agents. Anatomically, the megachiropteran immune system does not appear to be unique. Anatomical and histopathological analyses of *Rousettus* and *Pteropus* species indicate the presence of the usual mammalian immune organs such as the thymus, spleen, and lymphatics [130-133]. The thymus in young *Pteropus giganteus* is well organized and structurally similar to that of primates and humans. The organ is multi-lobed and distinct cortex and medulla regions are found within each lobe [130, 132]. Hassall's bodies are prominent in the medulla of the neonatal thymus similar to those seen in the human thymus. As the bats age, thymic involution is evidenced by large masses of fatty tissue that have infiltrated the thymic interior embedded with small 'islands' of lymphoid cells [130]. The spleen and lymph nodes were also structurally similar to other mammals with well-organized white and red pulp regions, and anti-bat immunoglobulin γ (IgG) immunostaining confirms the presence of B cells within germinal centers. While the thymus did not reveal many dissimilarities, hematoxylin and eosin and Masson-trichrome staining revealed most germinal centers in splenic white pulp and lymph nodes were hypertrophic although more studies need to be performed to verify these observations and determine if there are differences between wild caught and lab-contained animals [132, 133].

Only a few studies have examined the cells that make up the chiropteran immune system and these studies have not been performed at great depth. Cell surface topography,

cell surface adhesiveness to plastic or nylon wool, and scanning electron microscopy have been used to identify T cells, macrophages, B cells, eosinophils, basophils, monocytes, dendritic cells, and neutrophils [134-137]. Interestingly, the predominant leukocyte observed in peripheral blood varied from species to species with lymphocytes being detected in *P. hypomelanus* and *P. vampyrus*, whereas the neutrophil was the predominant leukocyte observed in *P. rodricensis* [136]. Upon immunization of *P. giganteus* with sheep red blood cells to generate a T-cell dependent antibody response, morphological changes were observed in cell surface topography such as elongation of spike-like filamentous projections and membrane ruffling suggested activation of lymphocytes [134]. As reagents become available, further characterization of function and faculty of immune cell populations will shed light on bats' immunological relationship with the viruses they host.

In addition to enabling reagent development, determination of cell surface molecule amino acid homology and heterogeneity among species can help predict viral tropism for host cell types during infection in multiple species. For example, different strains of influenza preferentially infect humans versus birds or upper versus lower respiratory tracts [138, 139]. Additionally, the inability of human or palm civet SARS-CoV to bind the bat ACE2 receptor was predicted and experimentally verified based on key residues known to be important for S protein binding to human ACE2 despite 81% amino acid sequence homology between bat and human ACE2 [68]. Recently the *Rousettus aegyptiacus* CD4 gene was cloned, sequenced, and compared to CD4 nucleotide and amino acid sequences of multiple mammals and one bird. Consistent with the predicted phylogeny (Figure 1), chiropteran

CD4 had a higher amino acid homology to cat and dog CD4 (60.6% and 59.4% respectively) than human, mouse, or chicken CD4 (56.4%, 47.6%, and 23.5% respectively). The CD4 Ig constant domain (IgC)-like region 1 in bats contained an 18 extra amino acid insertion that consisted mainly of glycine and serine residues as compared to this region in humans, monkeys, mice, rabbits, and pigs. Similar insertions of 9 and 16 amino acids are found in the cat and dog CD4 IgC-like region 1, respectively. Akin to the cat, dog, pig, and rabbit CD4 IgC-like region 1, a cysteine near the N-terminus of this region was replaced with a tryptophan, likely preventing the formation of a disulfide bond found in this human, mouse, and monkey CD4 region. The significance of the loss of the disulfide bond is unknown; however, it may result in a different conformation of the bat CD4 IgC-like region 1 than that of human and mouse. This conformation may influence major histocompatibility complex (MHC)-CD4 connection between antigen presenting cells and $CD4^+$ T cells and subsequently influence T cell activity [140].

Antibodies compose another important part of the immune system. Early research noted a delay in time to attain peak primary antibody response to antigen or stimulation in *Pteropus giganteus* compared to that in mice [133, 141-143]. This delay is likely due to T-cell mediated suppression of B cell activation, because blastogenic response and antibody responses were comparable to mice after cyclophosphamide depletion of T regulatory/suppressor cells. Cyclophosphamide has been shown to deplete $CD4^+CD25^+$ T cells and alter the ratios of $CD4^+CD25^+$ T cells to $CD4^+$ T cells in favor of $CD4^+$ T cells to enhance anti-tumor immunity in a $CD4^+CD25^+$ T cell dependent manner [144]. The reasons

behind why the delayed antibody response exists or may be favorable in bats are unknown, and unfortunately follow up studies were not performed due to lack of reagents and lab animal strains [133].

Recently, two groups have created monoclonal and polyclonal anti-megachiropteran bat IgG antibodies (*Rousettus aegyptiacus* [132, 145] and *Pteropus hypomelanus* [146]) with very low cross reactivity to non-human primate, human, dog, mole, and shrew IgG as sera from each species could only competitively inhibit anti-bat IgG from binding bat IgG by less than 20% [145]. Additionally, detection of purified bat IgG could not be detected by anti-mouse, -rat, -sheep, -goat, -rabbit, -horse, -guinea pig, -bovine, -manatee, and -black rhino IgG. In an ELISA system, an anti-human IgG λ chain reagent bound bat IgG weakly, showing three-fold lower absorbance compared to binding of bat IgG by protein G [146]. These results suggest that bats have highly divergent IgG chains from other mammals and as reagents become available, further characterization of function and faculty of immune cell populations will shed light on bats' immunological relationship with the viruses they host.

Different animals rely on different means to form a diverse antibody repertoire. Mammals with many variable and constant chain genes, like humans, utilize somatic hypermutation, nucleotide addition and subtraction, and VDJ recombination to generate increased diversity due to the ability to initially form a large number of joining and junctional gene combinations. On the other hand, animals, such as chickens, that have limited numbers of gene combinations utilize gene conversion with pseudogenes to create a diverse set of antibody specificities [147]. Recently, the expression of Ig heavy chains was analyzed in

Pteropus alecto splenocytes and compared to the *Pteropus vampyrus* genome for a germline repertoire. Mammalian Ig variable heavy (VH) genes and gene families can be grouped into three clans according to nucleotide sequence conservation in two of the three framework intervals that flank the first and second complementarity determining regions (CDR) [148, 149]. Comparable to humans and rodents and in contrast to most other mammals (*e.g.*, cattle, swine, rabbits, and sheep), *Pteropus* had over 20 VH genes that were distributed in all three mammalian VH clans. In addition, at least five different joining heavy segments were identified which is comparable more to the human repertoire of six as opposed to one identified in the chicken [149]. The CDR3 ranged from six to 18 amino acid residues in length and were quite different from each other consistent with extensive diversity of the heavy genes. Interestingly, the *P. alecto* CDR3 regions contain fewer tyrosine residues and a greater proportion of arginine and alanine residues, which suggests the formation of antibodies with weaker avidity but greater specificity. Tyrosine residues have been correlated with greater 'sticky' antigen binding and arginine residues have been reported to be detrimental to antigen binding. The low tyrosine and high arginine-containing antibodies may be unable to bind with the same avidity as the 'sticky' antibodies thus reducing polyreactivity, although they may have greater specificity for particular antigens when they do bind. All of the sequences were obtained from splenocytes of a wild-caught adult specimen, so more analysis needs to be performed to examine antibody development and repertoire development throughout age and antigen exposure, as viral infections could have contributed to the selection of antibodies and germline negative selection during B cell

development [149]. Viral infection contribution to antibody selection could be another mechanism that Nipah virus employs to maintain infection in the bat population.

Overall, the bat immune system does not appear to be vastly different from other mammals, including humans, as noted in the immuno-anatomical and cellular studies mentioned above. Differences become apparent in structural and molecular studies as noted in the studies that examined the bat CD4 protein and the bat antibody repertoire. From the information above, why bats might be resistant to certain viruses remains unclear. However, as reagents become available, studies can examine individual cell populations and their effect on the immune system as noted in the T cell dependent delay of antibody response. Interferons and the antiviral state comprise another important arm of the immune system in the fight against viruses.

1.5. Type I and III interferons are key cytokines in the fight against viruses

Type I and III interferons (IFNs) are key cytokines in the rapid response to infection by a multitude of pathogens, including viruses. Interferons render cells refractive to viral infection/replication, which is commonly referred to as the "antiviral state" and is induced prior to onset of the adaptive immune system response [150-153]. Type I and type III interferons are initially induced in response to recognition of pathogen-associated molecular patterns (PAMPs) by cell surface and endosomal pattern-recognition receptors (PRRs), such as toll-like receptors (TLRs), or by intracellular cytosolic receptors, such as retinoic acid inducible gene I (RIG-I) and melanoma differentiation-associated gene-5 (MDA5) [151, 153-

155]. Once IFN is produced and secreted by the infected cell, it can bind IFN receptors on the same or neighboring cells to increase further IFN production via a positive feedback loop (Figure 3) [150, 153, 156].

The production of hundreds of proteins that are induced and/or activated by IFN signaling to control almost all steps in viral replication is broadly referred to as the antiviral state [150, 152, 153, 156]. I will briefly describe a few of the most studied and major effector proteins in the antiviral state: interferon stimulated gene (ISG)-15, Mx guanosine triphophatases (Mx GTPases, also referred to as Mx), 2'5'-oligoadenlyate synthetases (OAS), and protein kinase R (PKR) [150, 152, 153]. Animal models have demonstrated how defects in one of these effector molecules can render an otherwise immunocompetent animal susceptible to certain viruses. For example, the Mx proteins are important for conferring resistance to orthomyxoviruses in mice and one of the OAS proteins is important for directly mediating inhibition of West Nile virus (WNV) replication and natural resistance of mice to WNV [150]. ISG15 has multiple functions in the antiviral state, many of which are not fully understood. ISG15 has been shown to covalently attach to other antiviral proteins, such as PKR, likely to enhance activation [152, 157], or interferon regulator factor 3 (IRF3) to prevent virus mediated degradation [158]. ISG15 can covalently bind to influenza A non-structural 1 (NS1A) proteins to impair influenza replication by blocking the ability of NS1A to bind the nuclear import factor importin-α and to bind double-stranded RNA (dsRNA). In addition, ISG15 has been shown to bind human papillomavirus capsid proteins to impair virion infectivity through an undetermined mechanism, possibly through impairment of entry

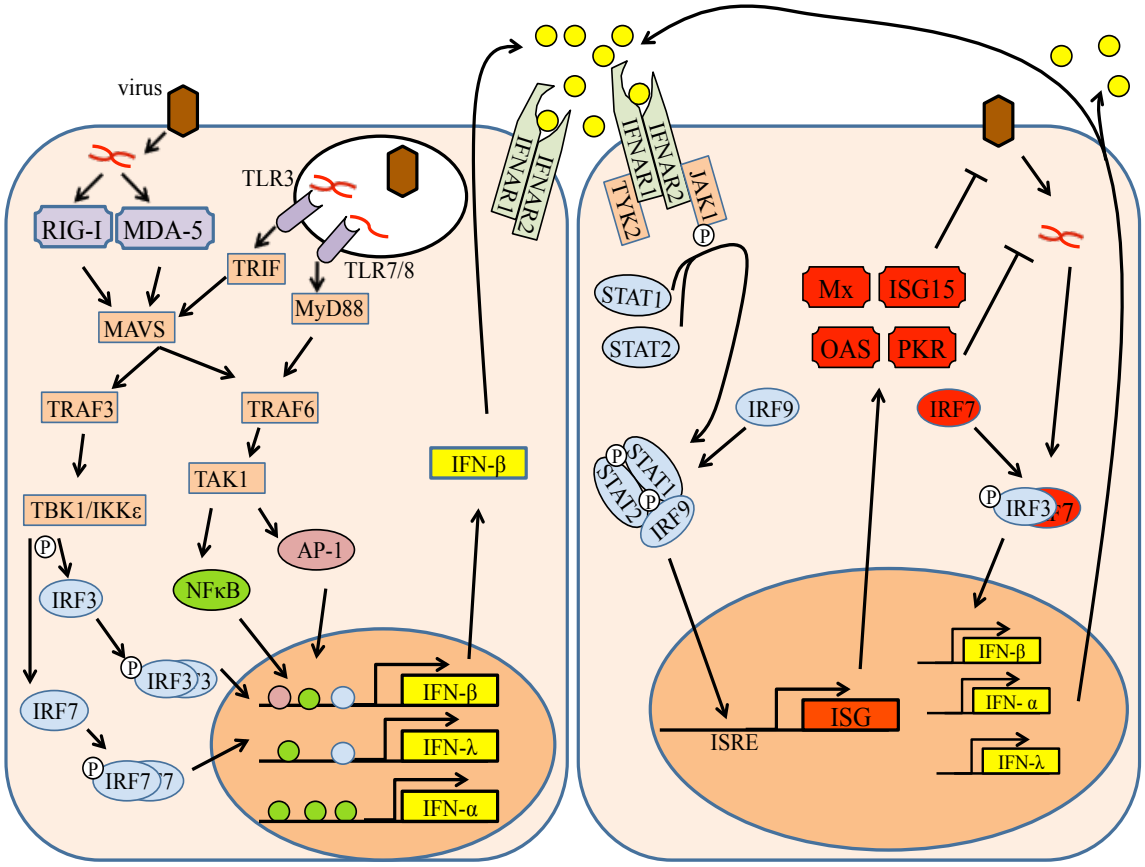

Figure 3. Simplified pathway of IFN induction and signaling. RIG-I, MDA5, TLR3, and TLR7/8 signal through different pathways to stimulate Type I and Type III IFNs. The different promoter binding requirements by IRFs, NF-κB, and AP1 are demonstrated in the figure. IFN-β production is followed in the figure for simplicity as IFN-β production normally precedes IFN-α induction. IFNs can bind back to IFN receptors on the same or neighboring cells to increase (via a feedback loop) further IFN production. Once IFN is bound to Type I or Type III IFN receptor, JAK1 phosphorylates STAT1 and STAT2. Phosphorylated STAT1 and STAT2 form homo- and hetero-dimers , then IRF9 binds. The STAT complexes translocate to the nucleus and bind interferon stimulate response elements (ISRE) to promote transcription of interferon stimulated gene (ISGs). ISGs like Mx GTPases, PKR, OAS, and ISG15 are described further in the body [55, 150, 152, 153, 159, 160].

or release of viral DNA into new cells [161]. The Mx GTPases are important inhibitors of early viral transcription and replication. While their precise function is unknown, Mx GTPases have been shown to inhibit early viral transcription and replication by trapping nucleocapsid structures, thus inhibiting their function and restricting cellular localization [162]. To inhibit viral replication, transcription, and translation, OAS proteins act as PRRs and are activated by viral dsRNA to produce 2'5'-oligoadenylates that in turn activate ribonuclease L (RNase L) to cleave viral and cellular RNAs [150, 152, 153]. Cleavage of viral genomic (in ssRNA viruses) and viral mRNA can eliminate the viral genome and inhibit viral protein synthesis, respectively. Additionally, cleavage of cellular mRNAs and ribosomal RNAs leads to damage of host cell machinery required for viral replication, production of small duplex RNAs that induce more IFN, and induction of apoptosis that could eliminate the virally infected cell prior to assembly of progeny virions [163]. PKR is an important factor in control of translation of viral proteins. PKR can be activated by dsRNA, short 5' triphosphate ssRNAs, tumor-necrosis factor (TNF)-receptor-associated factors (TRAFs), PACT, and caspase-mediated cleavage of the PKR inhibitory domain [150, 152, 153, 164]. Activated PKR phosphorylates eukaryotic translation initiation factor 2α (eIF2α), and consequently halts guanosine di-phophaste (GDP) recycling, thus inhibiting viral and cellular protein translation [150, 152, 153]. While inhibition of viral translation has its obvious advantages, inhibition of cellular protein translation can lead to apoptosis and cell-cycle arrest to clear viral infection or stall cell-cycle transforming viruses [153]. While

both type I and type III interferons induce this general and vital antiviral state [150, 156], the complexity of the type I and type III interferon systems will be described in greater detail.

The type I interferon family consists of a continually expanding catalog of subfamilies including the most well-known and studied IFN-α and IFN-β and the less well-understood IFN-ω, ε, κ, δ, τ, and ζ [159, 165, 166]. While interferon-α, β, and ω can be produced by almost all mammalian cells and encompass the majority of the interferons initially induced, the ratios produced vary with the cell type. IFN-β is secreted primarily by fibroblasts whereas plasmacytoid dendritic cells secrete high levels of IFN-α [150, 159]. In addition, other interferons are only produced by certain cell types, for instance IFN- κ production by keratinocytes [159, 167]. In the human, thirteen IFN-α species and a single species of IFN-β, IFN-κ, IFN-ω, and IFN-ε comprise the type I IFN family [159], although this expression profile is not conserved between animals [159, 165, 168, 169]. For example, 17 IFN-α species, eleven IFN-δ species, seven IFN-ω species, and a single species of IFN-β, IFN- ε, and IFN-κ were identified in the porcine type I IFN family, although the significance of these differences between species is not fully understood [168].

All type I interferons share a similar multi-helix structure and signal through the same receptor: the interferon-α/β receptor (IFNAR). The IFNAR is a heterodimeric receptor of chains IFNαR1 and IFNαR2c [159], and signaling through the IFNAR is highly conserved among species (Figure 3) [170-172]. Despite the structural similarities, the individual type I IFN species each seem to exhibit different activity profiles. For instance, IFN-αF human IFN-α1, -α2, -α6, -α8, -α10, -α17, and -α21 were all able to boost natural killer cell activity

although human IFN-α7 was shown to be unable to boost natural killer activity [173]. Human IFN-β was shown to preferentially induce β-R1 gene compared with IFN-α subtypes [174]. Subtle differences in structure, glycosylation status, and receptor affinity have all been implicated in differential binding of the IFNAR1 and IFNAR2 subunits and subsequent different biological actions of individual interferons [175-177]. How different interferons are able to produce different biological actions through the same receptor and highly conserved downstream signaling is not fully understood. Speculatively, these differences in binding could affect strength of Janus kinase (JAK)-signal transducer and activator of transcription (STAT) (JAK-STAT) binding and phosphorylation levels, in addition to differential IRF9 and p48 association with the STAT dimers resulting in different biological consequences [159, 177]. Remarkably many of the type I IFNs have been found to be animal species-specific, and the ones that can cross-react with IFNARs from other species do so unpredictably [178, 179]. The concept of animal species controlling and responding to viruses differently is strengthened by the facts that species express multitudes of interferon subtype expression profiles and individual interferon subtypes have distinct biologic actions.

In the past decade, type III interferons were identified as another set of interferons important in setting up and regulating the immediate antiviral response [151, 156]. Three type III IFNs have been identified in humans: IFN-λ1, λ2, and λ3, also known as interleukin (IL) 29, IL28A, and IL28B, respectively. Unlike the type I interferons, type III interferons are multi-exon genes and utilize a heterodimeric receptor composed of the unique IFN-λR1 and shared IL10R2 chains. The IFN-λ receptor complex utilizes the same JAK-STAT

pathway of the IFNAR, with some slight differences, to initiate the antiviral pathway [156]. *In vitro* cell cultures have shown that most cell types can produce IFN-λs; however, epithelial cells appear to be the main target of the IFN-λ as they express high levels of the IFN-λR1 chain. While cells express varying levels of the IL10R2 chain, the sensitivity of cells to IFN-λ correlates with expression of the IFN-λR1 chain [151, 156, 180, 181]. Like the type I IFNs, different animal species have differential expression of the IFN-λ1 genes. Humans express all three IFN-λs but only IFN-λ2 and IFN-λ3 are functional in the mouse [156, 182] while only IFN-λ1 and IFN-λ3 have been identified in the pig [183]. The type III IFNs similarly activate the antiviral state but with varying degrees as compared to the type I IFNs. The exact roles of type III interferons in viral defense are still being examined [156, 180, 183]. However, evidence of differential expression patterns of the type III IFNs, their receptors, and induction and interference of type III IFNs by certain viruses supports the idea that IFN-λ has a unique and specific role in the antiviral response and is not just redundant with the type I IFN system [156, 180].

As described above, many aspects of the type I and III interferon systems are highly homologous between animal species (*e.g.* receptor signaling, induction of a general antiviral state) while many aspects, namely usage of different IFN subtypes, differ between species. IFNs are targets of inhibition by viral proteins as will be discussed further in Chapter 1.7.. The evolution of different pathways to initiate the interferon induced antiviral pathway in spite of viral interference further substantiates the importance of the interferon system. In the next chapter, the megachiropteran immune system and interferon system will be described.

1.6. Bats and Interferons

Only in the last half decade have the innate immune receptors and pathogen recognition pathways in megachiropteran bats been explored. TLRs 1 through 10 were identified in the *P. alecto* genome [184] and TLRs 3, 7, and 9 in *Rousettus leschenaultii* [185]. TLR amino acid sequences were highly homologous to human sequences at 71%-86% homology depending on TLR type. Expression was verified by quantitative RT-PCR and, unlike in humans and mice, TLR3 was highly expressed in the liver of megachiropteran bats. Analysis of protein levels (by Western blot for example) needs to be performed to verify expression levels. In other mammals, TLR3 is predominately expressed in dendritic cells (DCs); therefore, higher TLR3 expression in the liver may signify greater numbers of DCs in the liver. On the other hand, the atypical characteristics of the bat response to viruses may be due to different expression of TLRs on bat cells compared to human cells [184, 185]. Individual cell types express certain TLRs in particular and future research will explore cellular TLR expression profiles.

Because bats appear to have a high level of resistance to viral infections, there has been great interest in characterizing the antiviral immune responses of bats. Two of the major components of the antiviral response conserved in all vertebrates are Type I IFNs and the newly recognized Type III IFNs. Omatsu *et al.* identified an interferon-α and interferon-β in *Rousettus aegyptiacus* [132, 186] and confirmed expression by semi-quantitative PCR in *Rousettus leschenaultii* primary kidney cells after poly(I:C) stimulation. In addition, bat primary kidney cells were stimulated for three hours with poly(I:C), a known inducer of IFN

through TLR3 stimulation, washed twice to ensure removal of any poly(I:C), and cultured in fresh media overnight. This interferon-containing media from the stimulated bat primary kidney cells was transferred to new cells and IFN-β transcript levels were measured by semi-quantitative PCR [132, 186]. The *R. aegyptiacus* IFN-β amino acid sequence was 64.2%, 61.8%, 61.3%, and 49.5% homologous to the human, cat, horse and mouse IFN-β genes respectively, and was most homologous to the pig IFN-β protein sequence at 72% [186, 187].

A rare Type I IFN was recently identified from megachiropteran and microchiropteran bat genomes of *Pteropus vampyrus* and *Myotis lucifugus*, respectively [165]. IFN-δ is a Type I IFN subtype not found in humans or mice but has been identified in pigs, sheep, horse, alpaca, bottlenose dolphin, armadillo, two species of shrews, kangaroo rat, and hedgehog. IFN-δ is a trophoblastic IFN found only during pregnancy, expressed by the blastocyst and its role during pregnancy remains to be characterized. Cochet *et al.* identified three and four IFN-δ subtypes in *M. lucifugus* and *P. vampyrus* respectively [165]. It is unclear what role, if any, IFN-δ has in prevention of viral infection.

Type III interferon genes for IFN-λ1 and IFN-λ2 were recently identified and cloned from *Pteropus alecto* and, although IFN-λ3 was identified from *P. vampyrus* genome, only IFN-λ1 and λ2 were confirmed to be transcribed in *P. alecto*. IFN-λ1 and λ2 amino acid sequences were 64% and 67% homologous to humans, respectively. In poly(I:C) stimulated bat primary cell lines, IFN-β had higher transcript induction than IFN-λ1 or λ2, and IFN-λ2 was induced to a much greater extent than IFN-λ1. However, when bat splenocytes were infected with Tioman virus, a paramyxovirus hosted by bats, IFN-β was not induced whereas

IFN-λ2 was greatly induced [188]. The expression dynamics between poly(I:C) stimulation and Tioman virus infection was possibly due to differential TLR stimulation and immune modulation by the virus to inhibit IFN-β signaling and/or response. Tioman virus is a distantly related paramyxovirus like Nipah virus but has not been found to infect other species naturally and only causes asymptomatic or mild illness upon experimental inoculation [189, 190]. All of the possible mechanisms of antiviral modulation by Tioman virus are unknown [190]; however, like other related paramyxovirus V proteins, the Tioman virus V protein binds MDA5 and could inhibit IFN-β induction [191]. Furthermore, IFN-λ2 containing media from IFN-λ2 producing 293T cells was able to protect a *P. alecto* stable cell line from Palau virus replication and measurably induce ISG56 and RIG-I, further demonstrating IFN-λ2's ability to stimulate antiviral activity much like a type I or III interferons from other species. This work is some of the first research extensively measuring the bat immune system to TLR stimulation and viral infection [188].

STAT1 is a major component of signaling through the interferon receptor and a common viral target to inhibit antiviral activity (Figure 3) [150]. STAT1 was sequenced and cloned from *Rousettus aegyptiacus*, and amino acid sequence was determined to be 97% homologous to horse STAT1 and 96% homologous to dog, human, and pig STAT1. Transfection experiments determined that bat STAT1 was phosphorylated and translocated to the nucleus, functionally similar to other mammals using anti-STAT1 and anti-phospho-STAT1 (Tyr701) antibodies known to bind mouse and human STAT1 and verified to bind bat STAT1 [172]. Basal levels of STAT1 in multiple tissues was examined by quantitative

real-time RT-PCR (qRT-PCR) analysis and STAT1 levels were high in the liver [172] much like was seen for TLR3 in *P. alecto* [184], further identifying the liver as an organ with unique immunological expression characteristics in bats.

As described above for the pig [168], Type I IFN profiles can differ between animal species. Further characterization of the bat interferon expression profile is needed to identify possible reasons for high resistance to infection in bats. To that end, one goal of this project was to identify, clone, and sequence the different Type I interferon species of *P. vampyrus*.

1.7. Viral evasion of IFN

If viruses had not evolved successful strategies to inhibit IFN production and signaling and suppress induction of the antiviral state, viruses would not be such successful pathogens [150, 153]. Virus-mediated interference with induction of the antiviral state can occur through one or more stages: (1) global interference with host gene expression and/or translation; (2) inhibition of signaling from PRRs and prevention of IFN induction; (3) interference of IFN signaling; (4) blocking antiviral action of ISGs; and (5) having a replication strategy that is mainly insensitive to the action of IFN [153].

As example of global interference with host gene expression (stage 1 above), the M protein of vesicular stomatitis virus suppresses IFN-β in a nonspecific manner through manipulation of host RNA polymerases and global shut-off host gene transcription [192, 193]. Poxviruses have large double stranded DNA (dsDNA) genomes and can encode for many interferon pathway antagonists. One smallpox protein sequesters dsRNA away from

PRRs to inhibit signaling from PRRs (stage 2), and another acts as an eIF2α mimetic to prevent PKR inactivation of eIF2α and block the antiviral translation inhibition (stage 4). In addition, smallpox encodes for a large soluble IFN binding protein to stop interferon from binding its own receptor on the host and neighboring cells, thus preventing induction of the IFN induced antiviral response (stage 3) [194]. Some viral proteins target multiple pathways and host cell components [153]. NS1 of influenza A virus sequesters dsRNA molecules to prevent PRR and PKR recognition (stage 2) and inhibits processing of cellular pre-mRNAs (stage 1) to respectively inhibit induction and translation of host cell genes such as IFNs and IFN effector proteins [150, 153]. The preceding examples illustrate the diversity of means by which viruses antagonize the IFN response. We hypothesize that viruses that evolve in a particular reservoir host will have had to evolve mechanisms to effectively antagonize the array of IFN proteins produced in that organism. The converse of this theory is that if a virus has a particularly highly developed array of IFN antagonists, the IFN mediated defenses of its reservoir host may have been highly effective. To begin to illustrate these points, the following section describes the IFN-antagonist proteins of three viruses for which pteropid bats are the reservoir host, namely SARS-CoV, Ebola virus, and Nipah virus.

1.7.1. SARS-CoV encodes several proteins to evade IFN mediated defenses

The SARS coronavirus has a particularly large genome for an RNA virus and encodes multiple different proteins that have multiple functions to inhibit induction of the antiviral state (Figure 4). In addition, the virus inhibits PRR detection by sequestering dsRNA

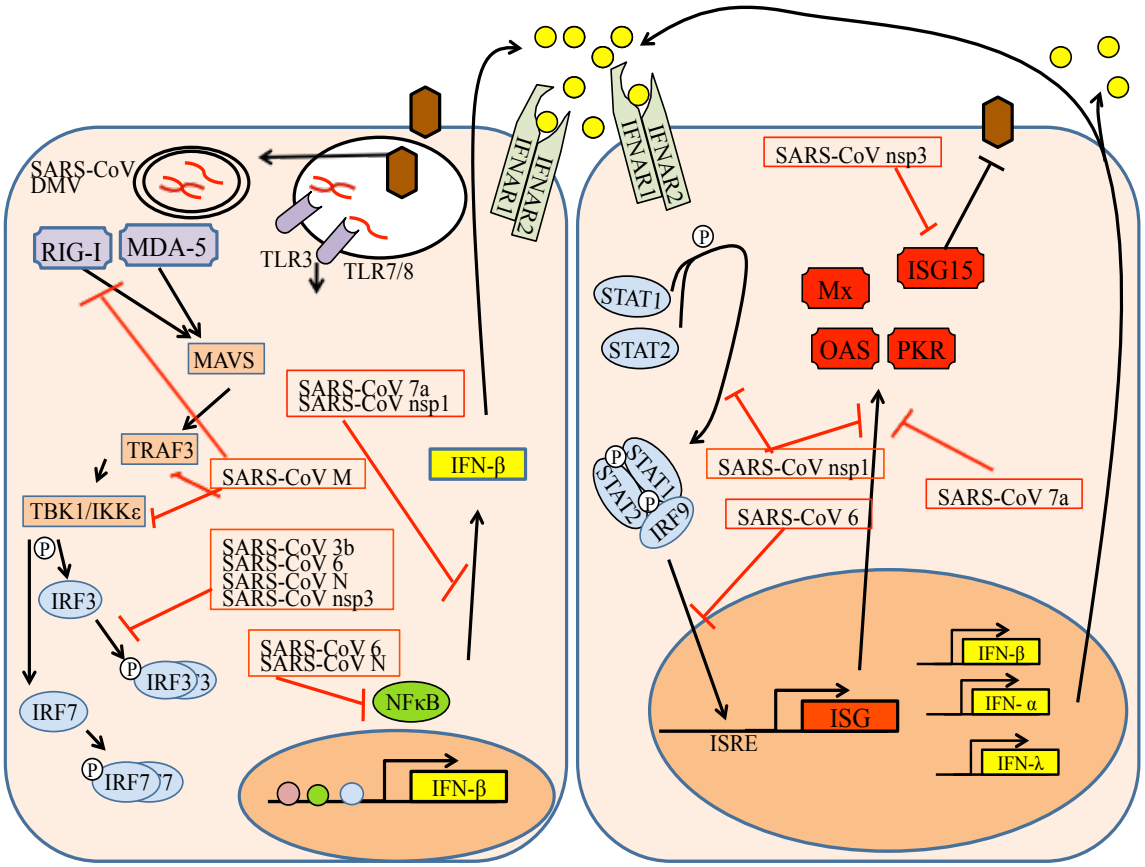

Figure 4. Interferon interference by SARS-CoV. SARS-CoV encodes multiple different proteins that have multiple functions to inhibit induction of the antiviral state. Most SARS-CoV interferon antagonists have specific target proteins while SARS-CoV nsp1 and SARS-CoV 7a promote host cell degradation and inhibit cellular protein synthesis respectively.

products in double membrane vesicles to prevent IRF-3 activation and subsequent IFN-α/β induction [55]. To suppress initial induction of IFNs, the SARS-CoV 3b protein, SARS-CoV 6, and SARS-CoV N inhibit phosphorylation of IRF-3 and translocation to nucleus to the IFN-β promoter while SARS-CoV 6 and SARS-CoV N also reduce nuclear factor kappa-light-chain-enhancer of activated B cells (NF-κB) activation [195]. The SARS coronavirus papain-like protease (nsp3) physically interacts with non-phosphorylated IRF3 to prevent IRF3 phosphorylation and activation [196]. The SARS-CoV papain-like protease has been shown to preferentially cleave ISG15 from other proteins, suggesting inhibition of ISG15ylation mediated effects [197]. The SARS-CoV M protein associates with and sequesters RIG-I, TRAF family member-associated NF-κB activator (TANK)-binding kinase 1 (TBK1), inhibitor of NF-κB kinase subunit epsilon (IKKε), and TRAF3 to prevent activation of IRF3 and IRF7 [198]. As well as inhibiting interferon transcription, SARS-CoV 3b and SARS-CoV 6 inhibit IFN signaling. SARS-CoV 6 prevents nuclear translocation of STAT1 by tethering and sequestering away the nuclear import factors necessary for STAT1 nuclear translocation [195, 199].

In a more global modulation of the host antiviral response, SARS-CoV 7a inhibits cellular protein synthesis [200], and SARS-CoV nsp1 has been suggested to promote host cell mRNA degradation and inhibition of STAT1 phosphorylation [55, 201-203]. In summary, SARS-CoV use not one but multiple separately encoded proteins to modulate host IFN production and signaling [55]. This is consistent with our hypothesis predicting that bat-vectored viruses will encode a robust and diverse array of IFN-antagonist factors.

1.7.2. EBOV utilizes a different strategy to evade IFN

Unlike SARS-CoV, which uses multiple ORFs to produce its IFN antagonist proteins, Ebola virus encodes only two IFN antagonist proteins, each of which antagonize the IFN response at multiple points [204-206]. EBOV VP35 and VP24 both have dual activity as viral polymerase co-factors and matrix proteins, respectively, and as suppressors of the interferon induced antiviral response [75] (Figure 5). VP35 suppresses production of IFN-β mRNA and activation of IFN-β promoter region by preventing activation/phosphorylation, dimerization, and nuclear accumulation of IRF3 [207, 208]. VP35 contains a dsRNA binding region likely to block dsRNA recognition by RIG-I and PKR [208-210]. However, VP35 was also shown to prevent, and even reverse, PKR phosphorylation in a manner independent of dsRNA binding [209, 210]. To inhibit IRF3 and IRF7 activation, VP35 competitively binds and acts as an alternate phosphorylation substrate for IRF3 kinases, IKKε, and TBK1, and subsequently prevents association of IRF3/7 with IKKε and TBK1 [211]. Normally IRF3 and IRF7 are small ubiquitin-like modifier (SUMO)-ylated (SUMOylated) by ubiquitin carrier protein 9 (Ubc9) and protein inhibitor of activated STAT1 (PIAS1) to contribute to negative feedback regulation of IFN-α/β production [212]. VP35 induces IRF3/7 SUMOylation to impair IFN-β gene transcription [213]. In contrast to VP35, VP24 targets IFN signaling. VP24 inhibits STAT1 nuclear accumulation by disrupting phosphorylated-STAT1 interactions with karyopherin-α1, the nuclear import factor necessary for transport of activated STAT1 complexes into the nucleus. VP24 was shown to competitively bind karyopherin-α1, although other mechanisms are possible [214]. In summary, EBOV, like

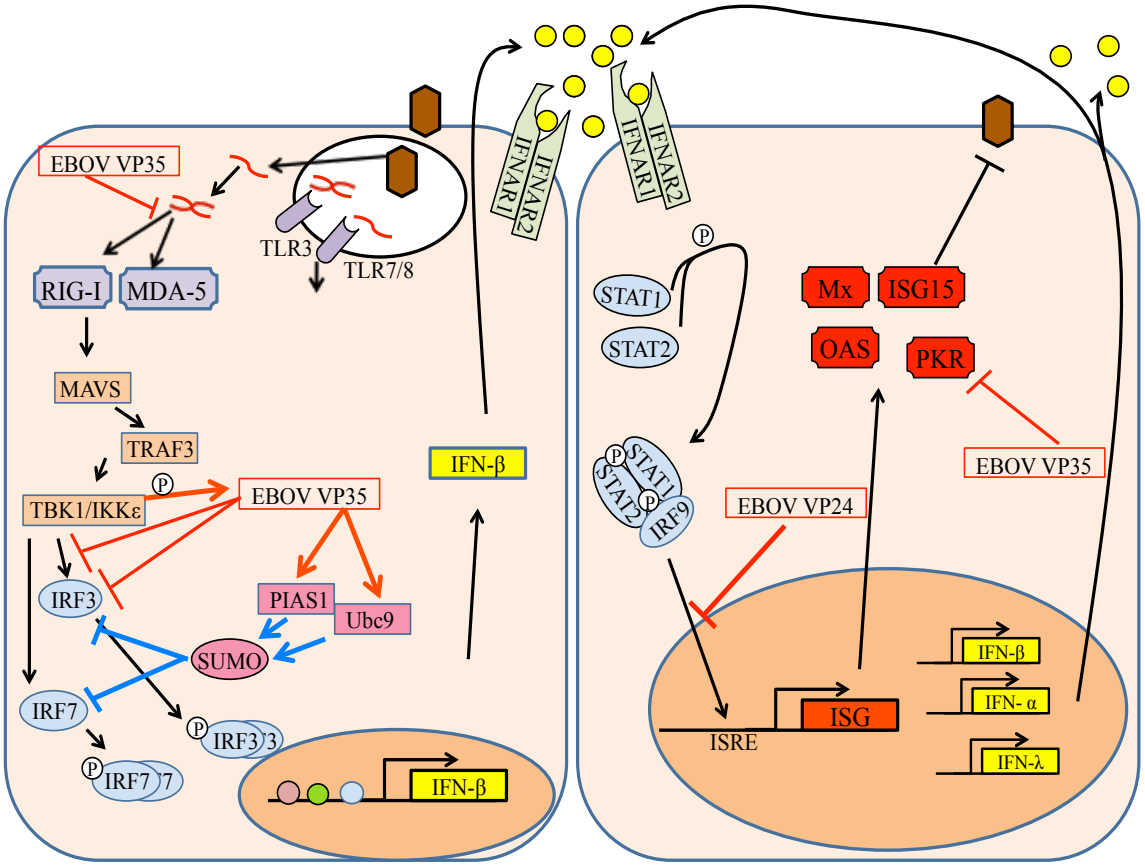

Figure 5. Interferon interference by EBOV. EBOV VP35 and EBOV VP24 function as structural proteins and potent interferon antagonists.

SARS-CoV, encodes potent IFN antagonist proteins capable of interfering with the host IFN response at multiple points. This is once again consistent with our hypothesis that bat-evolved viruses have superior IFN-antagonist activity in order to propagate within the bat population reservoir.

1.7.3. NiV antagonizes IFN response from distinct cellular compartments

As described in Section 1.3.3., Nipah virus is an RNA virus with a relatively small (18kb) genome. Despite this limited genome capacity, NiV encodes four proteins with IFN antagonist activity (Figure 6). The NiV P ORF encodes NiV P, NiV V, and NiV W, which are generated via transcriptional addition of one or two guanine nucleotides respectively [96]. The NiV C protein is generated from an alternate start side within the NiV P ORF [96].

The C protein has been shown to inhibit IFN activity through an unknown target by rescue of interferon sensitive Newcastle Disease virus replication expressing a green fluorescent protein (GFP) [215], and further experiments found that NiV C could only partially block ISREs [215, 216]. A mutation of the NiV C translational start codon has shown that NiV C was dispensable for the interferon antagonist function of NiV V and NiV W [215]. However, a recombinant Nipah virus with a knockout of the NiV C gene was associated with reduction in virulence suggesting an alternative important role [216]. The NiV P protein localizes to the cytoplasm where it acts as a viral polymerase cofactor. NiV P inhibits STAT1 phosphorylation and the activity of an ISRE, although inhibition of the ISRE by NiV P was less complete than that mediated by NiV V and NiV W [97].

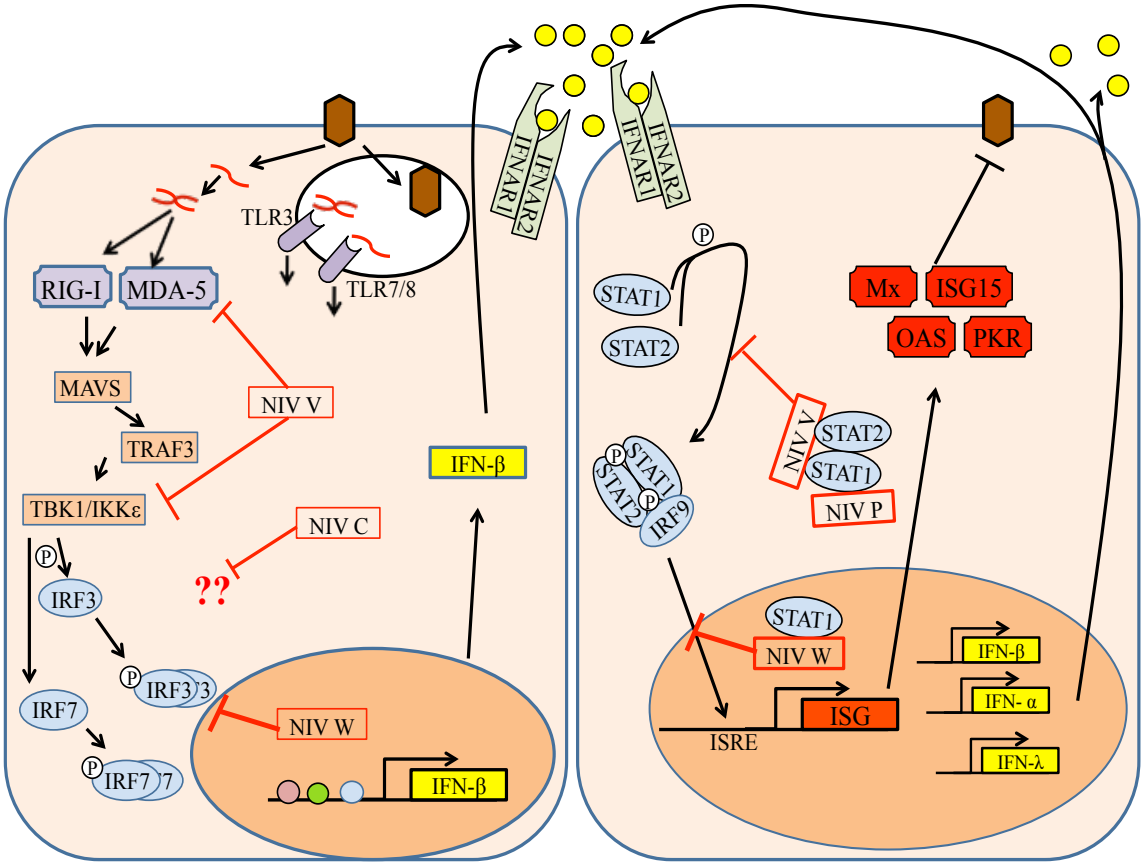

Figure 6. Interferon interference by NiV. The professional NiV interferon antagonists, NiV V and NiV W, act on the interferon pathways interferon from their cellular localization.

The NiV V and W proteins block IFN induction and IFN signaling via multiple pathways. NiV V blocks activation of the IFN-β gene and IRF3 dependent genes [216, 217] by binding the cytosolic PRR MDA5 [191] and inhibits signaling downstream of IKKε and TBK1 activation [217]. NiV V cannot bind RIG-I nor inhibit its activity [191], nor does NiV V suppress TLR3 stimulated promoter activity. However, the lack of TLR3 blockade is likely due to the fact that NiV V did not completely block signaling in response to TBK1, a kinase with a major role in TLR3 signaling [217]. NiV V protein can shuttle between the nucleus and cytoplasm, but a nuclear export signal transports NiV V back to cytoplasm at net steady state distribution. NiV V also redistributed the latent STAT1 from uniform whole cell dispersion to entirely cytoplasmic suggesting NiV V antagonist activity directly targeted to the cytoplasm [218, 219]. NiV V binds STAT1 and STAT2 in the cytoplasm in high molecular weight complexes to prevent IFN induced STAT phosphorylation/activation, and translocation to the nucleus [97, 218, 219].

NiV W protein inhibits IFN-β induction, IRF3 dependent genes, and IFN signaling but from a different cellular compartment than that of NiV V [97, 215, 217]. NiV W carboxyl-terminal domain contains a nuclear localization signal that interacts with karyopherin-α3 and -α4 to accumulate NiV W in the nucleus [217]. In contrast to NiV V protein, NiV W inhibits TLR3 mediated signaling and is dependent upon nuclear localization of NiV W. In addition, NiV W induces loss of phosphorylated IRF3 and subsequent promoter activation by both activated IKKε and TBK1. The exact mechanism that explains how Nipah W induces this loss has yet to be determined. However, the IRF3 nuclear

localization signal displays the same preference for binding the same karyopherins as does NiV W, although interactions between the karyopherins, IRF3, and NiV W have not been determined experimentally [217]. NiV W has also been shown to inhibit STAT1 phosphorylation, possibly via the same mechanism as that utilized by the NiV V protein. In support of that idea, both NiV V and NiV W promote redistribution of latent STAT1 to the cytoplasm and nucleus, respectively, and NiV V and NiV W also share the same STAT1 binding domain [97]. The localization of NiV V and NiV W provide Nipah virus with a dual and targeted strategy for blocking both cytoplasmic and nuclear forms of STAT1 [97].

In conclusion, the NiV IFN antagonist proteins have some common activities but are also distinguished by unique cellular distributions and some individual functions. A full mechanistic understanding of the NiV IFN antagonists awaits further study, which may also help to elucidate the effects of these proteins on pathogenesis and host range restriction [216].

1.8. Species host range can depend on virus' ability to effectively antagonize the IFN response

The preceding sections describe the multiple ways in which three different bat-associated zoonotic viruses antagonize the interferon inducible antiviral response. While the general mechanisms employed appear to be similar among SARS-CoV, Ebola, and Nipah, the specific mechanisms by which each virus achieves IFN suppression are quite different. It is worth noting that henipaviruses are the only known zoonotic paramyxoviruses that are

highly pathogenic in humans [96]. Nipah virus does not encode more genes than some of the other paramyxoviruses like Sendai virus, which is pathogenic for mice but not humans [220, 221]. In contrast to the other paramyxoviruses, Nipah utilizes different mechanisms of STAT and IRF3 inhibition [96] and Nipah edits the P gene at almost two-fold higher frequencies to produce more V and W transcripts [222, 223]. This evidence supports the hypothesis that Nipah virus evolved highly developed mechanisms to effectively antagonize the highly effective array of IFN proteins produced in the pteropid reservoir host.

For many viruses, host range can depend on IFN antagonist activity. While the human and murine STAT1 proteins are 92.4% identical at the amino acid level, the human and murine STAT2 proteins share only 68.6% amino acid identity [224, 225]. Both human and murine STAT2 are activated by IFN, translocate to the nucleus, bind DNA, and activate reporter genes. The C-terminus of human STAT2 was shown to encode a transactivator domain [8] for interferon-stimulated gene factor 3 (ISGF-3), a critical component mediating the biological response to Type I IFNs [224, 226]. While the human and murine STAT2 C-termini bound a similar pattern of proteins as determined by protein pull-down and gel electrophoresis, they display distinct binding preferences. Proteins with molecular weights of ~250 and ~52 kilodaltons (kDa) preferentially bound human STAT2 C-terminus while proteins of ~60, ~30, and ~22kDa preferentially bound the murine STAT2 C-terminus [224]. Differences in STAT2 between mice and humans were shown to mediate the ability of the primate-tropic paramyxovirus simian virus 5 to productively infect mouse cells. The simian virus 5 V protein was only able to induce degradation of murine STAT1 in the presence of

human STAT2 to efficiently suppress IFN signaling [225]. Similarly, the interferon antagonistic ability of EBOV VP24 has been suggested to be a major determinant in resistance of mice to the *Zaire ebolavirus* through an unknown mechanism. However, inability to block the murine STAT2 nuclear translocation could be a factor as EBOV VP24 functions in humans to prevent activated STAT nuclear translocation [214, 227, 228]. In another example, lower susceptibility of mice to influenza B virus can be partly attributed to the fact that influenza NS1B cannot bind and antagonize ISG15 and ISG15 mediated effects in mice as it can in humans. The region responsible in ISG15 for binding of influenza NS1B is highly conserved among primates but divergent in other mammalian species such as mouse and dog [161]. As described above, viruses target the antiviral pathway in many ways to become successful pathogens, and the importance of the interferon system is highlighted further by host range specificity that can incur from differences in just one viral or host protein. The highly pathogenic bat-derived viruses may be able to more efficiently antagonize the human interferon response due to one or more host proteins that are divergent enough between the human and bat interferon response.

1.9. Aims and hypothesis

Pteropid bats are the reservoir hosts of Nipah virus, Ebola virus, and SL-CoV. These viruses are considerably more pathogenic in humans than they are in bats. This raises the question of whether viral factors, host factors, or a combination of the two are responsible for the difference in pathogenicity between species. We hypothesize that for SARS-CoV, EBOV, and NiV the interferon system of the host is largely responsible for the differences in

pathogenicity between bats and humans. In support of this, as described in section 1.3., both the EBOV [81, 84] and NiV [106, 107, 127, 128] strains sequenced from bats are highly homologous to those infecting humans. In addition, both EBOV [76] and NiV [129] have cellular receptors that are highly conserved between bats and humans suggesting receptor differences are not involved in virulence differences between bats and humans. The inability of SL-CoVs to infect humans and SARS-CoV to infect bats is largely due to differences in the SARS-CoV S protein as insertion of a minimal region into the SL-CoV S backbone was able to convert the SL-CoV S to bind human ACE2 [68]. While pathogenicity experiments in humans or palm civets have not been performed with this ACE2 binding SL-CoV chimera, experimental infection in bats with SL-CoV is asymptomatic [65], like Nipah [108] and Ebola [78] infection. In addition, the genes responsible for interferon antagonism in SL-CoV appear to be highly homologous at the amino acid level to SARS-CoV [59] and may not account for differences in infection beyond receptor binding, suggesting that a ACE2 binding SL-CoV conceivably could infect humans with similar pathogenicity to SARS-CoV. The evidence above for the homology of SARS-CoVs, EBOVs, and NiVs that infect humans and bats strongly suggests that host factors are responsible for the differences in pathology between the species.

In some cases, the host range of a virus has been shown to depend on the ability to antagonize the new host's immune system. Because bats have a high level of resistance to some viral infections that are lethal in humans (NiV, SARS, EBOV), we predicted that bats might have superior anti-viral responses to those viruses. One of the major components of

the antiviral response conserved in all vertebrates is the type I IFN system. We hypothesize that the megachiropteran bat interferon system is qualitatively and quantitatively more effective in controlling these highly pathogenic zoonotic viruses than the human interferon system and these viruses have consequently coevolved a highly effective antagonistic means to control the bat interferon system thus maintaining viral infection and transmission.

As described above, different animals genetically encode different arrays of interferon subtypes. We predicted that the bat might have a larger number of IFN genes relative to humans, or that the subtype distribution might be different. To address these hypotheses we established the following four goals for this project: (1) identify the type I interferons from *Pteropus vampyrus*; (2) quantitatively measure the response of *P. vampyrus* cells to viral stimulation; (3) clone and purify recombinant *P. vampyrus* IFNs; and (4) develop a bioassay to measure antiviral activity of *P. vampyrus* recombinant IFNs.

1.10. Experimental Approach

We began by using a statistical gene assembler to infer possible interferon gene sequences from the *P. vampyrus* genome traces to identify the type I interferons encoded by the *Pteropus vampyrus* genome. The validity of the inferred sequences was then confirmed by direct cloning and sequencing from *P. vampyrus* genomic DNA. To address the second goal, we treated peripheral blood mononuclear cells (PBMCs) with interferon inducing stimuli and used transcriptome deep sequencing to measure expression of both IFNs and of IFN-responsive genes.

The third goal of the project was to clone the *P. vampyrus* IFN-β gene into an expression vector and purify IFN-β recombinant protein. Interferon-β is considered a major initiator and component of the interferon induced antiviral pathway [150, 153]. Like other type I IFNs, IFN-β is expressed by a single exon gene with no post-transcriptional modification. In addition, most animals express only one IFN-β gene [159]. These factors made IFN-β an ideal first candidate for recombinant protein production and purification. The IFN-β protein is only one of a few type I IFNs that are glycosylated, and this glycosylation has been shown to affect the stability and solubility of IFN-β [176, 229-232]. Both the glycosylated and non-glycosylated forms of human IFN-β have been approved for human use and differences in biological activity have been attributed to the stabilizing effect of the glycosylation [230].

Interferon-β has been purified with many systems [168, 231-237] and we carefully considered the pros and cons before choosing a system to produce the *P. vampyrus* IFN-β. The baculovirus system was chosen for production of a glycosylated IFN-β and an *Escherichia coli* (*E. coli)* system was chosen for production of a non-glycosylated IFN-β. Both of these systems were chosen for the ease of cloning, because no endogenous interferon was produced by the host cells, and these systems were low-cost and easily scalable.

The fourth goal of the project was the development of a bioassay to test the antiviral action of the *P. vampyrus* IFNs. The *P. vampyrus* IFN-β gene was cloned into a mammalian expression vector and then was stably transfected into baby hamster kidney (BHK) cells that do not produce endogenous interferon. Supernatants from the IFN-β expressing BHKs were

used to treat an IFN responsive immortalized lung cell line from *Pteropus alecto*, a bat closely related to *Pteropus vampyrus*. Protection of the lung cells conferred by IFN-β from infection by vesicular stomatitis virus (VSV) expressing GFP was measured by GFP expression, cytopathic effect, and viral progeny levels released into the supernatant.

2. MATERIALS AND METHODS

2.1. Ethics Statement

All animals were handled in strict accordance with good animal practice as defined by the relevant national and/or local animal welfare bodies, and all animal work was covered by an Institutional Animal Care and Use Committee (IACUC) protocol from the Lubee Bat Conservancy (USDA Research Facility #58-R-0131).

2.2. Animals and sample collection

Subjects for this study included 10 male Large Flying Foxes (*Pteropus vampyrus*). Some of the animals were wild caught, and some were laboratory born; all were reproductively mature, ranging in age from 4 to 21 yrs. Animals were housed in captivity at the Lubee Bat Conservancy in Gainesville, Florida, USA. Animals were housed together with conspecifics in an indoor/outdoor circular flight enclosure and were fed a mixture of fruit, vegetables, commercial primate chow, and a vitamin supplement. Water was provided *ad libitum*. The bats were captured manually, anesthesia was mask-induced with 5% isoflurane in oxygen (3 L/min), and the bats were maintained with 2.5% isoflurane. Blood was collected from the left and right brachial veins using 3-ml syringes and 25-gauge needles. Blood samples were transferred to Ethylenediaminetetraacetic acid (EDTA) containing vacutainer collection tubes, maintained and shipped at room temperature (RT) (22°C) via overnight courier.

2.3. Human sample collection

Blood was drawn from visually asymptomatic human volunteers and collected into EDTA containing vacutainer tubes (BD, Franklin Lakes, NJ). To simulate shipping conditions of bat blood samples, human blood samples were rocked gently overnight on nutator at room temperature (22°C).

2.4. Cloning and Sequencing of Pteropus Vampyrus Interferon Genes

Genomic DNA was prepared from whole unfractionated peripheral blood from *Pteropus vampyrus* bats. Using primers (Table 1) derived from the inferred interferon gene sequences [187], short (~200 basepair (bp)) internal sections of the interferon genes were amplified from the genomic DNA as proof of concept. The PCR program consisted of an initialization step at 94°C for 5 minutes, then 30 cycles of amplification consisting of denaturation at 94°C for 1 minute, annealing at 55°C for 30 seconds, and elongation at 72° for 1 minute. Amplification was followed by a final elongation step at 72°C for 5 minutes and samples were held at 4°C. PCR was performed on a Px2 Thermal Cycler from ThermoElectron Corporation (Waltham, MA). PCR products were gel extracted using Qiaex II gel extraction kit (Qiagen, Valencia, CA) as per manufacturer's protocol. DNA sequencing was performed by the Duke University DNA Analysis Facility, a shared resource of the Duke Cancer Institute (Durham, NC).

Using primers derived from the inferred interferon gene sequences (Table 1), full-length genes were PCR amplified from the genomic DNA. The forward and reverse primers

Table 1. Primer sequences. Primer sequences used for *Pteropus vampyrus*. All primer sequences read 5' to 3'. Primers were purchased from Invitrogen (Carlsbad, CA).

Species: *Pteropus vampyrus*	
Internal Short Section Primers	Primer sequence (5'→3')
IFN-α forward	cctgggacaaatgaggagaa
IFN-α reverse	tctgcctagcagggtctcat
IFN-β forward	ctccctgcggagattaaaca
IFN-β reverse	catgctttcccaggtgaagt
IFN-δ forward	cagctccatcctgatttgct
IFN-δ reverse	gcgttcaacaggctgaagat
IFN-κ forward	cctacaggccttcgacatct
IFN-κ reverse	gtcagctgggagaccatagc
Full Length Primers	
NheI IFN-α forward	gactcatttcagctagcatggccctgccctgttccttt
XhoI IFN-α reverse	cgatgcagtctcgagttaatccttactctttgatt
NheI IFN-β forward	gactcatttcagctagcatgaccaacaggtgcatcct
XhoI IFN-β reverse	cgatgcagtctcgagtcagttttggaggtattctg
NheI IFN-δ forward	gactcatttcagctagcatggcccagtgcagttcgtg
XhoI IFN-δ reverse	cgatgcagtctcgagtcacatgagaaaaaggcgcgctgtg
NheI IFN-κ forward	gactcatttcagctagcatgagca ccaagcctcatat
XhoI IFN-κ reverse	cgatgcagtctcgagttatttttttcctgagtagtgctgtg
NheI IFN-ω1 forward	gactcatttcagctagcatggcccccctttctctctct
XhoI IFN-ω1 reverse	cgatgcagtctcgagtcgaggtgagtccatgcctc
NheI IFN-ω2 forward	gactcatttcagctagcatggcccccctgctccctct
XhoI IFN-ω2 reverse	cgatgcagtctcgagtcaaggtgactccatgtctc
NheI IFN-ω3 forward	gactcatttcagctagcatggcccccctgctctctct
XhoI IFN-ω3 reverse	cgatgcagtctcgagtcaaagagaccccaggtctc
NheI IFN-ω4 forward	gactcatttcagctagcatggcctccctgctccctct
XhoI IFN-ω4 reverse	cgatgcagtctcgagtcaaggagaccgcaggtctc
NheI IFN-ω5 forward	gactcatttcagctagcatggcccccctgttctctct
HindIII 6xHT rEK IFN-β forward	atcccaagcttatgaagcatcaccatcaccatcacgatgacgacgacaagatgaccaacaggtgcatcct
HindIII 6xHT rEK IFN-βΔsig forward	atcccaagcttatgaagcatcaccatcaccatcacgatgacgacgacaagatgagctacaactggcttcg
BamHI rEK IFN-βΔsig forward	gactcatttcaggatccgatgacgacgacaagatgagctacaactggcttcg

encoded restriction sites for NheI and XhoI respectively, which allowed cloning of the full length gene into mammalian expression vector pcDNA3.1(+). After purification, the inserted genes were sequenced using vector primers downstream and upstream of the insert site. Sequences of clones were aligned to form consensus sequences. *Pteropus vampyrus* IFN-β, IFN-κ, IFN-δ, and IFN-α sequences have been submitted to Genbank (GU126493, HM63650, HM636501, and HM636502).

From pcDNA3.1(+) IFN-β clone, IFN-β consensus sequence with or without the sequence encoding the signal peptide (IFN-βΔsig) was PCR amplified and cloned into baculovirus transfer vector pBAC-1 (Novagen, Gibbstown, NJ) with forward primer encoding HindIII restriction site, N-terminal 6x-Histine tag and recombinant enterokinase protease recognition site; and reverse primer encoding XhoI restriction site (Table 1). Proper expression from purified clonal plasmid expression was confirmed by DNA sequencing as above.

pGEX-4T-3 *E. coli* expression plasmid (GE Healthcare, Piscataway, NJ) was kindly provided by Scott Soderling (Duke University, Durham, NC). From pcDNA3.1(+) IFN-β clone, IFN-βΔsig was PCR amplified with forward primer encoding BamHI restriction site and N-terminal recombinant enterokinase (rEK) site, and reverse primer encoding XhoI restriction site (Table 1). PCR product was cloned into pGEX-4T-3 to generate glutathione S-transferase (GST) N-terminal fusion protein. Purified plasmid was confirmed by DNA sequencing as above.

2.5. Cell culture and transfections

All mammalian cell lines were grown at 37°C and 5% CO_2. Baby hamster kidney (BHK-21) cells were cultured in Dulbecco's modified eagle medium (DMEM) supplemented with 5% heat inactivated fetal bovine serum (HI-FBS), penicillin, and streptomycin. Transfections were performed using Effectene transfection reagent (Qiagen, Valencia, CA) as per the manufacturer's protocol. Stable clones were selected and cultured in media supplemented with 0.5mg/mL G418 (SigmaAldrich, St. Louis, MO).

P. alecto lung clonal cells (PaLuSD8) immortalized by simian virus 40 (SV40) small and large T antigen were generated by Crameri *et al.* [238] and were generously given by Michelle Baker (Commonwealth Scientific and Industrial Research Organisation (CSIRO) Livestock Industries, Geelong, Australia). PaLuSD8 cells were cultured in DMEM:Nutrient Mixture F-12 (DMEM/F-12) supplemented with 10% HI-FBS, penicillin, streptomycin, and amphotericin B.

Spodoptera fugiperda insect cells (SF9), spinner flasks, and culture incubator were generously provided by Greg Sempowski (Duke Human Vaccine Institute (DHVI), Durham, NC). Spinner suspension cultures of SF9 cells were cultured and passaged in HyClone SFX-Insect cell culture medium (ThermoFisher Scientific, Waltham, MA) in 28°C incubator and spun at 80 RPM.

2.6. Recombinant baculovirus generation and recombinant 6x-histidine tag (6xHT) IFN-β protein purification

Transfection of SF9 cells and baculovirus growth in SF9 cells was performed in BacVector Insect cell medium (Novagen, Gibbstown, NJ). Prior to transfection and baculovirus growth, SF9 cells were passaged once in BacVector Insect cell medium to adapt cells to the new medium. Recombinant baculoviruses were generated using BacMagic DNA kit (Novagen, Gibbstown, NJ) and amplified as per the manufacturer's protocol. Virus stocks were stored at -80°C.

For protein expression and purification, a 100mL spinner culture of $2x10^6$ cells/mL in log phase growth was infected at a multiplicity of infection (MOI) of one pfu/cell. After 72 hours or when all cells appear infected under a phase-contrast inverted microscope, cells were pelleted by centrifugation at 1000xg for 10 minutes. The cell pellet was lysed in 1mL/10^7 cells of insect cell lysis buffer (10mM Tris-Cl pH7.5, 130mM NaCl, 1% Triton X-100, 10mM NaF, 10mM sodium phosphate pH7.5, 10mM sodium pyrophosphate, Complete Mini EDTA-free protease inhibitor cocktail (Roche, Indianapolis, IN)) at 4°C for 45 minutes. Lysate were clarified by centrifugation at 40,000xg for 30' at 4°C. Protein was purified with HisPur Purification kit (Pierce, Rockford, IL) following manufacturer's protocol. Eluates were stored at 4°C.

2.7. E. coli expression of GST tagged IFN-βΔsig and protein purification

E. coli BL21 cells were a kind gift from Scott Soderling (Duke University, Durham, NC) and chemically competent stocks were prepared in lab. pGEX-4T-3 EK IFN-βΔsig was transformed into *E. coli* BL21 and clones selected by ampicillin resistance and expression as confirmed by Western blot of cell lysates. Glycerol stocks of individual clones were stored at -80°C.

For large-scale protein production, a 20mL starter culture of LB with ampicillin was inoculated and cultured overnight in 30°C shaking incubator. The next morning 1L of LB with ampicillin was inoculated with 10mL of the overnight culture and incubated shaking at 30°C. When the culture reached an OD600 of 0.4-0.6, IPTG was added to a final concentration of 0.1mM. Culture was incubated at 15°C with shaking overnight. The next day, bacteria were pelleted by centrifugation. If needed, pellets were stored at -80°C.

Alternatively, 1L of LB with ampicillin was inoculated, incubated shaking at 30°C, and IPTG was added as above. Culture was incubated shaking at 30°C for 4 hours. Bacteria were pelleted by centrifugation.

Bacterial pellets were lysed in 50mL lysis/sonication buffer pH7.5 (50mM Tris pH7.5, 100mM NaCl, 1mM EDTA pH8.0, 1mM ethylene glycol tetraacetic acid (EGTA) pH8.0, 2% NP-40) with freshly added 200ug/mL lysozyme, 3mM DTT, 1mM AEBSF, 2ug/mL Leupeptin, and 2ug/mL Pepstatin. Lysates were nutated 30 minutes at 4°C followed by three rounds of sonication for one minute with icing in between sonication. Lysates were clarified by centrifugation at 38,000xg for 30 minutes at 4°C. Glutathione Sepharose 4B

beads (GE Healthcare, Piscataway, NJ) were loaded onto a disposable column (Bio-Rad, Hercules, CA) and buffer was allowed to run through. Beads were washed with several volumes of lysis/sonication buffer with lysozyme, DTT, and protease inhibitors to equilibrate the column. Cleared lysate was loaded onto the column, and the top and bottom of the column was capped. Column was rotated for 1 to 16 hours to allow the tagged protein to bind. After the incubation, lysates were drained from the column and washed with several volumes of lysis/sonication buffer with lysozyme, DTT, and protease inhibitors followed by one wash with wash buffer A pH7.5 (50mM Tris pH7.5, 100mM NaCl, 1mM EDTA pH8.0, 1mM EGTA pH8.0) with freshly added DTT, AEBSF, Leupeptin, and Pepstatin as before. Column was washed once with wash buffer B pH7.5 (50mM Tris pH7.5, 100mM NaCl) with freshly added DTT, AEBSF, Leupeptin, and Pepstatin. To remove traces of protease inhibitors that could negatively affect downstream rEK removal of the GST tag, column was washed several times in wash buffer B with freshly added 3mM DTT. Column was capped and one volume of release buffer pH7.5 (50mM Tris pH7.4, 150mM NaCl, with freshly added 3mM DTT and 25mM reduced glutathione) was loaded onto the column. Column was rotated for one hour. After incubation, eluate was fraction or batch collected. A second volume of release buffer was added to the column, allowed to drip through to collect remaining protein, and combined with first eluate. All column steps were performed at 4°C.

2.8. Protein concentration

Proteins were concentrated using an Amicon (Millipore, Billerica, MA) or Spin-X UF (Corning, Lowell, MA) 30,000 molecular weight cut-off (MWCO) spin concentrator following manufacturer's protocol. Flowthrough from the 30,000 MWCO concentrator was applied to an Amicon (Millipore, Billerica, MA) or Spin-X UF (Corning, Lowell, MA) 10,000 MWCO spin concentrator following manufacturer's protocol.

2.9. Removal of GST tag with rEK

Concentrated eluates from glutathione column containing GST tagged IFN-βΔsec were cleaved and rEK removed using Tag•off rEK Cleavage Capture Kit (Novagen, Gibbstown, NJ) as per the manufacturer's protocol. Eluates were concentrated as before.

For in-column digestion, lysate was loaded and the Glutathione Sepharose 4B column was washed twice with several volumes of 1x cleavage/capture buffer (50mM NaCl, 20mM Tris-HCl, 2mM $CaCl_2$, pH7.4). Tag•off High Activity rEK (Novagen, Gibbstown, NJ) was diluted in 1 column volume of 1x cleavage/capture buffer according to manufacturer's protocol and loaded onto the column. Column was capped and rotated for 6 hours at room temperature to digest. After digestion, eluate was collected. One volume of cleavage/capture buffer was applied to the column, collected, and repeated. rEK was removed from the eluates using Tag•off rEK Cleavage Capture Kit (Novagen, Gibbstown, NJ) as per manufacturer's protocol. rEK-free samples were concentrated with 10,000 MWCO Spin-X UF (Corning, Lowell, MA) concentrator and stored at 4°C.

2.10. SDS-PAGE and Western blot

Sample and eluate protein concentrations were determined with Coomassie (Bradford) Protein Assay kit (Pierce, Rockford, IL) as per manufacturer's protocol prior to SDS-PAGE and Western blot. Total protein separation was stained with Bio-Safe Coomassie (Bio-Rad, Hercules, CA). To detect 6xHisTagged proteins, the following antibodies and detection reagents were tested according to their manufacturer's protocols: rabbit anti-6-His antibody HRP conjugated (A190-114P; Bethyl Laboratories, Montgomery, TX) kindly provided by Frank Mason (Soderling lab, Duke University, Durham, NC), anti-HisG antibody (R940-25; Invitrogen, Carlsbad, CA) kindly provided by Haiyen Chen (Liao Lab, DHVI, Durham, NC), Ni-NTA-HRP conjugate (34530; Qiagen, Valencia, CA), HisProbe-HRP conjugate (15165; Pierce, Rockford, IL), Tetra-His antibody (34670; Qiagen, Valencia, CA), His•Tag monoclonal antibody (70796-4; Novagen, Gibbstown, NJ), mouse anti-histidine tag antibody (MCA1396; AbD Serotec, Raleigh, NC), Penta-His antibody (34660; Qiagen, Valencia, CA), Anti-His_6-Peroxidase (clone His-2) (04905270001; Roche, Indianapolis, IN), Anti-His_6 (clone BMG-His-1) (11922416001; Roche, Indianapolis, IN), and Anti-His_6 (clone His-2) (04905318001; Roche, Indianapolis, IN). GST was detected with Upstate rabbit anti-GST Tag antibody (06-332; Millipore, Billerica, MA). Alkaline phosphatase (AP) conjugated secondary antibodies were purchased from SigmaAldrich (St. Louis, MO) and were developed with Western Blue Stabilized Substrate for Alkaline Phosphatase (Promega, Madison, WI). Blots probed with HRP conjugated antibodies were developed with TMB Stabilized Substrate for HRP (Promega, Madison, WI).

2.11. Protein sequencing

Using practices to reduce keratin contamination, GST IFN-β was purified and digested with rEK as described, and proteins were separated with SDS-PAGE and Coomassie stained. Bands corresponding to the sizes of GST IFN-β, GST alone, and potentially cleaved IFN-β product were cut out with glass coverslips. Samples were submitted to the Duke Proteomics Core Facility, a shared resource of the Duke Institute for Genome Sciences and Policy (Durham, NC), for protein analysis by trypsin digest followed by liquid chromatography and tandem mass spectrometry (LC-MS/MS). In brief, to achieve an amino acid sequence, the first round of MS is used to identify the dominant peptide species. These peptides are then selected for in a quadrupole electric field. One at a time these peptides are collided with argon gas and broken up into smaller peptides and amino acids. These are further analyzed with time of flight MS to determine the amino acid sequence of the selected peptides. The identity of a protein is confirmed from the amino acid sequences of multiple peptides.

2.12. PBMC isolation

Whole anticoagulated blood from *P. vampyrus* and humans was diluted in phosphate buffered saline (PBS) pH7.4 and was layered over Lympholyte-M (Cedarlane, Burlington, NC) and Lympholyte-H (Cedarlane, Burlington, NC) respectively and centrifuged 2,000 RPM for 30 minutes at room temperature. Cells were collected from the interface, washed, and counted on a hemacytometer (Hausser Scientific, Horsham, PA).

2.13. Transcriptome deep sequencing

To accumulate enough PBMCs from the same bat, blood was drawn three times with one-week rest between bleeds. Time points and conditions performed on each week are shown in Figure 7, and RNA samples from cells treated under the same conditions were combined. For the human samples, enough PBMCs were isolated from a single draw for all time points, treatments, and independent biological replicate wells (Figure 7). One difference of note was that buffy coats from human PBMC isolation had a large red blood cell (RBC) contamination. RBCs were removed from the human samples with RBC lysis buffer (Sigma, St. Louis, MO) following the manufacturer's protocol.

PBMCs ($20x10^6$ cells/well) were plated on 6 well flat-bottom ultra-low attachment tissue culture plates (3471; Corning, Lowell, MA) in a total volume of 1mL. Cells were treated as indicated with either poly(I:C) (Invivogen, San Diego, CA) or VSV (Ramsburg lab stocks were previously confirmed endotoxin free using Limulus amebocyte lysate (LAL) assay). Stimulants were diluted such that the addition of 1mL stimulant would give a final concentration of 10 μg/mL poly(I:C) or an MOI of 5 for VSV. 1mL of complete medium was added to the unstimulated control wells. Cells were incubated at 37°C and 5% CO_2 for the indicated times, after which cells were harvested into RNA lysis buffer (RNeasy kit; Qiagen, Valencia, CA) according to the manufacturer's instructions.

Purified RNA was prepared from these whole-cell lysates as described in the protocols accompanying the Qiashedder (Qiagen, Valencia, CA), RNeasy Mini kit (Qiagen, Valencia, CA), and DNase-Free DNase Set (Qiagen, Valencia, CA). RNA samples were

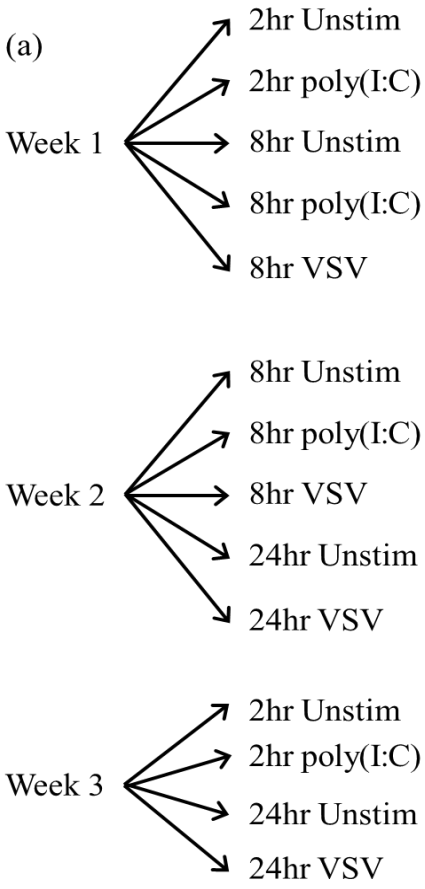

(b)

2hr Unstim	2hr poly(I:C)	
2hr Unstim	2hr poly(I:C)	

8hr Unstim	8hr VSV	8hr poly(I:C)
8hr Unstim	8hr VSV	8hr poly(I:C)

24hr Unstim	24hr VSV	
24hr Unstim	24hr VSV	

Figure 7. Deep sequencing sample and plating layout. (a) Draw and sample strategy to accumulate enough cells from the same bat for deep sequencing. Only seven samples could be submitted for deep sequencing so 2, 8 and 24 hour time points were chosen with Unstimulated (Unstim) and either VSV, poly(I:C), or both for each time point. (b) Plating strategy for the one human draw to replicate the bat sample biological duplicates.

combined and submitted to the David H. Murdock Research Institute (DHMRI, Kannapolis, NC) for Illumina-based transcriptome deep sequencing analysis. Initial analysis of the sequences and generation of the gene expression database was performed by Dr. Tom Kepler (Duke University, Durham, NC). Sequences were compared to the human transcriptome to identify genes and expression levels (methodology manuscript in progress). I analyzed the generated database set to isolate the genes of interest presented in this manuscript.

2.14. Bioassay for detection of P. vampyrus IFNs

To determine the ability of PaLuSD8 cells to respond to interferons, $0.1x10^6$ cells/well were grown on coverslips in 6 well tissue culture plates. Wells were treated with media alone or with 1 unit (U), 10U, 100U, 1000U, or 10,000U of universal Type I IFN (IFNαA/D) (PBL Interferon Source, Piscataway, NJ) in complete media. IFNαA/D is a recombinant human IFN-α hybrid known to have cross-species activity on many mammalian cell lines [178, 239]. Cells were treated for 16 hours. Media was removed and cells infected with $2.5x10^5$ PFU (MOI 3) VSV expressing enhanced GFP protein (VSV EGFP) in complete media to bring inoculum to a total volume of 200μL. Virus was incubated on the cells for 30 minutes in tissue culture (TC) incubator set to 37°C and 5% CO_2 with rocking every 5 minutes to prevent cells from drying out. 2mL of complete media was added to the wells and incubated for up to 48 hours and checked for cytopathic effect (cpe) at 8, 24, and 48 hours.

To determine if poly(I:C) could render PaLuSD8 cells refractive to VSV infection, $0.1x10^6$ cells/well were grown in 6 well tissue culture plate. Poly(I:C) at 0.1μg, 1μg, 10μg,

and 100µg was mixed with 2µL Lipofectamine 2000 (Invitrogen, Carlsbad, CA) in 100µL PBS for five minutes at RT prior to adding to 2mL complete media each. Wells were treated with PBS or the various amounts of poly(I:C) for 4 hours. Media was removed and cells infected with VSV EGFP as before. Wells were checked for cpe at 8, 24, and 48 hours.

To determine the ability of PaLuSD8 cells to produce IFN-like activity and protect naïve cells, $5x10^6$ PaLuSD8 cells in a 10cm TC dish were infected with VSV EGFP (MOI of .25) in 4mL serum free media. After 30 minutes, 5mL of complete media was added to the dish and the virus was incubated on the cells for 8 hours. Supernatant was collected onto a clean TC dish and ultraviolet (UV) inactivated twice with CL-1000 UV Crosslinker (UVP, Upland, CA) set to 500 mJ/cm^2 with one-minute rests in between pulses. 2mL of inactivated supernatants either undiluted or diluted 1:1, 1:10, 1:100 in complete media were incubated on naïve cells in a 6 well plate for 16 hours. Fresh complete media was used as a negative control. Wells were infected with VSV as before and incubated 24 hours and GFP expression was imaged with Nikon Eclipse TE2000-S (Melville, NY). As a control for complete VSV inactivation, 1:1 diluted inactivated supernatant was incubated on an uninfected well and monitored for 48 hours for cpe and GFP expression.

To determine the ability of PaLuSD8 cells to detect our recombinant IFN-β, BHKs stably expressing pcDNA3.1(+) IFN-β or pcDNA3.1(+) Empty were grown to ~80% confluence in 10 cm plates without G418. pcDNA3.1(+) is a mammalian plasmid vector that will highly express an inserted gene, in our case *P. vampyrus* IFN-β, under the human cytomegalovirus immediate early promoter. Supernatants were collected and diluted in

complete media as indicated. PaLuSD8 cells ($0.25x10^6$ cells/well) were grown with and without coverslips in a 6 well plate. Diluted media (2mL/well) of was incubated on the PaLuSD8 plates for 16 hours. IFNαA/D (1000 U) was used as a positive control, and complete media alone was used as a negative control. After treatment, supernatants were removed and cells were infected with VSV EGFP as before except at an MOI of 5 in a total inoculum volume of 0.5mL.

After 4 hours, supernatants were removed from the plates with coverslips and wells washed twice with 1mL PBS. Cells were fixed in the wells in 2mL of 3% paraformaldehyde (PFA) in PBS overnight at 4°C. Nuclei were stained, coverslips mounted, and imaged.

VSV titers were checked on plates without coverslips at 8 and 24 hours. At 8 hours, 1mL of supernatant was collected and stored at 4°C. The removed media was replaced with complete media in the well. At 24 hours, supernatant was collected off the wells and titered along with the 8 hour time point. Due to replacement of half of the media in the well at 8 hours, calculation of total plaque forming units (pfu) at 24 hours was determined using equation $pfu_{24hr}=0.5*pfu_{8hr}+2*titer_{24hr}$.

2.15. VSV titering

BHK cells ($1x10^6$ cells/plate) or PaLuSD8 cells ($0.4x10^6$ cells/well) were distributed into a 6 well plate the evening before titering. VSV EGFP virus stock or collected supernatants were serial diluted tenfold to 10^{-6} in serum free media in glass tubes. Media was removed from the wells and 200μL of dilutions was applied to the respective duplicate

wells. Plates were incubated for 45 minutes with occasional rocking. Overlay (2mL/well, 1% Methyl Cellulose (Sigma, St. Louis, MO), 1xDMEM (SAFC Biosciences, Lenexa, KS), 5% HI-FBS, 1.5g/L $NaHCO_3$ (Gibco/Invitrogen, Carlsbad, CA)) was added to each well. Plates were incubated with overlay for 48 hours. Overlay was removed by aspiration. Wells were stained and fixed for at least 16 hours in crystal violet stain (PML Microbiologicals, Wilsonville, OR) at room temperature. Plates were washed in tap water, dried, and counted. When indicated, titers are reported as the average ± the standard deviation and significance was determined by Student *t* test (n=3).

2.16. Staining and fluorescent imaging

All steps were performed at RT. PFA was removed from wells and 2mL PBS-Glycine (1xPBS, 10mM Glycine (Sigma, St. Louis, MO)) was incubated on each well for 30 minutes. Wells were washed one more time in PBS-Glycine. Cells were permeabilized with PBS-Glycine with 0.5% Triton X-100 for 5 minutes. Wells were washed twice with PBS-Glycine. Nuclei were stained with 0.5 μg/mL Hoechst 33258 (Invitrogen, Carlsbad, CA) in PBS-Glycine for 5' in the dark. Wells were washed 3x with PBS-Glycine and mounted in antifade and sealed with nail polish. Slides were imaged with Nikon Eclipse TE2000-S (Melville, NY) and NIS-Elements F2.30 software (Nikon, Melville, NY).

3. RESULTS

3.1. Identification of Pteropus vampyrus interferons

Our central hypothesis was that the interferon system of the bat is largely responsible for the differences in pathogenicity of various viruses between bats and humans. To begin to address that overall hypothesis, we sought to determine the number of Type I IFN genes and/or pseudogenes encoded in the *P. vampyrus* genome. The usual approach to that type of question is to use the sequences of the gene(s) of interest from a closely related species to "fish out" the novel sequences in the genome to be interrogated. Although genome sequencing of *P. vampyrus* is underway at Baylor College of Medicine [240], the genome is incomplete and slated for completion with 2x coverage [187, 240]. Because the complete genome was not available when we began this work, we created a statistical gene-family assembler used it to infer possible Type I IFN gene sequences from the *P. vampyrus* genome traces [187]. The genome assembler was created by Dr. Tom Kepler, with whom we have collaborated on this project. Detailed description of the assembler has been published [187], but in brief, we used human IFN sequences to "fish" the *P. vampyrus* trace archives for *P. vampyrus* IFN sequences. The assembler predicted one IFN-β sequence, seven IFN-α sequences, one IFN-κ sequence, five IFN-δ sequences, and 18 IFN-ω sequences (Table 2). Once the sequences had been inferred, we experimentally confirmed the presence of the predicted genes within the genome by performing PCR on genomic DNA isolated from individual *P. vampyrus* bats. We used genomic DNA as the template due to the ease of purification and because the Type I IFNs are single exon genes without transcriptional

Table 2. Verification of inferred sequences by cloning and DNA sequencing. Using primers described in the Methods, IFN subtypes were cloned into plasmid vector pcDNA3.1(+) and the inserted genes of individual clones were sequenced with vector based primers. IFN-β consensus was confirmed from two individual bats while other subtypes have only been sequenced from one animal thus far. Number of genes identified was determined from distinct genes that could be identified from multiple clones. The greater than sign indicates that more possible genes were suggested by the sequencing however sequencing of more clones is needed to differentiate distinct genes from sequencing error. *n.d.* = not determined. * from Kepler *et al.* [187].

Interferon Subtype	# sequences inferred*	# clones sequenced	# genes identified
IFN-α	7	52	>4
IFN-β	1	19	1
IFN-δ	5	32	>3
IFN-κ	1	7	2
IFN-ω	18	0	*n.d.*

modification [159]. Because the IFNs are single exon genes, it is likely that the sequence of the genes encoded in the genome will match the mRNA sequences that encode the protein amino acid sequence. In addition, IFNs are not constitutively expressed, and therefore require stimulation for mRNA expression and complementary DNA (cDNA) construction. As described in Section 1.5., some interferon subtypes are only produced by specific cell types and sequencing from mRNA would only provide the IFN subtypes specific to the cells examined. Therefore because cells isolated from the blood were the only cells available to us, we used genomic DNA as our PCR template to determine the sequence of all pteropid IFN genes.

The validity of the inferred sequences was first confirmed by PCR amplifying an internal segment of an IFN gene from *P. vampyrus* genomic DNA (gDNA) with primers designed from the inferred sequences (Figure 8, lanes 4 and 5). The validity of the full-length inferred sequences was then confirmed by PCR amplification from *P. vampyrus* gDNA (Figure 8, lanes 2 and 3) and direct cloning into a plasmid vector. Inferred primers were also able to specifically PCR amplify IFN-α, IFN-δ, IFN-κ, and IFN-ω at their predicted sizes (results not shown). Multiple clones of IFN-α, IFN-β, IFN-δ, and IFN-κ were purified, sequenced, and aligned to identify individual genes and to form consensus sequences of individual *P. vampyrus* IFN genes and sequencing of IFN- ω is still ongoing (Table 2). For determination of a gene versus sequencing error, I defined an independent gene as having met the following conditions: (a) a full length sequence should contain a stop codon to produce a protein in length similar to the anticipated length, (b) any full length

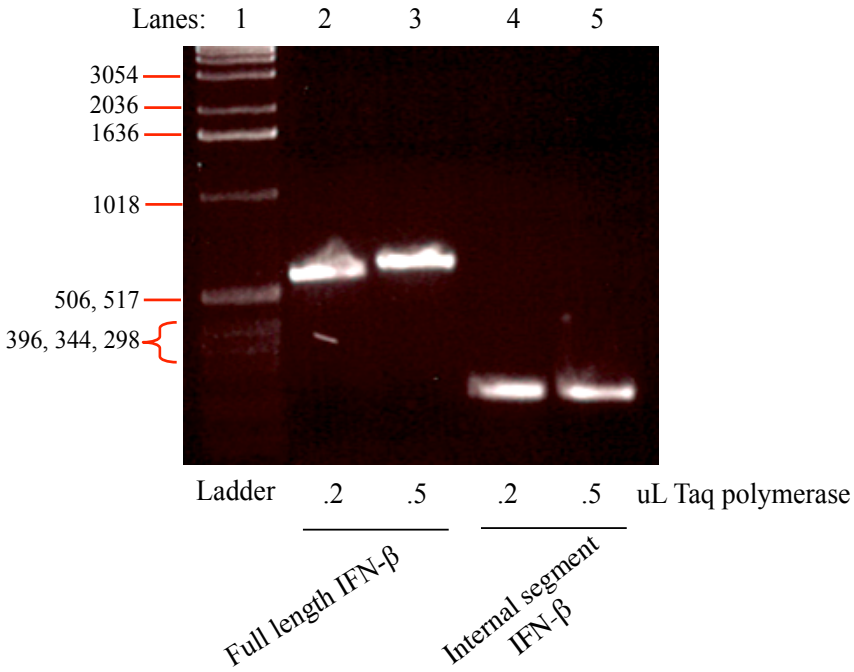

Figure 8. PCR primers derived from inferred IFN gene sequences amplify internal segment and full length IFNs from *P. vampyrus* genomic DNA. Using the indicated amounts of Taq polymerase, an internal segment of *P. vampyrus* IFN-β was PCR amplified at the predicted size of 228 bp (lanes 4 and 5). Full length IFN-β was PCR amplified at the predicted size of 558 bp.

inferred sequence or any individual base deviations from the inferred sequence or combination of base deviations had to be identified in at least five clones from at least two independent PCR amplifications, and (c) fell within statistical reasoning of Dr. Kepler's gene assembler [187].

Our efforts to clone the remainder of the predicted *P. vampyrus* IFN sequences are ongoing, but in the meantime we have proceeded with detailed analysis of the expression kinetics of *P. vampyrus* IFN-β. Interferon-β is considered a major initiator and component of the interferon induced antiviral pathway [150, 153]. For this reason and because we identified only one IFN-β gene, IFN-β was chosen as an ideal candidate for recombinant protein production and purification.

3.2. Quantitatively measure the response of P. vampyrus cells to viral stimulation

The second goal of this project was to quantitatively measure the response of *P. vampyrus* cells to viral infection. We hypothesized that expression of both IFNs and IFN-responsive genes is quantitatively different and is largely responsible for the differences in pathogenicity of various viruses between bats and humans. Because there are no available antibodies or other protein based assays to measure the bat interferon response, we could only utilize DNA and RNA based assays. To test our hypothesis, we treated purified *P. vampyrus* and human PBMCs with poly(I:C) or infected them with VSV and then harvested the cells for cellular RNA purification at 2 hours, 8 hours, or 24 hours (Figure 7).

To determine the mRNA expression profile, RNA samples were submitted to the DHMRI for transcriptome deep sequencing. Transcriptome deep sequencing or Illumina-based RNA-Seq is a powerful short-read high-throughput sequencing method that can provide the entire transcriptome profile without species, primer, or probe [241-243]. This assay returned millions of ~70 nucleotide long sequence reads. As no bat transcriptome is available, Dr. Kepler wrote a program to align the reads to the human transcriptome to identify individual genes and to quantify mRNA levels (manuscript in preparation). At this time, only the unstimulated and VSV-infected sample sequences at 8 and 24 hours have been analyzed. Over 17,000 genes were identified in the human samples and ~3,000 genes have been initially identified in the bat samples.

3.2.1. Method of analysis

Illumina sequencing generates sequence reads of ~70 nucleotides, which are then "mapped" to the relevant genome. This mapping generates a number of counts for each mRNA transcript. For example, if the transcript for β-actin has a count number of 500, that means that 500 of the RNA fragments in the sample pool mapped to somewhere within the β-actin gene. This does not mean that there were 500 whole copies of the β-actin gene present in the sample, nor can the number of counts be directly extrapolated to give a number of transcripts per cell.

Our first step, in analyzing the raw sequence data was to determine the number of counts for each transcript, and from that, to determine a fold-difference in the number of

counts between the uninfected and infected sample. For some transcripts, the count number was zero at one or more of the time points but was above zero at another time point. This created a mathematical problem, in which if we divided by zero, we would create infinity fold differences. Therefore, we added "one" to each count total for a gene transcript prior to calculating the $\log_2$ fold differences between the VSV-infected and unstimulated samples.

Dr. Kepler populated the bat and human datasets for each RNA sample sequenced. These datasets contained the gene mRNAs identified along with counts and $\log_2$ fold differences for each gene. I used Microsoft Excel PivotTables to align the >17,000 genes identified in each human dataset and the ~3,000 genes identified in each bat datasets for each time point. Genes were then sorted according to their name and RefSeq accession number, and separated into three groups based on their presence or absence in the two species at the different time points. The three groups were: 1) present in both bat and human dataset, 2) present only in the bat, and 3) present only in the human.

To first identify genes that were upregulated or downregulated significantly at either time point, I narrowed the list to include only genes having > 1 or < -1 $\log_2$ fold differences. Those $\log_2$ differences correspond to differences of at least two-fold between VSV-infected and unstimulated samples of the same species [244, 245]. Because the counts do not directly correspond to numbers of mRNA transcripts, but rather to overall mRNA levels that can be correlated to fold upregulation or downregulation, I reasoned that a two-fold difference might still be biologically significant. In addition, I did not want to exclude any IFNs from my initial analysis because IFN-β mRNA levels in a microchiropteran cell line peak at four hours

after poly(I:C) stimulation and are waning at eight hours while IFN-α mRNA levels were increasing from four to eight hours [186].

The filtered dataset contained approximately 2,600 genes matched in both the bat and human for each time point. The datasets were further grouped by whether the $\log_2$ fold difference between the human and bat was > 1 or < -1 at both 8 and 24 hours or unique to a time point. Our initial dataset to identify IFN related genes contained approximately 700 genes and was populated by the following conditions: 1) genes had to be present in both the human and the bat, 2) $\log_2$ fold difference between VSV-infected and unstimulated cells was > 1 or < -1, and 3) these differences were observed at both 8 and 24 hours. When we applied these stringent criteria, we did not identify many IFN-related genes, and therefore we expanded our search to include: 1) genes identified in the only the bat or human transcript read datasets at each time point, and 2) genes whose differences were observed at either 8 or 24 hours. After this list was populated to include genes that were only found at one time point with > 1 or < -1 $\log_2$ fold differences, I went back and retrieved values for the other time point. In addition, we included several highly expressed "housekeeping" genes [246-248]. Inclusion of these genes was important because we wanted to determine a proper housekeeping gene that does not change, or changes very little, in response to infection that could be used in qRT-PCR normalization to follow the deep sequencing results.

We next had to decide how to account for error inherent in the sequencing process and the transcript read sequence alignment process. Generally transcripts that are represented by a high number of counts (50 or more for example) are considered to be "real",

while transcripts that are represented by a very low number of counts (less than 8) may be artifacts of the sequencing process or the transcript read alignment process. To account for error but to avoid excluding genes that might simply be expressed at low levels, fold differences were compared to the absolute number of counts in a staggered cutoff scheme similar to but slightly more conservative than that described by Woodhouse, *et al.* for a study in which they compared Hepatitis C virus infected versus uninfected human hepatoma Huh-7.5 cells in order to analyze the full transcriptional activity of the hepatocyte upon Hepatitis C virus infection [245].

For genes with an absolute value fold-change of ≥1, I used a cutoff of 50 total counts; for genes with an absolute value fold-change of ≥2, I used a cutoff of ≥25 total counts; and for genes with an absolute value fold-change of ≥4, I used a cutoff of >8 total counts. Total counts equaled the sum of counts for the unstimulated and VSV-infected cells for a time point for each respective species.

The results of our expanded search are shown in Tables 3-5. Table 3 contains RefSeq accession numbers and gene abbreviations. Table 4 contains count numbers and the $\log_2$ fold change between unstimulated and VSV infected sample for each of the genes for each respective species and time point. Because the counts do not actually correspond to numbers of mRNA transcripts, we cannot compare counts from bats to humans directly. We can however compare the relative fold induction between the species for a particular gene. Table 5 contains the relative fold ratio of gene fold induction between human and bats at the respective time points. For example, for chemokine CXCL2, we found a fold difference of

Table 3. Deep sequencing gene reference table. RefSeq accession codes and abbreviations of genes included in Table Deep Seq.

Accession Code	mRNA Gene Name	Gene Abbreviation
NM_021130.3	Homo sapiens peptidylprolyl isomerase A (cyclophilin A)	PPIA
NM_001101.3	Homo sapiens actin, beta	ACTB
NM_002046.3	Homo sapiens glyceraldehyde-3-phosphate dehydrogenase	GAPDH
NM_000977.2	Homo sapiens ribosomal protein L13, transcript variant 1	RPL13
NM_003264.3	Homo sapiens toll-like receptor 2	TLR2
NM_138554.3	Homo sapiens toll-like receptor 4, transcript variant 1	TLR4 var1
NM_014314.3	Homo sapiens DEAD (Asp-Glu-Ala-Asp) box polypeptide 58	RIG-I
NM_022168.2	Homo sapiens interferon induced with helicase C domain 1	MDA5
NM_002177.1	Homo sapiens interferon, omega 1	IFNW1
NM_002176	Homo sapiens interferon, beta 1, fibroblast (IFNB1), mRNA	IFNB
NM_000605.3	Homo sapiens interferon, alpha 2	IFNA2
NM_007315.3	Homo sapiens signal transducer and activator of transcription 1, 91kDa	STAT1
NM_198332.1	Homo sapiens signal transducer and activator of transcription 2, 113kDa	STAT2
NM_005101.3	Homo sapiens ISG15 ubiquitin-like modifier	ISG15
NM_002201.4	Homo sapiens interferon stimulated exonuclease gene 20kDa	ISG20
NM_016816.2	Homo sapiens 2',5'-oligoadenylate synthetase 1, 40/46kDa, transcript variant 1	OAS1 var1
NM_001032409.1	Homo sapiens 2',5'-oligoadenylate synthetase 1, 40/46kDa, transcript variant 3	OAS1 var3
NM_016817.2	Homo sapiens 2'-5'-oligoadenylate synthetase 2, 69/71kDa, transcript variant 1	OAS2 var1
NM_002535.2	Homo sapiens 2'-5'-oligoadenylate synthetase 2, 69/71kDa, transcript variant 2	OAS2 var2
NM_001032731.1	Homo sapiens 2'-5'-oligoadenylate synthetase 2, 69/71kDa, transcript variant 3	OAS2 var3
NM_006187.2	Homo sapiens 2'-5'-oligoadenylate synthetase 3, 100kDa	OAS3
NM_003733.2	Homo sapiens 2'-5'-oligoadenylate synthetase-like, transcript variant 1	OASL var1
NM_001144925.1	Homo sapiens myxovirus (influenza virus) resistance 1, interferon-inducible protein p78 (mouse), transcript variant 1	MX1 var1
NM_001178046.1	Homo sapiens myxovirus (influenza virus) resistance 1, interferon-inducible protein p78 (mouse), transcript variant 3	MX1 var3
NM_002463.1	Homo sapiens myxovirus (influenza virus) resistance 2 (mouse)	MX2
NM_021133.3	Homo sapiens ribonuclease L (2',5'-oligoisoadenylate synthetase-dependent)	RNASEL
NM_002038.3	Homo sapiens interferon, alpha-inducible protein 6, transcript variant 1	IFI6 var1
NM_022873.2	Homo sapiens interferon, alpha-inducible protein 6, transcript variant 3	IFI6 var3
NM_032036.2	Homo sapiens interferon, alpha-inducible protein 27-like 2, mRNA	IFI27L2
NM_006417.4	Homo sapiens interferon-induced protein 44	IFI44
NM_006820.2	Homo sapiens interferon-induced protein 44-like	IFI44L
NM_001548.3	Homo sapiens interferon-induced protein with tetratricopeptide repeats 1, transcript variant 2	IFIT1 var2

Table 3 (Continued)

NM_001010987.2	Homo sapiens interferon-induced protein with tetratricopeptide repeats 1B	IFIT1B
NM_001547.4	Homo sapiens interferon-induced protein with tetratricopeptide repeats 2	IFIT2
NM_001549.4	Homo sapiens interferon-induced protein with tetratricopeptide repeats 3, transcript variant 1	IFIT3 var1
NM_001031683.2	Homo sapiens interferon-induced protein with tetratricopeptide repeats 3, transcript variant 2	IFIT3 var2
NM_012420.2	Homo sapiens interferon-induced protein with tetratricopeptide repeats 5	IFIT5
NM_003641.3	Homo sapiens interferon induced transmembrane protein 1 (9-27)	IFITM1
NM_006435.2	Homo sapiens interferon induced transmembrane protein 2 (1-8D)	IFITM2
NM_021034.2	Homo sapiens interferon induced transmembrane protein 3 (1-8U)	IFITM3
NM_000600.3	Homo sapiens interleukin 6 (interferon, beta 2)	IL6
NM_000572.2	Homo sapiens interleukin 10	IL10
NM_002188.2	Homo sapiens interleukin 13	IL13
NM_002089.3	Homo sapiens chemokine (C-X-C motif) ligand 2	CXCL2
NM_002993.3	Homo sapiens chemokine (C-X-C motif) ligand 6 (granulocyte chemotactic protein 2)	CXCL6

Table 4. Counts and log_2 fold differences of IFNs and IFN-stimulated genes from *P. vampyrus* and human PBMCs in response to VSV infection. Genes identified from deep sequencing. Counts and log_2 fold differences of counts (Log_2 Fold Δ) in VSV infected PBMCs (VSV) as compared to unstimulated PBMCs (UN) are displayed for the *P. vampyrus* bat and human for 8 and 24 hours respectively. Empty cell denotes gene was not detected for that species and/or time point. Values in light gray were did not meet the count number criteria as described in the text.

mRNA gene name	8 hours						24 hours					
	Bat			Human			Bat			Human		
	Counts		Log_2 Fold Δ	Counts		Log_2 Fold Δ	Counts		Log_2 Fold Δ	Counts		Log_2 Fold Δ
	UN	VSV		UN	VSV		UN	VSV		UN	VSV	
Housekeeping genes												
PPIA	116	102	**-0.184**	855	593	**-0.527**	98	71	**-0.459**	378	486	**0.362**
ACTB	23,273	15,489	**-0.587**	10,474	5,464	**-0.939**	15,503	11,472	**-0.434**	7,976	3,629	**-1.136**
GAPDH	690	770	**0.158**	6,790	4,726	**-0.523**	1,254	548	**-1.193**	3,260	1,553	**-1.069**
RPL13	337	309	**-0.125**	4,623	4,139	**-0.160**	274	241	**-0.184**	3,957	3,519	**-0.169**
PRRs												
TLR2	207	210	**0.021**	560	151	**-1.884**	352	435	**0.305**	115	19	**-2.537**
TLR4 var1	23	16	**-0.498**	148	32	**-2.175**	8	23	**1.415**	83	7	**-3.392**
RIG-I	1	8	**2.170**	179	294	**0.713**	6	51	**2.893**	54	518	**3.238**
MDA5	21	38	**0.826**	163	421	**1.364**	19	84	**2.087**	60	573	**3.234**
Interferons												
IFNW1	0	0	**0**	3	1	**1**	0	17	**4.170**	1	1	**0**
IFNB				2	73	**4.625**				0	152	**7.257**
IFNA2	0	1	**1**	0	0	**0**	0	12	**3.700**	0	6	**2.807**
IFNAR signaling												
STAT1	70	110	0.644	1615	1,857	0.201	224	225	**0.006**	502	4,077	3.019
STAT2	20	32	0.652	405	537	0.406	27	74	**1.422**	154	1,102	2.831
IFN stimulated genes												
ISG15	162	571	**1.811**	153	574	**1.901**	187	2,776	**3.885**	34	1,035	**4.888**
ISG20	663	716	**0.111**	134	332	**1.303**	1,182	3,930	**1.733**	66	525	**2.973**
OAS1 var1				21	78	**1.844**				9	123	**3.632**
OAS1 var3	2	30	**3.369**	103	329	**1.666**	18	130	**2.786**	57	672	**3.537**
OAS2 var1	0	0	**0**	34	107	**1.626**	0	11	**3.585**	13	183	**3.716**
OAS2 var2	15	31	**1.954**	374	984	**1.393**	50	519	**3.350**	89	1,689	**4.231**
OAS2 var3				12	26	**1.055**				4	46	**3.233**
OAS3	87	183	**1.064**	237	781	**1.716**	196	968	**2.298**	59	2,697	**5.350**
OASL var1	26	28	**0.103**	261	478	**0.871**	46	153	**1.712**	30	433	**3.807**
MX1 var1	10	43	**2**	18	123	**2.706**	29	172	**2.528**	7	261	**5.033**
MX1 var3	113	376	**1.726**	360	1,470	**2.027**	257	1,619	**2.651**	59	2,697	**5.491**
MX2	111	199	**0.837**	337	657	**0.961**	209	1,048	**2.321**	102	1,118	**3.442**
RNASEL	1	5	**1.585**	55	33	**-0.720**	7	25	**1.700**	44	36	**-.282**
IFI6 var1	0	1	**1**	14	32	**1.138**	0	30	**4.954**	8	122	**3.773**
IFI6 var3	1	1	**0**	90	204	**1.172**	4	94	**4.248**	38	898	**4.527**
IFI27L2	13	16	**0.280**	7	7	**0**	12	46	**1.854**	18	5	**-1.663**
IFI44				220	436	**0.984**				33	1,003	**4.884**
IFI44L				188	435	**1.206**				18	1,806	**6.572**
IFIT1 var2	5	23	**2**	57	339	**2.551**	9	77	**2.963**	4	767	**7.263**
IFIT1B	10	39	**1.863**	2	5	**1**	40	147	**1.852**	2	1	**-0.585**
IFIT2	1	13	**2.807**	371	1,483	**1.996**	34	458	**3.713**	39	1,519	**5.248**
IFIT3 var1	99	214	**1.104**	185	721	**1.957**	273	1,349	**2.301**	19	1,437	**6.168**
IFIT3 var2	4	7	**0.678**	1	3	**1**	5	59	**3.322**	0	5	**2.585**
IFIT5	0	2	**1.585**	89	179	**1**	0	16	**4.088**	27	304	**3.445**

Table 4 (Continued)

IFITM1				448	885	**0.981**				288	2,340	**3.018**
IFITM2	89	169	**0.918**	195	265	**0.441**	183	337	**0.877**	150	442	**1.553**
IFITM3	857	1,004	**0.228**	74	72	**-0.039**	1,458	3,723	**1.352**	15	177	**3.476**
Cytokines and Chemokines												
IL6				1	643	**8.331**				4	62	**3.655**
IL10	16	23	**0.498**	4	48	**3.293**	4	32	**2.723**	1	1	**0**
IL13	1	1	**0**	0	15	**4**	1	20	**3.392**	2	0	**-1.585**
CXCL2	552	1,525	**1.464**	176	2,029	**3.520**	2,251	4,625	**1.039**	96	81	**-0.242**
CXCL6	75	852	**3.489**	2	1	**-0.585**	1,830	1,209	**-0.598**	0	1	**1**

Table 5. IFN and IFN-stimulated gene mRNA induction is quantitatively different between *P. vampyrus* and human PBMCs in response to VSV infection. Relative fold ratio was calculated by taking the fold ratio of the fold ratio of gene induction in response to VSV infection between human and bats at the respective time points. Values in gray were calculated from fold ratios where the count numbers that did not meet count number criteria as described in text and depicted in Table 4.

mRNA gene name	Relative Fold Ratio	
	8 hours	24 hours
Housekeeping genes		
PPIA	-1.269	1.767
ACTB	-1.276	-1.626
GAPDH	-1.603	1.089
RPL13	-1.025	1.011
PRRs		
TLR2	-3.744	-7.164
TLR4 var1	-3.198	-28
RIG-I	-2.746	1.270
MDA5	1.452	2.214
Interferons		
IFNW1	1	-18
IFNA2	-2	-1.857
IFNAR signaling		
STAT1	-1.360	8.075
STAT2	-1.186	2.657
IFN stimulated genes		
ISG15	1.064	2.004
ISG20	2.284	2.363
OAS1 var3	-3.257	1.683
OAS2 var1	3.086	1.095
OAS2 var2	-1.475	1.842
OAS3	1.571	8.293
OASL var1	1.702	4.273
MX1 var1	1.632	5.679
MX1 var3	1.232	7.161
MX2	1.090	2.175
RNASEL	-4.941	-3.953
IFI6 var1	1.100	-2.268
IFI6 var3	2.253	1.213
IFI27L2	-1.214	-11.449
IFIT1 var2	1.466	19.692
IFIT1B	-1.818	-5.415
IFIT2	-1.755	2.898
IFIT3 var1	1.806	14.593
IFIT3 var2	1.250	-1.667
IFIT5	-1.500	-1.561
IFITM2	-1.392	1.597
IFITM3	-1.203	4.359
Cytokines and Chemokines		
IL10	6.942	-6.600
IL13	16	-31.500
CXCL2	4.156	-2.430
CXCL6	-16.836	3.027

4.156 at 8 hours post-infection. That number means that CXCL2 fold induction in human PBMCs when stimulated with VSV relative to unstimulated conditions was 4.156-fold more than the fold induction in bat PBMCs at that time. To better demonstrate the fold ratio when a gene in the human has a fold induction less than the bat, the inverse of the human-to-bat ratio is taken and a negative sign is used to signify this. For example, for the chemokine CXCL2 at 24 hours, instead of displaying 0.412 fold ratio that would be interpreted as "the fold-induction in human PBMCs is 0.412 fold of the fold-induction in bat PBMCs", the table shows -2.430 which means "the fold induction in human PBMCs was 2.430-fold less than the fold induction in bat PBMCs." Mathematically "0.412-fold" and "2.430-fold less" are identical.

Another consideration in interpreting our results is that many genes may not be expressed under unstimulated conditions and then may increase to only a modest number of counts after stimulation. If these genes still fall under our cutoff values and are removed computationally, we have to cautious when we analyze count numbers and what we consider "not real" or "not significant". For example, the bat cells have high CXCL6 counts at 8 and 24 hours after infection; however in the human cells, counts are near zero at all time points (Table 4). These extremely low counts in human samples may be considered "not real" by our cutoff rules (as depicted in grey in Tables 4 and 5), although the relative fold difference between bats and human may still be biologically significant. Instead of excluding these data and subsequent fold calculations, we kept the "below cutoff" values in our table for one species if there was a significant "above cutoff" change in the other species.

In both human and bat cells, we found robust induction of IFN-responsive genes after virus infection. This result was expected and was consistent with other published reports describing induction of IFN and IFN-responsive genes in human cells [162, 249-253]. There were also intriguing differences between the humans and the bat, which we discuss in detail in the Discussion section. Generally, these results provide evidence that IFNs and IFN-stimulated genes are differentially expressed in *P. vampyrus* PBMCs than human PBMCs which supports our overall hypothesis.

3.3. Expression and purification of recombinant P. vampyrus IFN-β

The third goal of the project was to clone the *P. vampyrus* IFN-β gene into an expression vector and purify recombinant IFN-β protein. Our central hypothesis was that the interferon system of the host is largely responsible for the differences in pathogenicity between bats and humans for SARS-CoV, EBOV, and NiV. To help address our central hypothesis, we needed to develop assays and reagents that could be used to further characterize the antiviral response of bats and the interferon modulation by highly pathogenic bat-derived viruses in the bat host. Therefore we decided to purify *P. vampyrus* recombinant IFN-β that could be used as a valuable reagent in the development of bioassays, gene expression profiling, enzyme-linked immunosorbent assays (ELISAs), and antibodies for immunofluorescence (IF) or immunocytochemistry (ICC).

Interferon-β proteins of other species have been purified using many different methodologies [168, 231-237], and therefore we carefully considered which system to use for

producing *P. vampyrus* IFN-β. The IFN-β protein is only one of a few type I IFNs that are glycosylated, and this glycosylation has been shown to affect the stability and solubility of IFN-β [176, 229-232]. The baculovirus system was chosen for production of a glycosylated IFN-β because of the ease of cloning, no endogenous interferon was produced by the host cells, and this system was low-cost and easily scalable.

3.3.1. rBacV expression system

We first used an rBacV expression system to produce a glycosylated form of IFN-β presumably similar to natural IFN-β produced by the bat. Because there are no anti-*P. vampyrus* IFN-β antibodies that could be used for affinity purification of the recombinant protein, and because high performance liquid chromatography (HPLC) and fast protein liquid chromatography (FPLC) purification are relatively expensive, we decided to use an affinity tag-based purification approach. To accomplish this we used primers to encode a N-terminal 6xHT followed by a rEK recognition site onto the 5' end of the IFN-β gene so that the protein could be purified using immobilized metal ion affinity chromatography (IMAC) and the tag removed post-purification. First, a rBacV expressing 6xHT rEK IFN-β was generated (Figure 9, Figure 10a lane 1) and this IFN-β construct contained the N-terminal 21 amino acid signal peptide that is cleaved to secrete mature IFN-β into the supernatant (Figure 11a). To avoid column-binding competition from cleaved and tagged IFN-β signal peptides, a recombinant rBacV expressing 6xHT rEK IFN-β without the signal peptide (6xHT rEK IFN-βΔsig) was generated (Figure 10a lane 2) that would not be cleaved nor secreted

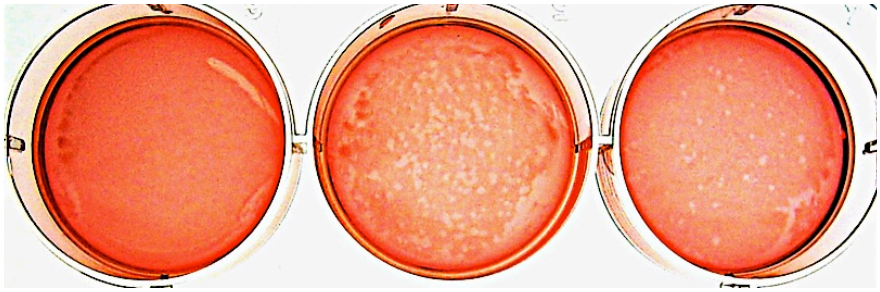

Figure 9. Generation of recombinant baculovirus. Titer plate of rBacV rEK HT IFN-β displays Neutral Red staining of live cells while unstained virus plaques remain visible as clearings in the cell monolayer. The virus plaques on the titer plate are the first definitive proof of successful generation of a rBacV.

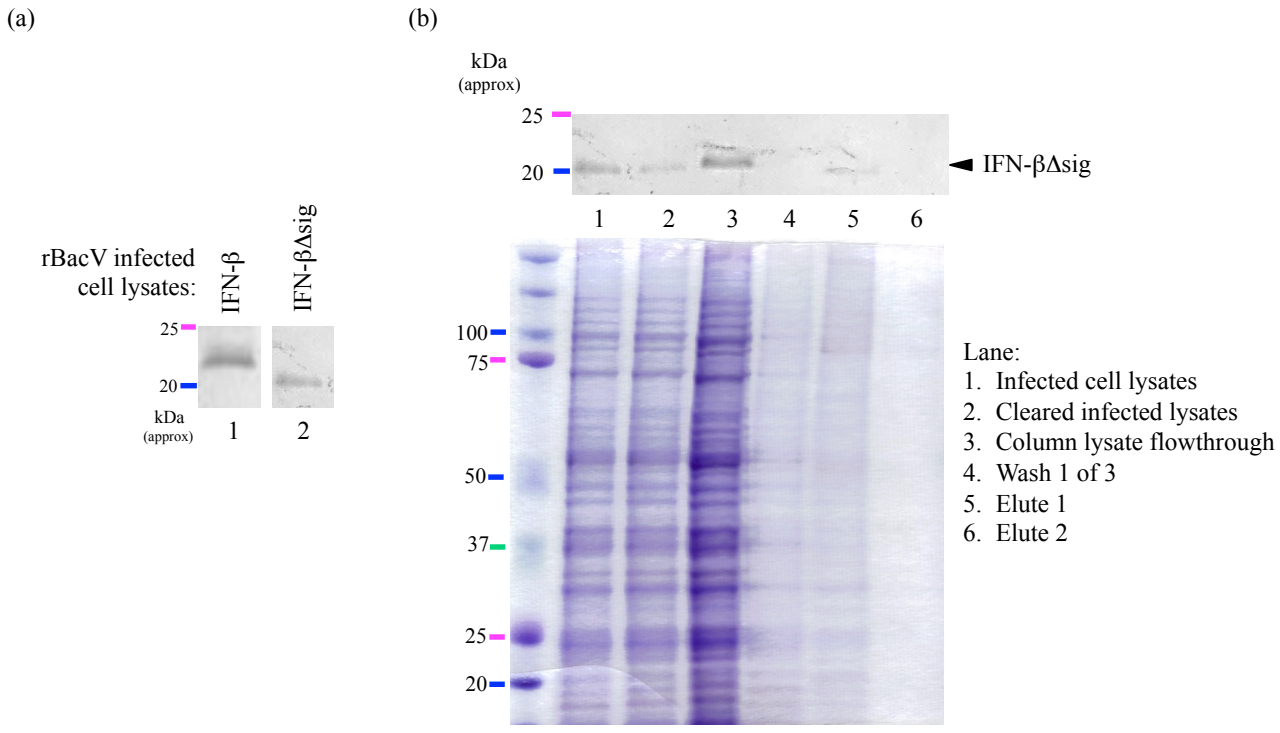

Figure 10. rBacV expression of *P. vampyrus* IFN-β. (a) Western blot of rBacV 6xHT rEK IFN-β (lane 1, 24 kDa) or rBacV 6xHT rEK IFN-βΔsig (lane 2, 21.7 kDa) infected cell lysates probed anti-6xHT antibody. (b) Anti-6xHT Western blot and Coomassie stained SDS-PAGE gel of lysates, wash, and eluates of IMAC purification process. Column was washed three times and wash 3 did not contain any visible protein (results not shown). Purification was extensively troubleshot but 6xHT rEK IFN-βΔsig could not be cleanly eluted.

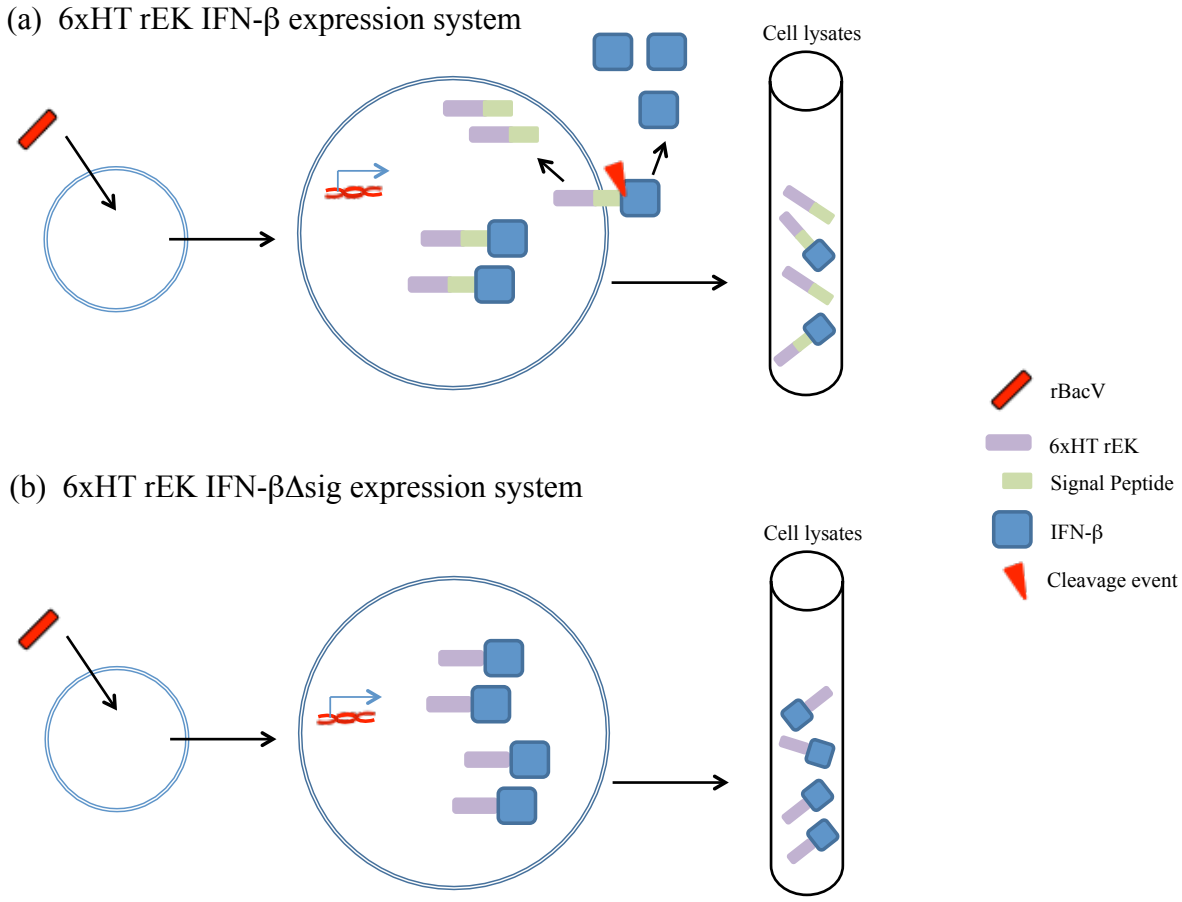

Figure 11. Elimination of the signal sequence improves purification of 6xHT IFN-β purification. (a) rBacV 6xHT rEK IFN-β infected cells would produce 6xHT rEK IFN-β that would be cleaved and IFN-β would be secreted into the supernatant. Cell lysates would contain both 6xHT rEK IFN-β and 6xHT rEK signal peptide and could competitively bind the purification column. (b) rBacV 6xHT rEK IFN-βΔsig infected cells would produce a non-secreted 6xHT rEK IFN-βΔsig that could be purified solely from cell lysates without risk of competition.

(Figure 11b).

After discussion with colleagues experienced in 6xHT purification, we realized that Western blot detection of 6xHT proteins was not as straightforward as purchasing any manufacturer's product but in practice required selection of an optimal anti-6xHT antibody for our specific protein. Eleven antibodies and conjugates in total were tested for their ability to detect our 6xHT rEK IFN-β with the strongest specific signal and lowest nonspecific binding (Figure 12 and results not shown). Based on these results, the AbD Serotec mouse anti-histidine tag antibody (Figure 12b) was chosen for all use in all further studies.

While 6xHT rEK IFN-βΔsig could be identified in the lysates of rBacV infected cells by Western blot (Figure 10b top panel), we were never able to recover pure 6xHT rEK IFN-βΔsig from the IMAC column (Figure 10b lane 5). We attempted to increase recovery via denaturing the protein with 8M urea, adjusting the imidazole concentration in the lysate and washes, using a concentrator to enrich proteins with the appropriate molecular weights, and by adjusting the pH in the lysate and wash buffers (results not shown). Because we could not recover a pure protein, we abandoned the rBacV system and moved to the *E.coli* system to purify the *P. vampyrus* IFN-β.

3.3.2. E. coli expression system

We then decided to produce *P. vampyrus* IFN-β in an *E. coli* expression system because it was easy to use and the *E.coli* system allowed us to progress rapidly from cloning to protein purification. Although *E. coli* produces non-glycosylated proteins, we predicted

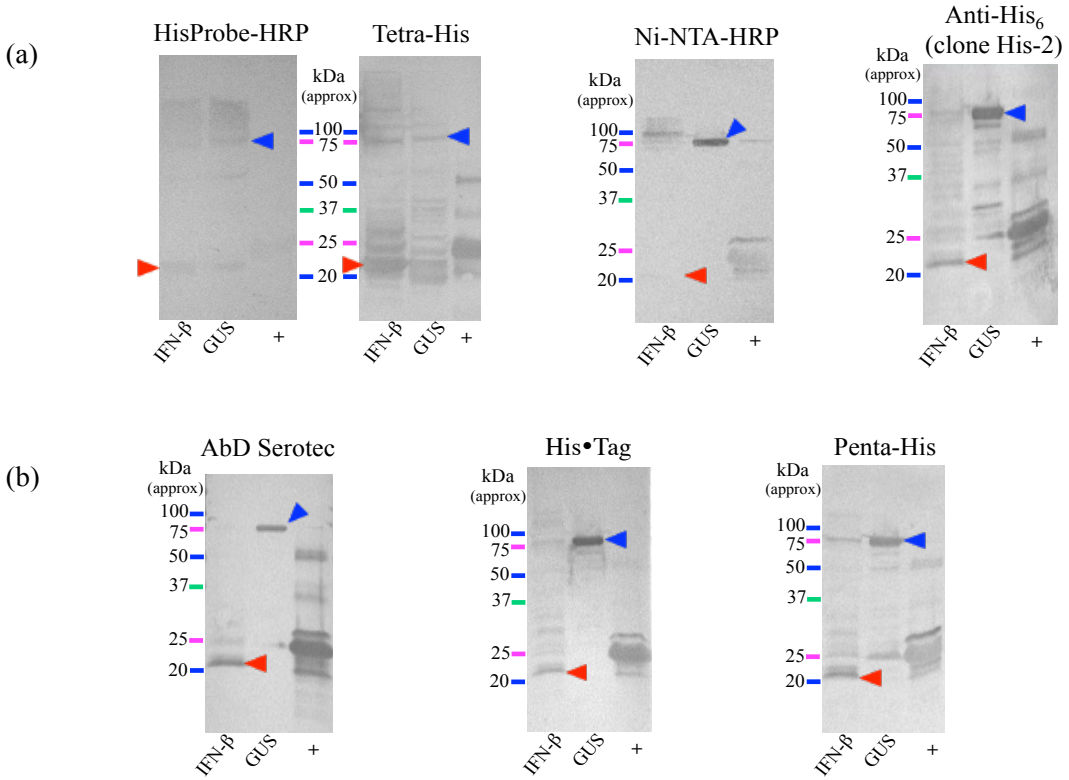

Figure 12. Selection of an optimal anti-HT antibody for detection of IFN-β. SF9 cells were infected with rBacV 6xHT rEK IFN-β (IFN-β lanes) or rBacV 6xHT beta-glucuronidase (GUS lanes). Lysates from infected cells were separated by SDS-PAGE and Western blotted. A 6xHT control protein (+ lanes) was run as a positive control. Eleven different anti-HT antibodies or conjugates were tested as probes for 6xHT IFN-β (24 kDa; red arrowhead) and 6xHT GUS (78kDa, blue arrowhead). Neither IFN-β nor the control protein were detected on blots probed with the anti-HisG antibody, Bethyl anti-6-His-HRP, Anti-His_6 (clone BMG-His-1), nor Anti-His_6-Peroxidase (clone His-2) (results not shown). Panel (a) shows Western blots probed with antibodies that gave a weak specific signal or high nonspecific binding. Panel (b) shows Western blots probed with antibodies that gave the strongest specific signal and lowest nonspecific binding. Based on these results, the AbD Serotec antibody was chosen for all use in all further studies.

that a non-glycosylated IFN-β might still be biologically active. For example, the glycosylated and non-glycosylated forms of recombinant human IFN-β are both biologically active, and the effect of the glycosylation appears to prevent aggregation and increase molecular stability [254].

To express *P. vampyrus* IFN-β in *E. coli* we used primers to encode a N-terminal rEK recognition site at the 5' end of the IFN-βΔsig gene, and then we cloned the construct into the plasmid vector pGEX-4T-3. This vector encodes an N-terminal GST tag so that the expressed protein could be purified using Glutathione Sepharose 4B beads (Figure 13a). To verify proper expression of our GST rEK IFN-βΔsig protein, we submitted the SDS-PAGE gel band of our putative GST rEK IFN-βΔsig to the Duke Proteomics Core Facility for sequencing. The pGEX-4T-3 vector encoded GST gel band was also submitted as a control protein. Proteins were trypsin digested and peptides separated by liquid chromatography prior to tandem mass spectrometry (LC-MS/MS). We chose to use LC-MS/MS rather than matrix-assisted laser desorption/ionization (MALDI) MS because LC-MS/MS gives us the amino acid sequence of the peptides identified by mass to charge ratios. LC-MS/MS identified pGEX-4T-3 vector GST peptides (results not shown) and five peptide amino acid sequences from our GST rEK IFN-βΔsig gel band (Figure 14). These peptide sequences encompass 50% of the IFN-βΔsig amino acid sequence and confirm the identity of the GST rEK IFN-βΔsig protein.

To remove the GST tag prior to immunologic or biologic studies, we digested the purified protein with rEK, leaving the native IFN-β N-terminus. GST rEK IFN-βΔsig

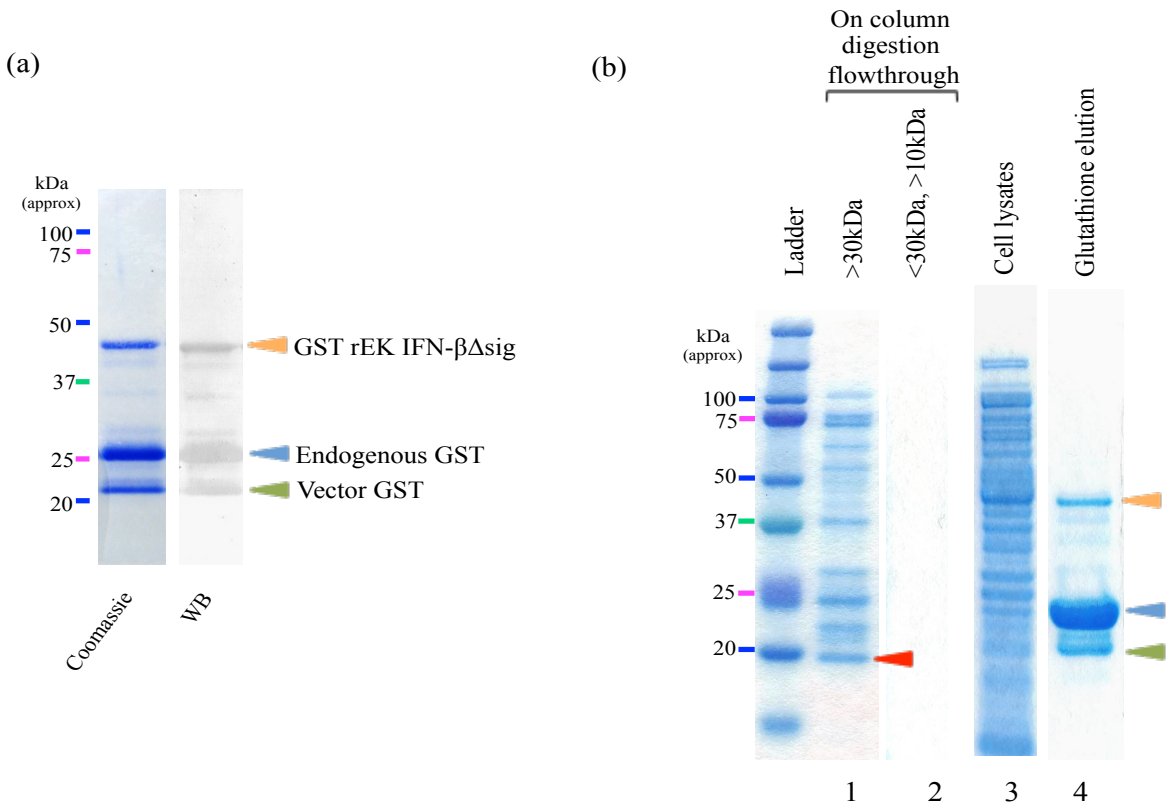

Figure 13. *E. coli* expression of GST rEK IFN-βΔsig and on column rEK digestion. (a) SDS-PAGE (Coomassie) and anti-GST Western blot (WB) analysis of eluate from glutathione column confirms expression of GST rEK IFN-βΔsig (orange arrowhead). Endogenous GST (blue arrowhead) and pGEX-4T-3 vector derived GST (green arrowhead) was also eluted from the column, likely heterodimerized with GST rEK IFN-βΔsig during expression. (b) GST rEK IFN-βΔsig was digested with rEK on the glutathione column as described in the Methods leaving GST and undigested GST rEK IFN-βΔsig bound to the column (lane 4). Putative IFN-βΔsig (red arrowhead, 19.9kDa) could be observed in the >30kDa fraction and was not detected in any other fraction.

GST Fusion Protein- MSYNWLRFQQ RSSNLACVKL LWQLNGTPQY
CHKDRMDFKL PAEIKQPQQF QKEDTVLIIH EMLRQIFDIF QRNFSSTGWN
ETIIMNLYVT LSGQMDRLET AMEEMEEENF TWESMTVLHL KNYYFRIMRY
LETKLYSRCA WTVVKAEILR NFFFLNGLTE YLQN

Figure 14. Protein sequencing of IFN-βΔsig. LC-MS/MS identified 5 peptide sequences within expected amino acid sequence of IFN-βΔsig. These identified peptides (red regions) confirm expression of IFN-βΔsig with 50% coverage.

containing lysates were bound to a glutathione sepharose column and digested with rEK. GST stays bound to the column while IFN-βΔsig elutes with the digestion reaction. Unexpectedly, a band at the projected 19.9kDa was observed in the >30kDa concentrated fraction (Figure 13b lane 1) but not in the 10-30kDa concentrated fraction (Figure 13b lane2) after rEK removal and protein concentration. In addition, multiple bands previously unseen in the purified GST rEK IFN-βΔsig eluates (Figure 13a) were observed in the >30kDa concentrated fraction (Figure 13b lane 1). Anti-GST Western blot did not detect any GST in the IFN-βΔsig containing >30kDa fraction (results not shown). Additionally, we eluted GST rEK IFN-βΔsig in the glutathione elution step (Figure 13b lane 4) suggesting further optimization of digestion conditions is needed. Our efforts to optimize the purification of *P. vampyrus* IFN-β are ongoing, but in the meantime we have proceeded with development of a bioassay to test recombinant *P. vampyrus* IFN-β.

3.4. Bioassay for the detection of biologically active P. vampyrus IFN-β

Once we had confirmed the inferred *P. vampyrus* IFN-β sequence by cloning and sequencing from *P. vampyrus* genomic DNA and confirmed proper *P. vampyrus* IFN-β protein sequence expression by LC-MS/MS, it was important to develop an assay which would allow us to determine whether our recombinant *P. vampyrus* IFN-β was biologically active. Demonstration of biological activity would serve to confirm the *P. vampyrus* IFN-β gene sequence to produce an active IFN-β protein similar to what is likely found in *P. vampyrus*, as opposed to just a protein that matches the inferred sequence. Additionally, the

bioassay would serve to determine the efficacy of the protein production/purification method to generate a biologically active *P. vampyrus* IFN-β. The standard bioassay for determining whether or not an IFN protein is functional is performed as followed: cells are treated *in vitro* with the novel interferon, later infected with an interferon-sensitive GFP-expressing virus, and monitored for GFP fluorescence as a measure of infection [215, 255]. In this assay, biological activity depends on a functional protein binding to IFNARs of the cells and stimulating the antiviral state. Pretreatment of cells with biologically active IFNs inhibits viral GFP expression [215].

Because many of the type I IFNs have been found to be animal species-specific [178, 179], in our bioassay we used PaLuSD8 cells, a lung cell line derived from the closely related *Pteropus alecto* [238], and infected the cells with a VSV expressing EGFP. VSV infection is rapid, lytic, and known to be sensitive to the effects of IFN treatment on cells [255]. The rapid and lytic infection allows us to monitor infection not only by GFP fluorescence levels but also by observing cpe and measuring levels of viral progeny released into the supernatant.

PaLuSD8 cells had not previously been utilized in an assay such as this so we first had to determine if PaLuSD8 cells were appropriate for our bioassay. Cells in this assay have to be permissive to virus infection and replication and be able to respond to IFNs. We first determined if PaLuSD8 cells were permissive to VSV EGFP infection and replication by infecting PaLuSD8 cells at various MOIs with VSV EGFP and observing cells for GFP fluorescence and cpe for up to 72 hours. By qualitative observation, VSV EGFP

productively infected PaLuSD8 at all the MOIs examined and all cells had lysed by 48-72 hours (results not shown). Consistent with VSV EGFP infection in many other mammalian cell types ([255, 256] and personal observations), GFP fluorescence was observed within 8-12 hours and at MOIs >1 all cells were lysed by 48 hours and at MOIs <1 all cells were lysed by 72 hours (results not shown). To verify the MOI calculations used in infection of PaLuSD8 cells, we titered our VSV EGFP stocks on PaLuSD8 cells and compared the results to titers of the same stock on BHK cells. There was no significant difference ($P > 0.05$) in titers of VSV EGFP assayed on PaLuSD8 cells ($4.50x10^7 \pm 0.48x10^7$ pfu/mL) compared to titers of VSV EGFP assayed on BHK cells ($4.15x10^7 \pm 0.54x10^7$ pfu/mL).

Next, I developed a positive control for the bioassay and determined if signaling through the IFNAR was intact. Expression of the IFNAR in PaLuSD8 cells had been previously determined by reverse transcriptase PCR (Michelle Baker, personal communication). To determine whether the receptor was functional, I treated cells with IFNαA/D prior to infection with VSV EGFP. IFNαA/D is a recombinant human IFN-α hybrid known to have cross-species activity on many mammalian cell lines [178, 239]. At 48 hours post-VSV EGFP challenge, cpe was observed in almost all cells of the untreated well (Figure 15 top row, right panel), cells treated with 10U IFNαA/D (Figure 15 middle row, rightmost panel), and cells treated with 1U IFNαA/D (results not shown). Partial protection was observed in cells pretreated with 100U IFNαA/D (Figure 15 middle row, center panel). The morphology of cells pretreated with 10000U IFNαA/D (results not shown) and 1000U IFNαA/D (Figure 15 middle row, leftmost panel) was comparable to uninfected cells (Figure

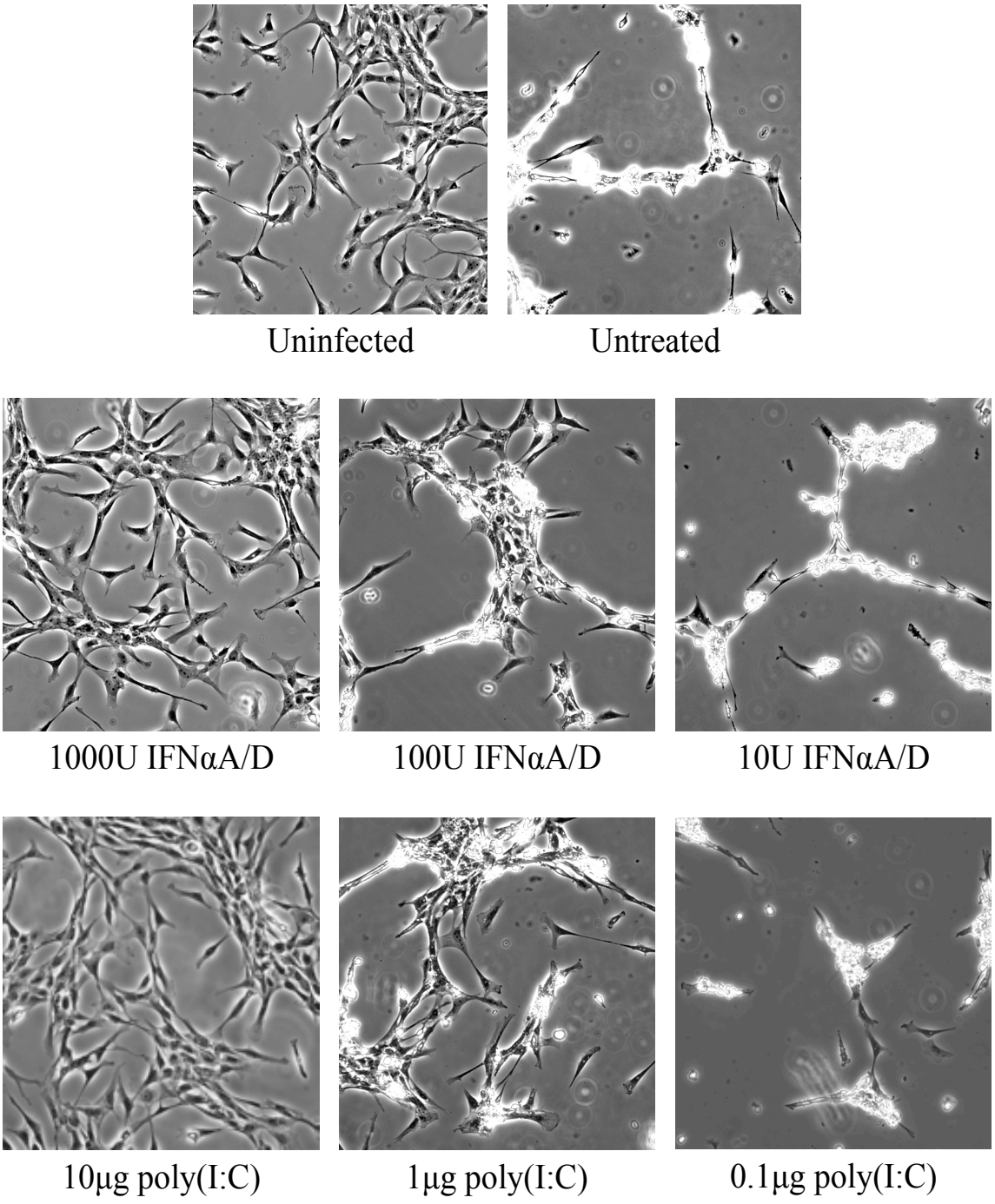

Figure 15. Universal IFN-α and poly(I:C) protect PaLuSD8 cells from VSV-mediated cpe. PaLuSD8 cells were pretreated with the indicated amounts of IFNαA/D or poly(I:C) and then infected with VSV EGFP. Brightfield images were taken at 48 hours post-infection. 1000U of IFNαA/D or 10ug poly(I:C) protects PaLuSD8 cells from VSV-induced cpe.

15 top row, rightmost panel) and showed no signs of cpe at 48 hours. These results confirm the expression and proper function of the IFNAR in PaLuSD8 cells and provide us with a positive control of 1000U IFNαA/D for our bioassay.

In addition, I evaluated sensitivity of PaLuSD8 cells to the anti-viral effects of poly(I:C) induced IFN or IFN-like effectors. Double-stranded viral RNA mimic poly(I:C) has been shown to induce IFN production in bat primary cells [186] and other *P. alecto* cell lines [238]. Monitoring cpe for 48 hours, I observed no changes in cell morphology in wells pretreated with 10μg (Figure 15 bottom row, leftmost panel) and 100μg poly(I:C) (results not shown) as compared to the uninfected well (Figure 15 top row, leftmost panel), while cells treated with 1μg poly(I:C) were only partially protected (Figure 15 bottom row, middle panel). No protection was observed with treatment of 0.1μg poly(I:C) (Figure 15 bottom row, leftmost panel) comparable to the untreated cells (Figure 15 top row, rightmost panel). Because no reagents are available to measure IFN protein production by PaLuSD8 cells, we could not determine if this protection was due to the effect of endogenous IFNs produced by the PaLuSD8 cells. As described in section 1.5., IFN production and IFN signaling through the IFNAR are necessary for effective induction of ISGs to protect cells from infection. Poly(I:C) treatment of cells deficient in interferon synthesis *e.g.* Vero cells [257] and BHK cells (Jason Tourigny, unpublished results) did not influence viral replication in these cell types. Although we could not measure IFN protein production directly, inhibition of VSV EGFP-mediated cpe after pretreatment of PaLuSD8 cells with poly(I:C) (Figure 15) suggests PaLuSD8 cells can produce endogenous IFNs or some unknown effector molecule with IFN-

like activity. In addition, these results provide us with another possible positive control for our bioassay.

Because not all cells respond to poly(I:C) stimulation [257], we also designed experiments to determine if PaLuSD8 cells could produce endogenous IFN-like activity in the more natural context of infection. I hypothesized that VSV EGFP could stimulate IFN-like activity in PaLuSD8 supernatants and these supernatants could inhibit VSV replication in separately infected PaLuSD8 cells. To test this, I first infected PaLuSD8 cells with VSV EGFP at a low MOI (0.25) to stimulate production of IFN-like effector molecules. The VSV matrix protein inhibits host gene expression in order to suppress interferon production [192] and a low MOI was used to ensure production of IFN-like effector molecules by infected cells and possibly by stimulated uninfected neighboring cells (Figure 3). Virus in the supernatant was UV-inactivated prior to incubating naïve PaLuSD8 cells with diluted supernatants. UV-inactivated supernatants inhibited VSV EGFP replication as measured by cpe and GFP expression (Figure 16). While all cells appeared infected as indicated by the GFP fluorescence, the 1:10 dilution of UV inactivated media (Figure 16, panel 3) and, to a lesser extent, the 1:100 dilution (Figure 16, panel 4) inhibited VSV replication as evidenced by the normal cell morphology and lack of cpe. GFP expression and cpe observed in cells treated with the 1:1 dilution of UV inactivated media was similar to that of the 1:10 dilution (results not shown). As a control for complete VSV inactivation, I incubated 1:1 diluted UV-inactivated supernatant on an uninfected well and observed no cpe or GFP expression up to 48 hours suggesting virus inactivation was complete (results not shown). Because a pure

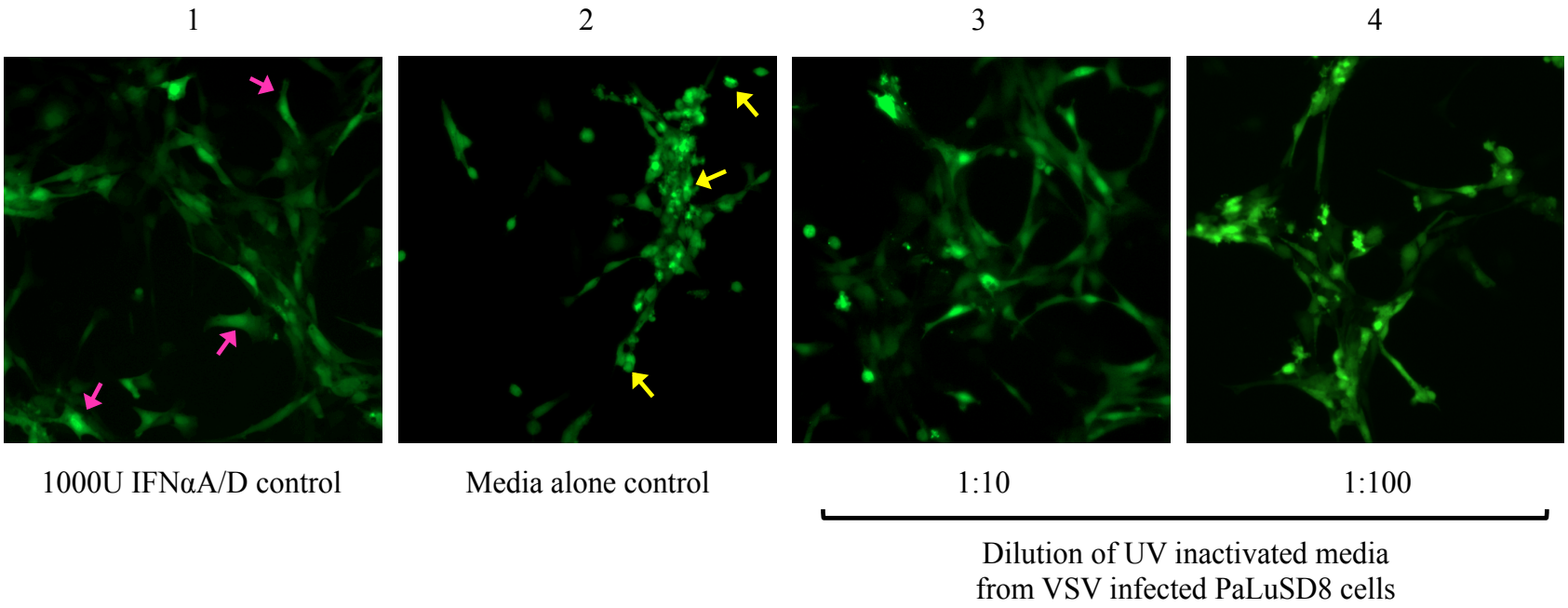

Figure 16. VSV-mediated CPE is inhibited after pretreatment with supernatants from infected PaLuSD8 cells. 1000U IFNαA/D (first panel) and media alone (second panel) were used as positive and negative controls, respectively. PaLuSD8 cells were pretreated for 16 hours prior to infection with VSV EGFP for 24 hours. After 24hours, GFP expression and cpe was imaged with fluorescence microscopy. Cytopathic effect (yellow arrows) is easily visible in media alone control (panel 2) due to advanced viral replication. In panels 1 and 3, infection is indicated by the GFP expression however normal cell morphology (purple arrows in panel 1) suggests inhibition of VSV EGFP replication. No background fluorescence was observed with uninfected cells (results not shown).

UV-inactivated VSV EGFP control was not performed, we do not know if UV-inactivated VSV EGFP virions could also have stimulated the cells to inhibit VSV EGFP replication upon challenge. However, it should be noted that previous studies using cells from other species indicate that UV-inactivated VSV does not induce IFN production [255, 258-261] and IFN induction by VSV requires initial viral transcription [260]. These results suggest production of endogenous IFN-like effectors by PaLuSD8 cells and provide us with an alternate positive control for our bioassay.

Once we established that PaLuSD8 cells were appropriate for the bioassay and we had a positive control, we sought to determine if our recombinant *P. vampyrus* IFN-β protein was biologically active. Because a pure preparation of our recombinant IFN-β was not yet available, we tested the hypothesis that our inferred *P. vampyrus* IFN-β gene could produce biologically active IFN-β, and therefore confirming the accuracy of the gene sequence used for protein expression and purification. To test this hypothesis, we used supernatant from BHK cells stably transfected with pcDNA3.1(+) *P. vampyrus* IFN-β. These cells should express and secrete *P. vampyrus* IFN-β. BHK cells do not produce their own IFN [262, 263], so if IFN-β secreted from transfected BHKs is biologically active, then pretreatment with the BHK supernatants should inhibit VSV EGFP infection and replication in PaLuSD8 cells in a dose-dependent manner. I pretreated PaLuSD8 cells with supernatants from BHKs expressing pcDNA3.1(+) *P. vampyrus* IFN-β or empty vector pcDNA3.1(+) prior to VSV EGFP challenge. GFP expression levels were imaged at four hours post-infection (Figure 17) and levels of viral progeny in the supernatants were measured at 8 and 24 hours (Figure

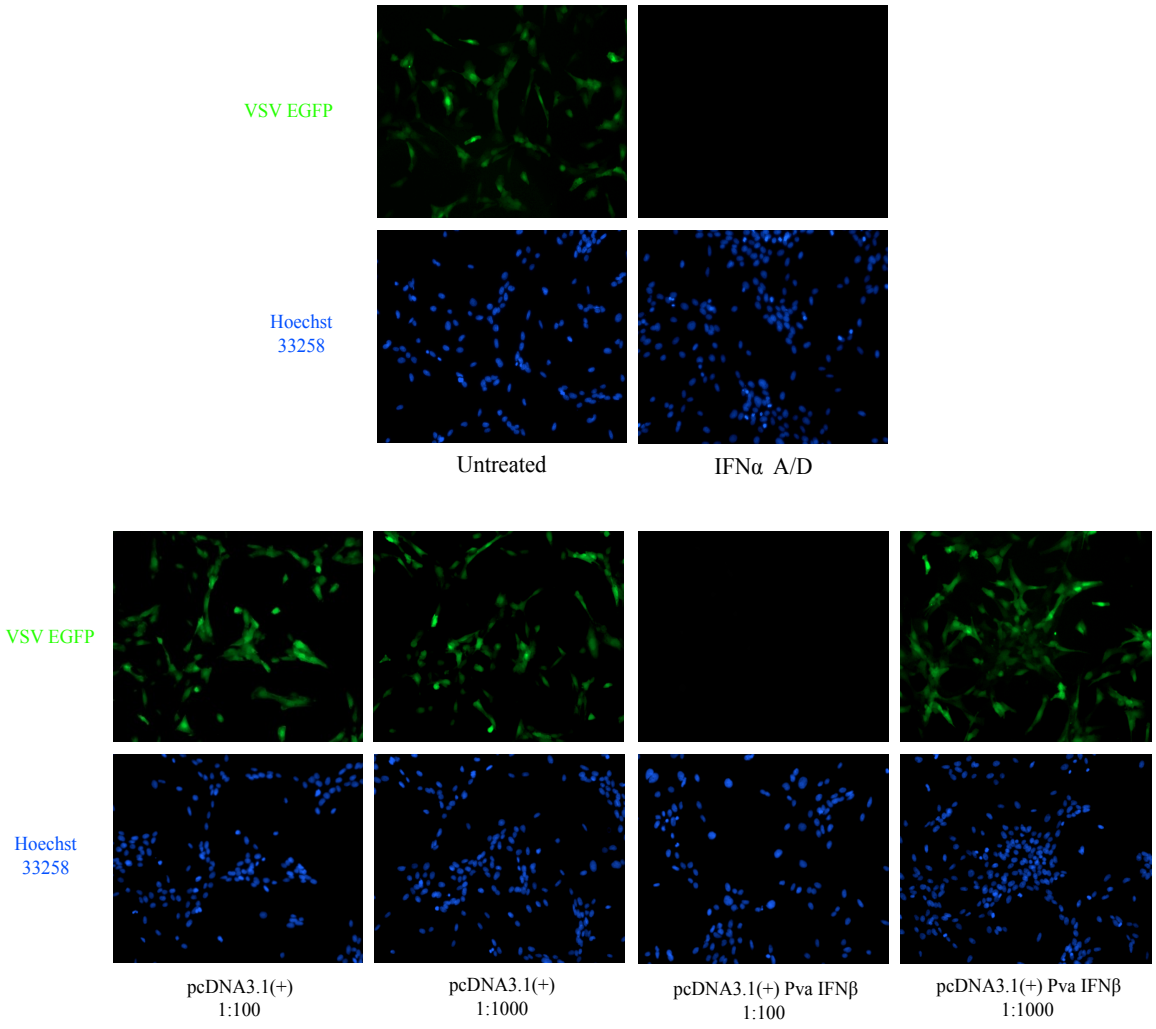

Figure 17. *P. vampyrus* IFN-β inhibits EGFP expression in VSV EGFP infected PaLuSD8 cells. PaLuSD8 cells were treated with supernatants from BHK cells stably expressing pCDNA3.1(+) *P.vampyrus* IFN-β (Pva IFN-β) or empty vector pcDNA3.1(+) at the dilutions indicated. Treated cells were then infected with VSV EGFP for 4 hours, fixed, nuclei stained, and imaged by fluorescence microscopy. GFP expression at 4 hours was not detected in cells treated with IFN-β containing sups at 1:100 dilution as compared to cells treated with any dilution of empty vector pcDNA3.1(+) sups. Images are representative of two experiments.

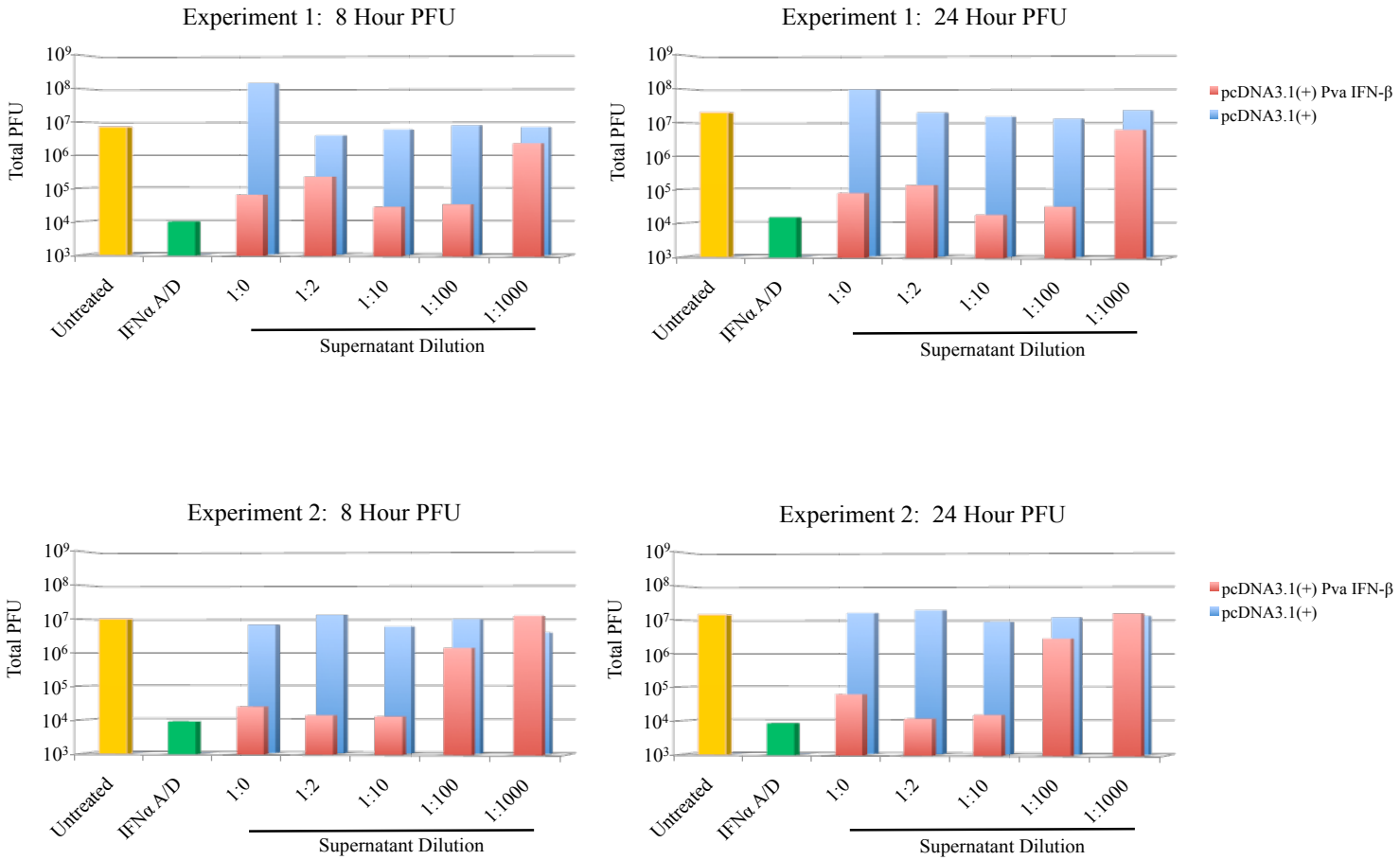

Figure 18. *P. vampyrus* IFN-β inhibits VSV replication in PaLuSD8 cells. PaLuSD8 cells were treated with supernatants from BHK cells stably expressing pCDNA3.1(+) *P.vampyrus* IFN-β (Pva IFN-β) or empty vector pcDNA3.1(+) at the dilutions indicated. Treated cells were then infected with VSV EGFP and samples of the supernatants were taken at 8 and 24 hours. Samples were titered on BHK cells and total pfu of infectious virus was calculated.

18). As evidenced by the Hoechst staining in Figure 17, many nuclei appear in a single GFP expressing area. PaLuSD8 cells grow in very close contact with other cells, often have thin and long morphologies, and tend to grow on top of each other as opposed to a single cell monolayer, thus confounding true enumeration of infected versus uninfected cells. We chose an early time point post-infection to best demonstrate a visually positive or negative infection. GFP expression in cells treated with IFNαA/D and the 1:100 dilution of *P. vampyrus* IFN-β containing supernatant was below detection while GFP expression was clearly evident in empty vector supernatant dilutions and untreated cells (Figure 17). Additionally over ten-fold fewer pfu were detected at 8 and 24 hours in the supernatants of wells pretreated with IFN-β containing supernatants at dilutions up to 1:100 for experiment 1 (Figure 18, top graphs) and up to 1:10 for experiment 2 (Figure 18, bottom graphs). Protection was concentration dependent as evidence by GFP expression (Figure 17) and virus levels (Figure 18) at the higher dilutions of IFN-β containing supernatant. These results indicate that our bioassay can be used to detect novel *P. vampyrus* type I IFNs and strongly suggest that the inferred *P. vampyrus* IFN-β gene can produce a biologically active protein.

4. DISCUSSION

As described in the Introduction, pteropid bats are the asymptomatic reservoir hosts of NiV, EBOV, and SARS-CoV; viruses that are considerably more pathogenic in humans than in bats. We hypothesized that host factors, in particular the type I IFN antiviral system, are largely responsible for the differences in pathogenicity of these viruses between bats and humans. In this study, we first identified the sequences of the type I IFNs from *P. vampyrus*. Because sequencing and assembly of the *P. vampyrus* genome is still under construction, we had to infer the sequences from the genome traces using a novel statistical gene family assembler developed by Dr. Tom Kepler [187]. In order to validate the inferred sequences, we PCR amplified and cloned the type I IFN genes from genomic DNA using primers derived from the inferred sequences and then sequenced the clones. For IFN-β, we sequenced multiple clones amplified from the genomic DNA of two individual *P. vampyrus* bats. Dr. Kepler's prediction worked well and we were able to identify the *P. vampyrus* IFN-β sequence. Initially the IFN-β consensus sequence that we identified experimentally differed from the inferred sequence by only two nucleotides. To resolve these differences, we analyzed the quality scores from the sequencing and adjusted the statistical gene assembler. The *P. vampyrus* IFN-β gene sequence inferred by the updated program then matched the consensus sequence derived from the sequences of the experimentally obtained clones. It is highly advantageous to utilize the feedback from the experimental sequences to refine the gene assembler, which in turn strengthens the confidence we have in the sequences inferred from the statistical gene assembler. Validation of the other inferred sequences by

direct cloning from the genomic DNA is still ongoing and as clones are sequenced, the program is being updated. Finally, genomic DNA has been prepared from whole blood of eight outbred *P. vampyrus* bats. We plan to confirm identity of the inferred sequences from at least two individual bats.

From the initial inferred and clonal sequencing results, we determined that the type I IFN profile in bats is qualitatively different from the type I IFN profile in humans. In contrast to humans that have 13 IFN-α subtypes and only a single IFN-ω [159], seven IFN-α genes and 18 IFN-ω genes were inferred for *P. vampyrus.* We cannot assess the full biological effect of these differences based on the data we have collected so far, however we speculate that the multiple IFN-ω genes could play significant role in defense against NiV or other viral infections. In support of this idea, pigs, which are an intermediate host for NiV-Malaysia [91, 92], have an expanded IFN-ω gene family and are far more resistant to NiV infection than are humans [168]. In addition, individual IFN subtypes can have different activity profiles [173, 177]. For example, human IFN-ω was shown to be a more potent antiviral agent than IFN-α against yellow fever virus and West Nile virus at the effective concentration of IFN-ω [264].

Once we had completed inference of the pteropid IFN gene family [187] and confirmed the nucleotide sequence of *P. vampyrus* IFN-β, our next goal was to clone the *P. vampyrus* IFN-β gene into an expression vector and purify recombinant IFN-β protein. Purification of our recombinant *P. vampyrus* IFN-β is still in progress. Once a pure preparation is achieved, our first priority will be to test the biological activity of the

recombinant protein using the bioassay developed in this project. In addition, we plan to use the protein to develop monoclonal and polyclonal antibodies that could be used in Western blots, immunoprecipitation, and the development of an ELISA. All of these reagents and assays will be instrumental in the measurement of the *P. vampyrus* interferon response at the protein level.

As part of this study, we developed a bioassay to detect the antiviral bioactivity of novel *P. vampyrus* type I IFNs. Our bioassay is modeled after the standard bioassay used for the detection of function IFN protein as described in Section 3.4. Our assay utilizes an immortalized *P. alecto* lung cell line (PaLuSD8) as the IFN-responsive cell line, and inhibition of VSV EGFP infection as the reporter. Briefly, IFN-responsive cells are pretreated *in vitro* with the novel interferon, infected with VSV EGFP, and monitored for GFP fluorescence, for cytopathic effects, or for secretion of viral progeny into the supernatant. VSV is an IFN-sensitive virus and if the infected cells are treated with a biologically active IFN, VSV infection, transcription, and replication are inhibited. Inhibition of viral infection and transcription results in a measurable lack of GFP fluorescence. The titer of virus from the supernatants of infected cells is a measure of viral replication inhibition.

Pretreatment of PaLuSD8 cells with a "universal" IFN-α inhibited VSV EGFP-mediated cpe (Figure 15) and demonstrated that expression of and signaling through the IFNAR is intact in PaLuSD8 cells. As a next step, we confirmed that the *P. vampyrus* IFN-β gene produced a biologically active protein because transferred supernatants from BHK cells

expressing pcDNA3.1(+) *P. vampyrus* IFN-β were able to inhibit VSV EGFP transcription and replication (Figures 17 and 18) in a dose dependent manner. Because a blocking antibody to our *P. vampyrus* IFN-β is unavailable and a blocking antibody to the *P. alecto* IFNAR is also currently unavailable, we could not formally exclude the possibility that the inhibition of VSV EGFP is not due to another factor in the supernatants from our BHKs expressing pcDNA3.1(+) *P. vampyrus* IFN-β, although this seems extremely unlikely in view of the fact that cells transfected with a control plasmid were not protected from infection.

Signaling through the IFNAR involves activation of JAK and subsequent phosphorylation and activation of STAT1 and STAT2 (Figure 3). Rabbit anti-human STAT1 and anti-human phopsho-STAT1 have been shown to bind to STAT1 and phospho-STAT1 respectively of *Rousettus aegyptiacus*, another pteropid bat [172]. As reagents like this are developed that can bind *P. vampyrus* IFNAR signaling proteins, we plan to further confirm the signaling of our recombinant *P. vampyrus* IFN-β through the IFNAR with Western blots and immunocytochemistry.

In the final part of this study, transcriptome deep sequencing analysis was used to quantitatively measure the response of *P. vampyrus* PBMCs to VSV infection. Because NiV and EBOV are biosafety level-4 (BSL-4) agents, we could not directly infect cells with NiV or EBOV in our laboratory. VSV was chosen for the infection experiments because we could perform experiments at BSL-2, and VSV is an enveloped virus with a single-stranded, negative-sense RNA genome like NiV and EBOV with similar viral transcription strategy as

NiV. In addition, we needed a virus that could infect both our human and *P. vampyrus* PBMCs, and VSV can infect all known mammalian cell types.

Transcriptome analysis allows us to compare the relative rate of change in expression level for a particular gene of interest in the two species before and after infection. For example, we might determine that when human PBMCs were infected with VSV, expression of IL2 increased 5x over uninfected human PBMCs, while in bat cells expression increased only 2x. To be able to draw conclusions from the transcriptome analysis, we had to select the best analysis method. In our initial analysis of the deep sequencing data, we chose a staggered cutoff scheme for the count numbers and fold differences to determine relevance of fold difference and account for some read count error as described in Section 3.2.1. Deep sequencing is still a relatively new RNA analysis technique and there are many techniques being proposed to normalize and analyze the large amount of data these studies generate [241, 242, 244, 245, 265-268]. We had to choose a method of analysis that would account for error inherent in the sequencing process and the transcript read sequence alignment process. Some studies normalized counts based on gene length or exon mapping to the genome of the species of interest [241, 242, 265, 267, 268]. The full bat transcriptome is unavailable for us to perform normalization calculations based upon gene lengths. In addition, exon mapping of every read to the unassembled *P. vampyrus* genome is not technically feasible [241, 242, 265, 267, 268]. For these reasons, we chose a staggered cutoff scheme similar to that described by Woodhouse, *et al.* (described in detail in Section 3.2.1)

over the other normalization analyses for its simplicity and because our study and the published study were both comparing virus-infected versus uninfected cells [245].

From our results, differential expression of many important chemokines and cytokines is evident. For example, induction of mRNA of inflammation associated cytokines, IL6, IL13, and CXCL2 at 8 hours post-VSV infection in human PBMCs is much greater than the induction in *P. vampyrus* PBMCs at 8 hours however induction of these cytokine mRNAs is greater in the bat cells at 24 hours post-VSV infection than induction in the human cells at 24 hours (Tables 4 and 5). The same differential induction pattern is noted for IL10, a pleiotropic cytokine more commonly associated with inhibition of the inflammatory response and type I IFNs [269]. Induction of CXCL6, a neutrophil chemoattractant [270], mRNA at 8 hours post-infection in the bat PBMCs is over 16-fold greater than CXCL6 induction in the human PBMCs. These results suggest that infection in humans and bats results in very different cytokine and chemokine profiles, however it is unclear exactly how these different cytokine profiles affect the response to infection *in vivo*.

Of the type I IFNs we detected IFN-α2, IFN-ω, and IFN-β (Table 4) from the human deep sequencing reads at 24 hours post-VSV infection. These results are consistent with previous studies that have shown that VSV infection of human PBMC induces type I IFN protein production by 8 hours post-infection [269, 271]. Counts for the other type I and type III IFNs were two or below at all time points and conditions in human cells. To our knowledge, this is the only study to examine the whole transcriptome response of human cells to short infection (≤24 hours) with a rapid cytolytic virus such as VSV. Consistent with

the idea that IFN-ω might be a key factor in the bat's defense against viral infection, at 24 hours post-VSV infection of bat PBMCs, IFN-ω mRNA was induced 18 fold over unstimulated samples while IFN-ω was not detected at all in the human samples (Tables 4 and 5). We plan to further investigate this result by comparing the individual *P. vampyrus* IFN-ω subtypes to the deep sequencing reads to determine which of the IFN-ω subtypes are being induced and if any reads are being excluded because they are divergent enough from the human IFN-ω.

One possibility is that, in bats, the more robust induction of inflammatory mediators, such as those discussed above, could act to synergistically inhibit viral infection. Synergy occurs when two or more cytokines function together to create a response that was not individually obtainable. Synergy could result in greater upregulation in some genes while others are downregulated compared to the responses to the individual cytokines. Consistent with this hypothesis, in human fibroblasts, TNF-α and IFN-β were able to induce a distinct antiviral state with a novel gene expression profile that was not induced when the cells were stimulated with the individual cytokines [272]. The synergistic antiviral state induced by TNF-α and IFN-β was necessary to sufficiently block myxoma virus, a poxvirus. Among the hundreds of genes that were differentially expressed, TNF-α treatment upregulated CXCL6 78-fold, however TNF-α and IFN-β treatment only upregulated CXCL6 10-fold in the human fibroblasts [272]. From our results, bat PBMCs greatly upregulated CXCL6 at 8 hours after VSV infection but human cells did not upregulate CXCL6 at 8 nor 24 hours. TNF-α and IFN-β treatment of human fibroblasts upregulated many antiviral pathway genes

such as OAS1, OAS2, OAS3, MX2, and RIG-I more than by treatment with the cytokines alone [272]. Many of the same genes were expressed differently in the bat and human cells. Many combinations of cytokine/cytokine mixtures and cytokine/IFN-α/β mixtures have been tested on human cells that result in unique synergistic patterns of gene induction [273]. Because cytokines most likely occur as a mixture during the in vivo response to infection, the study of their combined effect is physiologically relevant [273]. Greater upregulation of IL10 and IL13 in humans at 8 hours post-infection but greater upregulation in bats at 24 hours post- infection demonstrates a more temporal difference in gene induction, however it is unknown how these two cytokines may interact to create the gene induction profile from our results. The synergistic effects of cytokines have also been studied post-TLR stimulation [273]. At this time we cannot confirm if or how the different cytokines act synergistically to inhibit VSV replication in bat cells. As described above, IFN-ω has different actions than the other type I IFNs, and the bat IFN-ω subtype profile [187] and IFN-ω mRNA upregulation is different in the bat than the human. IFN-ω could act synergistically with another cytokine to create the response of the bat PBMCs measured by the deep sequencing.

If this synergistic activity of a cytokine and a Type I IFN were present in the bat but not in humans, it could explain why NiV infects bat cells but does not disseminate or cause pathologic responses in bats. On the other hand, if synergistic inhibition occurs in bat cells, then that raises the question of how these viruses persist long enough in the bat to be transmitted to other hosts. Recently it was discovered that human lymphocytes were not permissive to NiV infection, however NiV could bind the lymphocyte cell surface,

disseminate throughout the body, and productively transinfect other cells such as neurons [274]. If NiV could disseminate throughout the bat in a similar manner it might thereby avoid complete eradication by the synergistic cytokine and IFN response. This would serve to prolong infection until the virus could be established in an organ that would subsequently shed virus and facilitate spread to spread to a new host.

Alternatively, the actions of different IFN subtypes and production of a different cytokine profile in the bat could attract a different set of immune cells to the site of infection and those cells could control NiV infection and prevent dissemination. Consistent with that idea, *in vitro* and computational model studies have showed that production of IFN antagonists, NiV W and NiV V, is delayed in human cells. This leads to production of early inflammatory cytokines other than IFN, which was still efficiently inhibited [275]. This suggests that when NiV infects human cells, this early inflammatory cytokine production could increase infiltration by lymphocytes to the site of infection while still effectively antagonizing the human IFN antiviral response and then the lymphocytes could facilitate dissemination. SARS-CoV infection in humans has also been associated with early production and high plasma levels of IFN-α but not IFN-β suggesting that SARS-CoV suppresses the major human antiviral IFN and uses IFN-α to modulate cytokine production, cellular infiltration, and the immune response to support productive infection and increase pathogenicity [55]. Taking the aforementioned studies together with our findings that bats have a different type I IFN profile compared to humans [187] and the differential expression of cytokines and chemokines from our deep sequencing results, these data support our

hypothesis that the bat IFNs could direct a novel and highly effective antiviral that controls NiV, EBOV, and SARS-CoV infection.

Interestingly, we found a large induction of IL6 mRNA in human cells upon VSV infection at 8 and 24 hours but we were unable to detect IL6 mRNA in the bat cells (Table 4). This result is contrary to reports that *in vitro* VSV infection does not increase levels of secreted IL6 protein in human PBMCs [276] and human monocytes [277]. IL6 mRNA is degraded rapidly with a half-life of approximately 30 minutes and expression is partly controlled post-transcriptionally [278]. One major difference between the studies is that our study measured mRNA induction not protein. To resolve this issue, we will perform follow up experiments in which we will measure IL6 protein secreted by VSV infected human PBMCs. We have to be careful before we can state that IL6 mRNA is not upregulated in bat cells after VSV infection. IL6 upregulation in bat cells could have been rapid and the response had waned by eight hours or bat cells do not use or upregulate IL6 in response to VSV infection. Alternatively, the *P. vampyrus* IL6 mRNA sequence may be too divergent from the human IL6 mRNA sequence to be matched to *P. vampyrus* reads. The full IL6 gene in the bat has been identified from the genomic traces and Dr. Kepler is currently mapping the exons to identify the mRNA sequence so we can compare the *P. vampyrus* IL6 gene to the deep sequencing results as to be sure we have not missed identifying the bat IL6 response.

Because gene counts are not actual transcript numbers, one feature common to all of the aforementioned studies utilizing transcriptome deep sequencing is the verification and

transcript/protein quantitation of deep sequencing results with qRT-PCR or protein assays. As described in the Introduction, the interferon-induced antiviral response results in upregulation, downregulation, and activation of hundreds of genes and proteins [153]. The deep sequencing results provide a global guide to gene transcript induction or suppression and reveal genes that are differentially expressed in the bat and human that we may not have examined if we just used individual gene or protein specific assays like qRT-PCR or Western blots. Now that we have this global dataset, we plan to use qRT-PCR to verify the gene induction we see in the deep sequencing results.

We hypothesized that expression of both IFNs and IFN-responsive genes is quantitatively different and is largely responsible for the differences in pathogenicity of various viruses between bats and humans. In support of our hypothesis, our preliminary deep sequencing results provide evidence that IFNs and IFN-stimulated genes are differentially expressed in *P. vampyrus* PBMCs compared to human PBMCs. It is unclear the overall effect that each of these differences has *in vivo*. From these results, we have identified genes that appear to be induced differently either temporally or in magnitude between the human than the bat. Future plans include confirmation of our initial results using qRT-PCR and protein assays.

Recently, two studies have examined NiV infection in both human [279] and bat [280] cells and suggested that the IFN response was not responsible for the bats' ability to control infection. The authors measured IFN-α, IFN-β, ISG54, and ISG56 mRNA levels by qRT-PCR after a 3 hours infection with NiV and the closely related Hendra virus (HeV) in

human Hep-2 and 293T cells, and various *P. alecto* cell lines. Consistent with the studies that show NiV V and NiV W proteins effectively antagonize type I IFN induction and signaling, IFN-α and IFN-β expression was inhibited to almost basal levels in both human and bat cells. The authors report that ISG54 and ISG56 were completely inhibited in bat cells [280] but not at all in human cells [279] with the exception of some low level ISG54 and ISG56 activation in some bat cell lines infected with HeV, which the investigators attributed to a small percentage of uninfected cells [280]. Although the results of this study seem to directly oppose our hypothesis, the design of the study was flawed. Specifically bat cells were infected at an MOI of ten for all viruses [280] while human cells were only infected at an MOI of one [279]. Infecting the human cells at a lower multiplicity would significantly increase the number of uninfected cells in the culture, and those cells could upregulate ISG54 and ISG56. In addition, our deep sequencing results suggests that other ISGs, such as RNASEL or OAS1, may be more important for the different antiviral responses by bat and human cells (Table 5) than ISG54 or ISG56. While both IFN-α and IFN-β mRNA induction was efficiently inhibited by NiVs in human [279] and bat [280] cell lines, we have identified an expanded IFN-ω profile and our deep sequencing results show that IFN-ω was preferentially induced over other IFNs after VSV infection. I hypothesize that IFN-ω may not be efficiently antagonized by NiV or that IFN-ω could play an important role in directing an immune response against NiV. One way we could test this hypothesis is to infect IFN-ω competent and responsive bat and human cells with NiV and measure the different IFN-ω species in bat cells or the one IFN-ω in human cells with qRT-PCR.

In both our study and previous studies [279, 280], infection was examined in cell types that may not be physiologically relevant to natural infection. As described in the Introduction, different IFNs are produced by different cell types [159, 167] and these IFNs could affect cells differently [173, 281, 282]. IFNs have been shown to play an important role in influenza tissue tropism [283]. The respiratory tract is likely the site of initial infection and spread in humans [125], while, in bats infection seems to spread in a urine-to-respiratory tract manner [108]. Another important goal for our ongoing studies is to investigate the IFN response throughout the respiratory tract.

Even if the interferon-induced antiviral state is not the reason behind the differences in pathogenicity in bats and humans, type I and III IFNs could still be major players in the adaptive response to infection. Type I IFNs have been shown to enhance the cytolytic activity of memory $CD8^+$ T Cells [284] and regulate T cell differentiation [281]. Future work should not only examine the IFN induced antiviral states in bats and humans but also investigate how IFNs may shape the cellular and adaptive response to infection.

In conclusion, we have identified an expanded type I IFN repertoire in *P. vampyrus* bats through a statistical gene-assembler and shotgun sequencing from PCR of genomic DNA. We cloned the *P. vampyrus* IFN-β gene, evaluated its biological activity, and are currently purifying recombinant protein. Transcriptome deep sequencing of human and bat PBMCs post-VSV infection has provided us with a wealth of data and a guide to further investigate the antiviral response of bats to viral infection. The results from deep sequencing of samples from cells treated with poly(I:C) are currently being aligned to the human

transcriptome. In addition we report the development of a bioassay to test the antiviral activity of recombinant bat IFNs. We believe elucidation of the active *P. vampyrus* IFN molecules and downstream ISG candidates could suggest novel strategies to combat infection by highly pathogenic bat derived viruses.

5. REFERENCES

1. Kunz TH, Fenton MB. Bat Ecology. Chicago, Ill.: University of Chicago Press, 2003.

2. Barclay RMR, Harder LD. Life Histories of Bats: Life in the Slow Lane. In: Kunz TH, Fenton MB, eds. Bat Ecology. Chicago, Ill.:University of Chicago Press, 2003:209-56.

3. Willig MR, Patterson BD, Stevens RD. Patterns of Range Size, Richness, and Body Size in Chiroptera. In: Kunz TH, Fenton MB, eds. Bat Ecology. Chicago, Ill.:University of Chicago Press, 2003:580-621.

4. Nishihara H, Hasegawa M, Okada N. Pegasoferae, an unexpected mammalian clade revealed by tracking ancient retroposon insertions. Proceedings of the National Academy of Sciences 2006; 103(26):9929-34.

5. Shoshani J, McKenna MC. Higher Taxonomic Relationships among Extant Mammals Based on Morphology, with Selected Comparisons of Results from Molecular Data. Molecular Phylogenetics and Evolution 1998; 9(3):572-84.

6. Novacek MJ. Mammalian phylogeny: shaking the tree. Nature 1992; 356(6365):121-5.

7. Pumo DE, Finamore PS, Franek WR, Phillips CJ, Tarzami S, Balzarano D. Complete Mitochondrial Genome of a Neotropical Fruit Bat, *Artibeus jamaicensis*, and a New Hypothesis of the Relationships of Bats to Other Eutherian Mammals. Journal of Molecular Evolution 1998; 47(6):709-17.

8. Podlutsky AJ, Khritankov AM, Ovodov ND, Austad SN. A New Field Record for Bat Longevity. The Journals of Gerontology Series A: Biological Sciences and Medical Sciences 2005; 60(11):1366-8.

9. Neuweiler G. The Biology of Bats. New York, N.Y.: Oxford University Press, 2000.

10. Kunz TH, Lumsden LF. Ecology of Cavity and Foliage Roosting Bats. In: Kunz TH, Fenton MB, eds. Bat Ecology. Chicago, Ill.:University of Chicago Press, 2003:3-89.

11. Nishihara H, Hasegawa M, Okada N. Pegasoferae, an unexpected mammalian clade revealed by tracking ancient retroposon insertions. Proc Natl Acad Sci U S A 2006; 103(26):9929-34.

12. Dumont ER. Bats and Fruit: An Ecomorphological Approach. In: Kunz TH, Fenton MB, eds. Bat Ecology. Chicago, Ill.:University of Chicago Press, 2003:398-429.

13. Helversen Ov, Winter Y. Glossophagine Bats and Their Flowers: Costs and Benefits for Plants and Pollinators. In: Kunz TH, Fenton MB, eds. Bat Ecology. Chicago, Ill.:University of Chicago Press, 2003:346-97.

14. Patterson BD, Willig MR, Stevens RD. Tropical Strategies, Niche Partitioning, and Patterns of Ecological Organization. In: Kunz TH, Fenton MB, eds. Bat Ecology. Chicago, Ill.:University of Chicago Press, 2003:536-79.

15. Jones G, Rydell J. Attack and Defense: Interactions between Echolocating Bats and Their Insect Prey. In: Kunz TH, Fenton MB, eds. Bat Ecology. Chicago, Ill.:University of Chicago Press, 2003:301-45.

16. Williams-Guillén K, Perfecto I, Vandermeer J. Bats Limit Insects in a Neotropical Agroforestry System. Science 2008; 320(5872):70.

17. Boyles JG, Cryan PM, McCracken GF, Kunz TH. Economic Importance of Bats in Agriculture. Science 2011; 332(6025):41-2.

18. Cleveland CJ, Betke M, Federico P*, et al.* Economic value of the pest control service provided by Brazilian free-tailed bats in south-central Texas. Frontiers in Ecology and the Environment 2006; 4(5):238-43.

19. Frick WF, Pollock JF, Hicks AC, Langwig KE, Reynolds DS, Turner GG, Butchkoski CM, Kunz TH. An Emerging Disease Causes Regional Population Collapse of a Common North American Bat Species. Science 2010; 329(5992):679-82.

20. Simmons NB, Conway TM. Evolution of Ecological Diversity in Bats. In: Kunz TH, Fenton MB, eds. Bat Ecology. Chicago, Ill.:University of Chicago Press, 2003:493-535.

21. Epstein JH, Olival KJ, Pulliam JRC*, et al.* Pteropus vampyrus, a hunted migratory species with a multinational home-range and a need for regional management. Journal of Applied Ecology 2009; 46(5):991-1002.

22. Palmer C, Price O, Bach C. Foraging ecology of the black flying fox *Pteropus alecto* in the seasonal tropics of the Northern Territory, Australia. Wildlife Research 2000; 27(2):169-78.

23. Fleming TH, Eby P. Ecology of Bat Migration. In: Kunz TH, Fenton MB, eds. Bat Ecology. Chicago, Ill.:University of Chicago Press, 2003:156-208.

24. World Health Organization. Cause-specific mortality, 2008. In: global_burden_disease_DTH6_2008.xls ed. Excel. Geneva, Switzerland:Health Statistics and Informatics Department, World Health Organization, 2008.

25. Morse SS. Factors in the emergence of infectious diseases. Emerg Infect Dis 1995; 1(1):7-15.

26. Meslin FX. Global aspects of emerging and potential zoonoses: a WHO perspective. Emerg Infect Dis 1997; 3(2):223-8.

27. Hanada K, Suzuki Y, Gojobori T. A Large Variation in the Rates of Synonymous Substitution for RNA Viruses and Its Relationship to a Diversity of Viral Infection and Transmission Modes. Molecular Biology and Evolution 2004; 21(6):1074-80.

28. Morens DM, Folkers GK, Fauci AS. Emerging infections: a perpetual challenge. Lancet Infect Dis 2008; 8(11):710-9.

29. Morens DM, Folkers GK, Fauci AS. The challenge of emerging and re-emerging infectious diseases. Nature 2004; 430(6996):242-9.

30. World Health Organization. Zoonoses. Geneva, Switzerland, 2011.

31. Jones KE, Patel NG, Levy MA, Storeygard A, Balk D, Gittleman JL, Daszak P. Global trends in emerging infectious diseases. Nature 2008; 451(7181):990-3.

32. Parrish CR, Holmes EC, Morens DM*, et al.* Cross-species virus transmission and the emergence of new epidemic diseases. Microbiol Mol Biol Rev 2008; 72(3):457-70.

33. Ecker DJ, Sampath R, Willett P*, et al.* The Microbial Rosetta Stone Database: a compilation of global and emerging infectious microorganisms and bioterrorist threat agents. BMC Microbiol 2005; 5:19.

34. Belshaw R, Gardner A, Rambaut A, Pybus OG. Pacing a small cage: mutation and RNA viruses. Trends in Ecology & Evolution 2008; 23(4):188-93.

35. Ashford RW. When is a reservoir not a reservoir? Emerg Infect Dis 2003; 9(11):1495-6.

36. Haydon DT, Cleaveland S, Taylor LH, Laurenson MK. Identifying reservoirs of infection: a conceptual and practical challenge. Emerg Infect Dis 2002; 8(12):1468-73.

37. Nishiura H, Hoye B, Klaassen M, Bauer S, Heesterbeek H. How to find natural reservoir hosts from endemic prevalence in a multi-host population: a case study of influenza in waterfowl. Epidemics 2009; 1(2):118-28.

38. Messenger SL, Rupprecht CE, Smith JS. Bats, Emerging Virus Infections, and the Rabies Paradigm. In: Kunz TH, Fenton MB, eds. Bat Ecology. Chicago, Ill.:University of Chicago Press, 2003:622-79.

39. Calisher C, Childs J, Field H, Holmes K, Schountz T. Bats: important reservoir hosts of emerging viruses. Clin Microbiol Rev 2006; 19:531 - 45.

40. World Health Organization. Acute repiratory syndrome China, Hong Kong Special Administrative Region of China, and Viet Nam. Weekly epidemiological record, Vol. 78. Geneva, Switzerland:World Health Organization, 2003:73-80.

41. World Health Organization. Severe Acute Respiratory Syndrome (SARS): over 100 days into the outbreak. Weekly epidemiological record, Vol. 78. Geneva, Switzerland:World Health Organization, 2003:217-28.

42. Donnelly CA, Ghani AC, Leung GM*, et al.* Epidemiological determinants of spread of causal agent of severe acute respiratory syndrome in Hong Kong. Lancet 2003; 361(9371):1761-6.

43. World Health Organization. Summary of probable SARS cases with onset of illness from 1 November 2002 to 31 July 2003. Vol. 2011. Geneva, Switzerland:World Health Organization, 2011.

44. Peiris JS, Yuen KY, Osterhaus AD, Stohr K. The severe acute respiratory syndrome. N Engl J Med 2003; 349(25):2431-41.

45. Keogh-Brown MR, Smith RD. The economic impact of SARS: how does the reality match the predictions? Health Policy 2008; 88(1):110-20.

46. Smith RD. Responding to global infectious disease outbreaks: lessons from SARS on the role of risk perception, communication and management. Soc Sci Med 2006; 63(12):3113-23.

47. Peiris JSM, Lai ST, Poon LLM*, et al.* Coronavirus as a possible cause of severe acute respiratory syndrome. The Lancet 2003; 361(9366):1319-25.

48. Ksiazek TG, Erdman D, Goldsmith CS*, et al.* A Novel Coronavirus Associated with Severe Acute Respiratory Syndrome. New England Journal of Medicine 2003; 348(20):1953-66.

49. Rota PA, Oberste MS, Monroe SS*, et al.* Characterization of a novel coronavirus associated with severe acute respiratory syndrome. Science 2003; 300(5624):1394-9.

50. Marra MA, Jones SJ, Astell CR*, et al.* The Genome sequence of the SARS-associated coronavirus. Science 2003; 300(5624):1399-404.

51. Wang L, Eaton B. Bats, Civets and the Emergence of SARS. In: Childs JE, Mackenzie JS, Richt JA, eds. Wildlife and Emerging Zoonotic Diseases: The Biology, Circumstances and Consequences of Cross-Species Transmission, Vol. 315:Springer Berlin Heidelberg, 2007:325-44.

52. Perlman S, Netland J. Coronaviruses post-SARS: update on replication and pathogenesis. Nat Rev Microbiol 2009; 7(6):439-50.

53. Li W, Moore MJ, Vasilieva N*, et al.* Angiotensin-converting enzyme 2 is a functional receptor for the SARS coronavirus. Nature 2003; 426(6965):450-4.

54. Frieman M, Heise M, Baric R. SARS coronavirus and innate immunity. Virus Res 2008; 133(1):101-12.

55. Thiel V, Weber F. Interferon and cytokine responses to SARS-coronavirus infection. Cytokine & Growth Factor Reviews 2008; 19(2):121-32.

56. Guan Y, Zheng BJ, He YQ*, et al.* Isolation and characterization of viruses related to the SARS coronavirus from animals in southern China. Science 2003; 302(5643):276-8.

57. Wu D, Tu C, Xin C*, et al.* Civets are equally susceptible to experimental infection by two different severe acute respiratory syndrome coronavirus isolates. J Virol 2005; 79(4):2620-5.

58. Mickleburgh SP, Hutson AM, Racey PA. A review of the global conservation status of bats. Oryx 2002; 36(01):18-34.

59. Li W, Shi Z, Yu M, Ren W, Smith C. Bats Are Natural Reservoirs of SARS-Like Coronaviruses. Science 2005; 310:676 - 9.

60. Lau S, Woo P, Li K, Huang Y, Tsoi H-W. Severe acute respiratory syndrome coronavirus-like virus in Chinese horseshoe bats. Proceedings of the National Academy of Sciences of the United States of America 2005; 102:14040 - 5.

61. Gloza-Rausch F, Ipsen A, Seebens A*, et al.* Detection and prevalence patterns of group I coronaviruses in bats, northern Germany. Emerg Infect Dis 2008; 14(4):626-31.

62. Dominguez SR, O'Shea TJ, Oko LM, Holmes KV. Detection of group 1 coronaviruses in bats in North America. Emerg Infect Dis 2007; 13(9):1295-300.

63. Tong S, Conrardy C, Ruone S*, et al.* Detection of novel SARS-like and other coronaviruses in bats from Kenya. Emerg Infect Dis 2009; 15(3):482-5.

64. Woo PC, Lau SK, Li KS*, et al.* Molecular diversity of coronaviruses in bats. Virology 2006; 351(1):180-7.

65. Watanabe S, Masangkay JS, Nagata N*, et al.* Bat coronaviruses and experimental infection of bats, the Philippines. Emerg Infect Dis 2010; 16(8):1217-23.

66. Li F, Li W, Farzan M, Harrison SC. Structure of SARS coronavirus spike receptor-binding domain complexed with receptor. Science 2005; 309(5742):1864-8.

67. Li W, Zhang C, Sui J*, et al.* Receptor and viral determinants of SARS-coronavirus adaptation to human ACE2. EMBO J 2005; 24(8):1634-43.

68. Ren W, Qu X, Li W*, et al.* Difference in receptor usage between severe acute respiratory syndrome (SARS) coronavirus and SARS-like coronavirus of bat origin. J Virol 2008; 82(4):1899-907.

69. Feldmann H, Geisbert TW. Ebola haemorrhagic fever. Lancet 2011; 377(9768):849-62.

70. Georges A-J, Leroy EM, Renaut AA*, et al.* Ebola Hemorrhagic Fever Outbreaks in Gabon, 1994–1997: Epidemiologic and Health Control Issues. Journal of Infectious Diseases 1999; 179(Supplement 1):S65-S75.

71. Known Cases and Outbreaks of Ebola Hemorrhagic Fever, in Chronological Order. Vol. 2011:CDC/Special Pathogens Branch, 2010.

72. Barrette RW, Metwally SA, Rowland JM*, et al.* Discovery of Swine as a Host for the Reston ebolavirus. Science 2009; 325(5937):204-6.

73. Jaax N, Jahrling P, Geisbert T*, et al.* Transmission of Ebola virus (Zaire strain) to uninfected control monkeys in a biocontainment laboratory. The Lancet 1995; 346(8991-8992):1669-71.

74. Jaax NK, Davis KJ, Geisbert TJ, Vogel P, Jaax GP, Topper M, Jahrling PB. Lethal experimental infection of rhesus monkeys with Ebola-Zaire (Mayinga) virus by the oral and conjunctival route of exposure. Arch Pathol Lab Med 1996; 120(2):140-55.

75. Barrette RW, Xu L, Rowland JM, McIntosh MT. Current perspectives on the phylogeny of Filoviridae. Infection, Genetics and Evolution 2011; In Press, Uncorrected Proof.

76. Dolnik O, Kolesnikova L, Becker S. Filoviruses: Interactions with the host cell. Cellular and Molecular Life Sciences 2008; 65(5):756-76.

77. Peters CJ, Sanchez A, Feldmann H, Rollin PE, Nichol S, Ksiazek TG. Filoviruses as emerging pathogens. Seminars in Virology 1994; 5(2):147-54.

78. Swanepoel R, Leman PA, Burt FJ*, et al.* Experimental inoculation of plants and animals with Ebola virus. Emerg Infect Dis 1996; 2(4):321-5.

79. Leroy EM, Epelboin A, Mondonge V, Pourrut X, Gonzalez JP, Muyembe-Tamfum JJ, Formenty P. Human Ebola outbreak resulting from direct exposure to fruit bats in Luebo, Democratic Republic of Congo, 2007. Vector Borne Zoonotic Dis 2009; 9(6):723-8.

80. Pourrut X, Souris M, Towner J, Rollin P, Nichol S. Large serological survey showing cocirculation of Ebola and Marburg viruses in Gabonese bat populations, and a high seroprevalence of both viruses in Rousettus aegyptiacus. BMC Infectious Diseases 2009; 9:159.

81. Leroy EM, Kumulungui B, Pourrut X*, et al.* Fruit bats as reservoirs of Ebola virus. Nature 2005; 438(7068):575-6.

82. Pourrut X, Délicat A, Rollin PE, Ksiazek TG, Gonzalez J-P, Leroy EM. Spatial and Temporal Patterns of Zaire ebolavirus Antibody Prevalence in the Possible Reservoir Bat Species. Journal of Infectious Diseases 2007; 196(Supplement 2):S176-S83.

83. Hayman DTS, Emmerich P, Yu M, Wang L-F, Suu-Ire R, Fooks AR, Cunningham AA, Wood JLN. Long-Term Survival of an Urban Fruit Bat Seropositive for Ebola and Lagos Bat Viruses. PLoS One 2010; 5(8):e11978.

84. Biek R, Walsh PD, Leroy EM, Real LA. Recent Common Ancestry of Ebola Zaire Virus Found in a Bat Reservoir. PLoS Pathog 2006; 2(10):e90.

85. Kondratowicz AS, Lennemann NJ, Sinn PL*, et al.* T-cell immunoglobulin and mucin domain 1 (TIM-1) is a receptor for Zaire Ebolavirus and Lake Victoria Marburgvirus. Proceedings of the National Academy of Sciences 2011; 108(20):8426-31.

86. Wang J, Manicassamy B, Caffrey M, Rong L. Characterization of the receptor-binding domain of Ebola glycoprotein in viral entry. Virologica Sinica 2011; 26(3):156-70.

87. Chua KB. Nipah virus outbreak in Malaysia. J Clin Virol 2003; 26(3):265-75.

88. Chua KB, Goh KJ, Wong KT*, et al.* Fatal encephalitis due to Nipah virus among pig-farmers in Malaysia. Lancet 1999; 354(9186):1257-9.

89. Lo MK, Rota PA. The emergence of Nipah virus, a highly pathogenic paramyxovirus. J Clin Virol 2008; 43(4):396-400.

90. Parashar UD, Sunn LM, Ong F*, et al.* Case-Control Study of Risk Factors for Human Infection with a New Zoonotic Paramyxovirus, Nipah Virus, during a 1998–1999 Outbreak of Severe Encephalitis in Malaysia. Journal of Infectious Diseases 2000; 181(5):1755-9.

91. Middleton DJ, Westbury HA, Morrissy CJ, van der Heide BM, Russell GM, Braun MA, Hyatt AD. Experimental Nipah Virus Infection in Pigs and Cats. Journal of Comparative Pathology 2002; 126(2-3):124-36.

92. Chua KB, Bellini WJ, Rota PA*, et al.* Nipah virus: a recently emergent deadly paramyxovirus. Science 2000; 288(5470):1432-5.

93. Luby SP, Hossain MJ, Gurley ES*, et al.* Recurrent zoonotic transmission of Nipah virus into humans, Bangladesh, 2001-2007. Emerg Infect Dis 2009; 15(8):1229-35.

94. Hughes JM, Wilson ME, Luby SP, Gurley ES, Hossain MJ. Transmission of Human Infection with Nipah Virus. Clinical Infectious Diseases 2009; 49(11):1743-8.

95. World Health Organization. Chronology of Nipah virus outbreaks. In: nipah_chronology_en.pdf ed. Geneva, Switzerland, 2009.

96. Eaton BT, Broder CC, Middleton D, Wang LF. Hendra and Nipah viruses: different and dangerous. Nat Rev Microbiol 2006; 4(1):23-35.

97. Shaw ML, Garcia-Sastre A, Palese P, Basler CF. Nipah virus V and W proteins have a common STAT1-binding domain yet inhibit STAT1 activation from the cytoplasmic and nuclear compartments, respectively. J Virol 2004; 78(11):5633-41.

98. Bonaparte MI, Dimitrov AS, Bossart KN*, et al.* Ephrin-B2 ligand is a functional receptor for Hendra virus and Nipah virus. Proc Natl Acad Sci U S A 2005; 102(30):10652-7.

99. Negrete OA, Levroney EL, Aguilar HC, Bertolotti-Ciarlet A, Nazarian R, Tajyar S, Lee B. EphrinB2 is the entry receptor for Nipah virus, an emergent deadly paramyxovirus. Nature 2005; 436(7049):401-5.

100. Negrete OA, Wolf MC, Aguilar HC*, et al.* Two key residues in ephrinB3 are critical for its use as an alternative receptor for Nipah virus. PLoS Pathog 2006; 2(2):e7.

101. Bellini W, Harcourt B, Bowden N, Rota P. Nipah virus: An emergent paramyxovirus causing severe encephalitis in humans. Journal of NeuroVirology 2005; 11(5):481-7.

102. Diederich S, Maisner A. Molecular Characteristics of the Nipah Virus Glycoproteins. Annals of the New York Academy of Sciences 2007; 1102(1):39-50.

103. Pager CT, Craft Jr WW, Patch J, Dutch RE. A mature and fusogenic form of the Nipah virus fusion protein requires proteolytic processing by cathepsin L. Virology 2006; 346(2):251-7.

104. Diederich S, Moll M, Klenk HD, Maisner A. The nipah virus fusion protein is cleaved within the endosomal compartment. J Biol Chem 2005; 280(33):29899-903.

105. Yob JM, Field H, Rashdi AM*, et al.* Nipah virus infection in bats (order Chiroptera) in peninsular Malaysia. Emerg Infect Dis 2001; 7(3):439-41.

106. Chua K, Lek Koh C, Hooi P, Wee K, Khong J. Isolation of Nipah virus from Malaysian Island flying-foxes. Microbes and Infection 2002; 4:145 - 51.

107. Rahman SA, Hassan SS, Olival KJ*, et al.* Characterization of Nipah virus from naturally infected Pteropus vampyrus bats, Malaysia. Emerg Infect Dis 2010; 16(12):1990-3.

108. Middleton DJ, Morrissy CJ, van der Heide BM, Russell GM, Braun MA, Westbury HA, Halpin K, Daniels PW. Experimental Nipah virus infection in pteropid bats (Pteropus poliocephalus). J Comp Pathol 2007; 136(4):266-72.

109. Sohayati AR, Hassan L, Sharifah SH*, et al.* Evidence for Nipah virus recrudescence and serological patterns of captive Pteropus vampyrus. Epidemiol Infect 2011; 139(Special Issue 10):1570-9.

110. Wacharapluesadee S, Boongird K, Wanghongsa S, Ratanasetyuth N, Supavonwong P, Saengsen D, Gongal GN, Hemachudha T. A longitudinal study of the prevalence of Nipah virus in Pteropus lylei bats in Thailand: evidence for seasonal preference in disease transmission. Vector Borne Zoonotic Dis 2010; 10(2):183-90.

111. Epstein JH, Prakash V, Smith CS, Daszak P, McLaughlin AB, Meehan G, Field HE, Cunningham AA. Henipavirus infection in fruit bats (Pteropus giganteus), India. Emerg Infect Dis 2008; 14(8):1309-11.

112. Iehle C, Razafitrimo G, Razainirina J*, et al.* Henipavirus and Tioman virus antibodies in pteropodid bats, Madagascar. Emerg Infect Dis 2007; 13(1):159-61.

113. Olson JG, Rupprecht C, Rollin PE, An US, Niezgoda M, Clemins T, Walston J, Ksiazek TG. Antibodies to Nipah-like virus in bats (Pteropus lylei), Cambodia. Emerg Infect Dis 2002; 8(9):987-8.

114. Reynes JM, Counor D, Ong S*, et al.* Nipah virus in Lyle's flying foxes, Cambodia. Emerg Infect Dis 2005; 11(7):1042-7.

115. Hsu VP, Hossain MJ, Parashar UD*, et al.* Nipah virus encephalitis reemergence, Bangladesh. Emerg Infect Dis 2004; 10(12):2082-7.

116. Wacharapluesadee S, Hemachudha T. Duplex nested RT-PCR for detection of Nipah virus RNA from urine specimens of bats. Journal of Virological Methods 2007; 141(1):97-101.

117. Wacharapluesadee S, Lumlertdacha B, Boongird K*, et al.* Bat Nipah virus, Thailand. Emerg Infect Dis 2005; 11(12):1949-51.

118. Fogarty R, Halpin K, Hyatt AD, Daszak P, Mungall BA. Henipavirus susceptibility to environmental variables. Virus Res 2008; 132(1-2):140-4.

119. Luby SP, Rahman M, Hossain MJ*, et al.* Foodborne transmission of Nipah virus, Bangladesh. Emerg Infect Dis 2006; 12(12):1888-94.

120. Tan C-T, Chua K-B. Nipah virus encephalitis. Current Infectious Disease Reports 2008; 10(4):315-20.

121. Wong KT, Shieh W-J, Kumar S*, et al.* Nipah Virus Infection: Pathology and Pathogenesis of an Emerging Paramyxoviral Zoonosis. Am J Pathol 2002; 161(6):2153-67.

122. Hooper P, Zaki S, Daniels P, Middleton D. Comparative pathology of the diseases caused by Hendra and Nipah viruses. Microbes and Infection 2001; 3(4):315-22.

123. Salah Uddin Khan M, Hossain J, Gurley E, Nahar N, Sultana R, Luby S. Use of Infrared Camera to Understand Bats' Access to Date Palm Sap: Implications for Preventing Nipah Virus Transmission. Ecohealth 2011:1-9.

124. Montgomery JM, Hossain MJ, Gurley E*, et al.* Risk factors for Nipah virus encephalitis in Bangladesh. Emerg Infect Dis 2008; 14(10):1526-32.

125. Hossain MJ, Gurley ES, Montgomery JM*, et al.* Clinical presentation of nipah virus infection in Bangladesh. Clin Infect Dis 2008; 46(7):977-84.

126. Geisbert TW, Daddario-DiCaprio KM, Hickey AC*, et al.* Development of an Acute and Highly Pathogenic Nonhuman Primate Model of Nipah Virus Infection. PLoS One 2010; 5(5):e10690.

127. Harcourt BH, Lowe L, Tamin A*, et al.* Genetic characterization of Nipah virus, Bangladesh, 2004. Emerg Infect Dis 2005; 11(10):1594-7.

128. AbuBakar S, Chang LY, Ali AR, Sharifah SH, Yusoff K, Zamrod Z. Isolation and molecular identification of Nipah virus from pigs. Emerg Infect Dis 2004; 10(12):2228-30.

129. Bossart KN, Tachedjian M, McEachern JA, Crameri G, Zhu Z, Dimitrov DS, Broder CC, Wang LF. Functional studies of host-specific ephrin-B ligands as Henipavirus receptors. Virology 2008; 372(2):357-71.

130. Chakraborty AK, Chakravarty AK. Thymus in Different gaes of a Bat, *Pteropus Giganteus*. Current Science (Bangalore) 1984; 53:39-40.

131. Crowley G, Hall L. Histological Observations on the Wing of the Grey-Headed Flying-Fox (Pteropus-Poliocephalus) (Chiroptera, Pteropodidae). Australian Journal of Zoology 1994; 42(2):215-31.

132. Omatsu T, Watanabe S, Akashi H, Yoshikawa Y. Biological characters of bats in relation to natural reservoir of emerging viruses. Comparative Immunology, Microbiology and Infectious Diseases 2007; 30(5-6):357-74.

133. Chakravarty AK, Paul BN. Analysis of suppressor factor in delayed immune responses of a bat, Pteropus giganteus. Dev Comp Immunol 1987; 11(3):649-60.

134. Sarkar SK, Chakravarty AK. Analysis of immunocompetent cells in the bat, Pteropus giganteus: isolation and scanning electron microscopic characterization. Dev Comp Immunol 1991; 15(4):423-30.

135. Lewis JH. Comparative hematology: Studies on chiroptera, Pteropus giganteous. Comparative Biochemistry and Physiology Part A: Physiology 1977; 58(1):103-7.

136. Heard DJ, Darby AW. Hematologic and Plasma Biochemical Reference Values for Three Flying Fox Species (Pteropus sp.). Journal of Zoo and Wildlife Medicine 1997; 28(4):464-70.

137. Van Der Westhuyzen J. Haematology and iron status of the egyptian fruit bat, rousettus aegyptiacus. Comparative Biochemistry and Physiology Part A: Physiology 1988; 90(1):117-20.

138. Garcia-Sastre A. Influenza virus receptor specificity: disease and transmission. Am J Pathol 2010; 176(4):1584-5.

139. Suzuki Y, Ito T, Suzuki T, Holland RE, Jr., Chambers TM, Kiso M, Ishida H, Kawaoka Y. Sialic acid species as a determinant of the host range of influenza A viruses. J Virol 2000; 74(24):11825-31.

140. Omatsu T, Nishimura Y, Bak EJ, Ishii Y, Tohya Y, Kyuwa S, Akashi H, Yoshikawa Y. Molecular cloning and sequencing of the cDNA encoding the bat CD4. Veterinary Immunology and Immunopathology 2006; 111(3-4):309-13.

141. Chakraborty AK, Chakravarty AK. Antibody-mediated immune response in the bat, Pteropus giganteus. Dev Comp Immunol 1984; 8(2):415-23.

142. Paul BN, Chakravarty AK. In vitro analysis of delayed immune response in a bat, Pteropus giganteus: process of con-A mediated activation. Dev Comp Immunol 1986; 10(1):55-67.

143. Chakravarty AK, Chakraborty AK. Histophysiology of the White Pulp Follicles and the Germinal Centres in Spleen and Lymph Nodes of a Bat, Flying Fox *(Pteropus giganteus)*. Comparative Physiology and Ecology 1984; 9(3):197-200.

144. Ghiringhelli F, Larmonier N, Schmitt E*, et al.* CD4+CD25+ regulatory T cells suppress tumor immunity but are sensitive to cyclophosphamide which allows immunotherapy of established tumors to be curative. European Journal of Immunology 2004; 34(2):336-44.

145. Omatsu T, Ishii Y, Kyuwa S, Milanda EG, Terao K, Yoshikawa Y. Molecular evolution inferred from immunological cross-reactivity of immunoglobulin G among Chiroptera and closely related species. Exp Anim 2003; 52(5):425-8.

146. Wellehan JF, Jr., Green LG, Duke DG, Bootorabi S, Heard DJ, Klein PA, Jacobson ER. Detection of specific antibody responses to vaccination in variable flying foxes (Pteropus hypomelanus). Comp Immunol Microbiol Infect Dis 2009; 32(5):379-94.

147. Butler JE. Immunoglobulin gene organization and the mechanism of repertoire development. Scand J Immunol 1997; 45(5):455-62.

148. Kirkham PM, Mortari F, Newton JA, Schroeder HW, Jr. Immunoglobulin VH clan and family identity predicts variable domain structure and may influence antigen binding. EMBO J 1992; 11(2):603-9.

149. Baker ML, Tachedjian M, Wang LF. Immunoglobulin heavy chain diversity in Pteropid bats: evidence for a diverse and highly specific antigen binding repertoire. Immunogenetics 2010; 62(3):173-84.

150. Haller O, Kochs G, Weber F. The interferon response circuit: induction and suppression by pathogenic viruses. Virology 2006; 344(1):119-30.

151. Iversen MB, Paludan SR. Mechanisms of type III interferon expression. J Interferon Cytokine Res 2010; 30(8):573-8.

152. Sadler AJ, Williams BR. Interferon-inducible antiviral effectors. Nat Rev Immunol 2008; 8(7):559-68.

153. Randall RE, Goodbourn S. Interferons and viruses: an interplay between induction, signalling, antiviral responses and virus countermeasures. Journal of General Virology 2008; 89(1):1-47.

154. Onoguchi K, Yoneyama M, Takemura A, Akira S, Taniguchi T, Namiki H, Fujita T. Viral infections activate types I and III interferon genes through a common mechanism. J Biol Chem 2007; 282(10):7576-81.

155. Baum A, García-Sastre A. Induction of type I interferon by RNA viruses: cellular receptors and their substrates. Amino Acids 2010; 38(5):1283-99.

156. Donnelly RP, Kotenko SV. Interferon-lambda: a new addition to an old family. J Interferon Cytokine Res 2010; 30(8):555-64.

157. Zhao C, Denison C, Huibregtse JM, Gygi S, Krug RM. Human ISG15 conjugation targets both IFN-induced and constitutively expressed proteins functioning in diverse cellular pathways. Proc Natl Acad Sci U S A 2005; 102(29):10200-5.

158. Lu G, Reinert JT, Pitha-Rowe I, Okumura A, Kellum M, Knobeloch KP, Hassel B, Pitha PM. ISG15 enhances the innate antiviral response by inhibition of IRF-3 degradation. Cell Mol Biol (Noisy-le-grand) 2006; 52(1):29-41.

159. Pestka S, Krause CD, Walter MR. Interferons, interferon-like cytokines, and their receptors. Immunol Rev 2004; 202:8-32.

160. Kawai T, Akira S. TLR signaling. Cell Death Differ 2006; 13(5):816-25.

161. Skaug B, Chen ZJ. Emerging role of ISG15 in antiviral immunity. Cell 2010; 143(2):187-90.

162. Haller O, Kochs G. Human MxA Protein: An Interferon-Induced Dynamin-Like GTPase with Broad Antiviral Activity. Journal of Interferon & Cytokine Research 2011; 31(1):79-87.

163. Silverman RH. Viral Encounters with 2',5'-Oligoadenylate Synthetase and RNase L during the Interferon Antiviral Response. J Virol 2007; 81(23):12720-9.

164. Patel RC, Sen GC. PACT, a protein activator of the interferon-induced protein kinase, PKR. EMBO J 1998; 17(15):4379-90.

165. Cochet M, Vaiman D, Lefevre F. Novel interferon delta genes in mammals: cloning of one gene from the sheep, two genes expressed by the horse conceptus and discovery of related sequences in several taxa by genomic database screening. Gene 2009; 433(1-2):88-99.

166. Oritani K, Tomiyama Y. Interferon- ζ/Limitin: Novel Type I Interferon That Displays a Narrow Range of Biological Activity. International Journal of Hematology 2004; 80(4):325-31.

167. LaFleur DW, Nardelli B, Tsareva T*, et al.* Interferon-kappa, a novel type I interferon expressed in human keratinocytes. J Biol Chem 2001; 276(43):39765-71.

168. Sang Y, Rowland RR, Hesse RA, Blecha F. Differential expression and activity of the porcine type I interferon family. Physiol Genomics 2010; 42(2):248-58.

169. Schultz U, Kaspers B, Staeheli P. The interferon system of non-mammalian vertebrates. Dev Comp Immunol 2004; 28(5):499-508.

170. Horvath CM. STAT proteins and transcriptional responses to extracellular signals. Trends in Biochemical Sciences 2000; 25(10):496-502.

171. Levy DE, Garcia-Sastre A. The virus battles: IFN induction of the antiviral state and mechanisms of viral evasion. Cytokine Growth Factor Rev 2001; 12(2-3):143-56.

172. Fujii H, Watanabe S, Yamane D*, et al.* Functional analysis of Rousettus aegyptiacus "signal transducer and activator of transcription 1" (STAT1). Developmental & Comparative Immunology 2010; 34(5):598-602.

173. Ortaldo JR, Herberman RB, Harvey C, Osheroff P, Pan YC, Kelder B, Pestka S. A species of human alpha interferon that lacks the ability to boost human natural killer activity. Proc Natl Acad Sci U S A 1984; 81(15):4926-9.

174. Rani MRS, Foster GR, Leung S, Leaman D, Stark GR, Ransohoff RM. Characterization of β-R1, a Gene That Is Selectively Induced by Interferon β (IFN-β) Compared with IFN-α. Journal of Biological Chemistry 1996; 271(37):22878-84.

175. Karpusas M, Whitty A, Runkel L, Hochman P. The structure of human interferon-beta: implications for activity. Cell Mol Life Sci 1998; 54(11):1203-16.

176. Sommereyns C, Michiels T. N-glycosylation of murine IFN-beta in a putative receptor-binding region. J Interferon Cytokine Res 2006; 26(6):406-13.

177. Slutzki M, Jaitin DA, Yehezkel TB, Schreiber G. Variations in the Unstructured C-terminal Tail of Interferons Contribute to Differential Receptor Binding and Biological Activity. Journal of Molecular Biology 2006; 360(5):1019-30.

178. Rehberg E, Kelder B, Hoal EG, Pestka S. Specific molecular activities of recombinant and hybrid leukocyte interferons. J Biol Chem 1982; 257(19):11497-502.

179. Lin LS, Abreu SL. Production, purification and characterization of rat interferon. Arch Virol 1979; 62(3):221-7.

180. Ank N, Iversen MB, Bartholdy C*, et al.* An important role for type III interferon (IFN-lambda/IL-28) in TLR-induced antiviral activity. J Immunol 2008; 180(4):2474-85.

181. Pagliaccetti NE, Robek MD. Interferon-λ in the Immune Response to Hepatitis B Virus and Hepatitis C Virus. Journal of Interferon & Cytokine Research 2010; 30(8):585-90.

182. Lasfar A, Lewis-Antes A, Smirnov SV*, et al.* Characterization of the mouse IFN-lambda ligand-receptor system: IFN-lambdas exhibit antitumor activity against B16 melanoma. Cancer Res 2006; 66(8):4468-77.

183. Sang Y, Rowland RR, Blecha F. Molecular characterization and antiviral analyses of porcine type III interferons. J Interferon Cytokine Res 2010; 30(11):801-7.

184. Cowled C, Baker M, Tachedjian M, Zhou P, Bulach D, Wang LF. Molecular characterisation of Toll-like receptors in the black flying fox Pteropus alecto. Dev Comp Immunol 2011; 35(1):7-18.

185. Iha K, Omatsu T, Watanabe S*, et al.* Molecular Cloning and Expression Analysis of Bat Toll-Like Receptors 3, 7 and 9. The Journal of Veterinary Medical Science 2010; 72(2):217-20.

186. Omatsu T, Bak E-J, Ishii Y, Kyuwa S, Tohya Y, Akashi H, Yoshikawa Y. Induction and sequencing of Rousette bat interferon [alpha] and [beta] genes. Veterinary Immunology and Immunopathology 2008; 124(1-2):169-76.

187. Kepler T, Sample C, Hudak K, Roach J, Haines A, Walsh A, Ramsburg E. Chiropteran types I and II interferon genes inferred from genome sequencing traces by a statistical gene-family assembler. BMC Genomics 2010; 11(1):444.

188. Zhou P, Cowled C, Todd S*, et al.* Type III IFNs in Pteropid Bats: Differential Expression Patterns Provide Evidence for Distinct Roles in Antiviral Immunity. The Journal of Immunology 2011; 186(5):3138-47.

189. Yaiw KC, Bingham J, Crameri G*, et al.* Tioman virus, a paramyxovirus of bat origin, causes mild disease in pigs and has a predilection for lymphoid tissues. J Virol 2008; 82(1):565-8.

190. Chua KB, Wang L-F, Lam SK*, et al.* Tioman Virus, a Novel Paramyxovirus Isolated from Fruit Bats in Malaysia. Virology 2001; 283(2):215-29.

191. Childs K, Stock N, Ross C, Andrejeva J, Hilton L, Skinner M, Randall R, Goodbourn S. mda-5, but not RIG-I, is a common target for paramyxovirus V proteins. Virology 2007; 359(1):190-200.

192. Ahmed M, McKenzie MO, Puckett S, Hojnacki M, Poliquin L, Lyles DS. Ability of the matrix protein of vesicular stomatitis virus to suppress beta interferon gene expression is genetically correlated with the inhibition of host RNA and protein synthesis. J Virol 2003; 77(8):4646-57.

193. Yuan H, Yoza BK, Lyles DS. Inhibition of host RNA polymerase II-dependent transcription by vesicular stomatitis virus results from inactivation of TFIID. Virology 1998; 251(2):383-92.

194. Smith GL, Symons JA, Alcamí A. Poxviruses: Interfering with Interferon. Seminars in Virology 1998; 8(5):409-18.

195. Kopecky-Bromberg SA, Martinez-Sobrido L, Frieman M, Baric RA, Palese P. Severe acute respiratory syndrome coronavirus open reading frame (ORF) 3b, ORF 6, and nucleocapsid proteins function as interferon antagonists. J Virol 2007; 81(2):548-57.

196. Devaraj SG, Wang N, Chen Z*, et al.* Regulation of IRF-3-dependent Innate Immunity by the Papain-like Protease Domain of the Severe Acute Respiratory Syndrome Coronavirus. Journal of Biological Chemistry 2007; 282(44):32208-21.

197. Lindner HA, Lytvyn V, Qi H, Lachance P, Ziomek E, Ménard R. Selectivity in ISG15 and ubiquitin recognition by the SARS coronavirus papain-like protease. Archives of Biochemistry and Biophysics 2007; 466(1):8-14.

198. Siu K-L, Kok K-H, Ng M-HJ, Poon VKM, Yuen K-Y, Zheng B-J, Jin D-Y. Severe Acute Respiratory Syndrome Coronavirus M Protein Inhibits Type I Interferon Production by Impeding the Formation of TRAF3·TANK·TBK1/IKKϵ Complex. Journal of Biological Chemistry 2009; 284(24):16202-9.

199. Frieman M, Yount B, Heise M, Kopecky-Bromberg SA, Palese P, Baric RS. Severe acute respiratory syndrome coronavirus ORF6 antagonizes STAT1 function by sequestering nuclear import factors on the rough endoplasmic reticulum/Golgi membrane. J Virol 2007; 81(18):9812-24.

200. Kopecky-Bromberg SA, Martinez-Sobrido L, Palese P. 7a protein of severe acute respiratory syndrome coronavirus inhibits cellular protein synthesis and activates p38 mitogen-activated protein kinase. J Virol 2006; 80(2):785-93.

201. Kamitani W, Narayanan K, Huang C, Lokugamage K, Ikegami T, Ito N, Kubo H, Makino S. Severe acute respiratory syndrome coronavirus nsp1 protein suppresses host gene expression by promoting host mRNA degradation. Proc Natl Acad Sci U S A 2006; 103(34):12885-90.

202. Zust R, Cervantes-Barragan L, Kuri T, Blakqori G, Weber F, Ludewig B, Thiel V. Coronavirus non-structural protein 1 is a major pathogenicity factor: implications for the rational design of coronavirus vaccines. PLoS Pathog 2007; 3(8):e109.

203. Wathelet MG, Orr M, Frieman MB, Baric RS. Severe acute respiratory syndrome coronavirus evades antiviral signaling: role of nsp1 and rational design of an attenuated strain. J Virol 2007; 81(21):11620-33.

204. Harcourt BH, Sanchez A, Offermann MK. Ebola Virus Selectively Inhibits Responses to Interferons, but Not to Interleukin-1beta , in Endothelial Cells. J Virol 1999; 73(4):3491-6.

205. Kash JC, Muhlberger E, Carter V*, et al.* Global suppression of the host antiviral response by Ebola- and Marburgviruses: increased antagonism of the type I interferon response is associated with enhanced virulence. J Virol 2006; 80(6):3009-20.

206. Basler CF, Amarasinghe GK. Evasion of interferon responses by Ebola and Marburg viruses. J Interferon Cytokine Res 2009; 29(9):511-20.

207. Basler CF, Mikulasova A, Martinez-Sobrido L*, et al.* The Ebola virus VP35 protein inhibits activation of interferon regulatory factor 3. J Virol 2003; 77(14):7945-56.

208. Cardenas WB, Loo YM, Gale M, Jr., Hartman AL, Kimberlin CR, Martinez-Sobrido L, Saphire EO, Basler CF. Ebola virus VP35 protein binds double-stranded RNA and inhibits alpha/beta interferon production induced by RIG-I signaling. J Virol 2006; 80(11):5168-78.

209. Feng Z, Cerveny M, Yan Z, He B. The VP35 protein of Ebola virus inhibits the antiviral effect mediated by double-stranded RNA-dependent protein kinase PKR. J Virol 2007; 81(1):182-92.

210. Schumann M, Gantke T, Muhlberger E. Ebola virus VP35 antagonizes PKR activity through its C-terminal interferon inhibitory domain. J Virol 2009; 83(17):8993-7.

211. Prins KC, Cardenas WB, Basler CF. Ebola virus protein VP35 impairs the function of interferon regulatory factor-activating kinases IKKepsilon and TBK-1. J Virol 2009; 83(7):3069-77.

212. Kubota T, Matsuoka M, Chang T-H, Tailor P, Sasaki T, Tashiro M, Kato A, Ozato K. Virus Infection Triggers SUMOylation of IRF3 and IRF7, Leading to the Negative Regulation of Type I Interferon Gene Expression. Journal of Biological Chemistry 2008; 283(37):25660-70.

213. Chang T-H, Kubota T, Matsuoka M, Jones S, Bradfute SB, Bray M, Ozato K. Ebola Zaire Virus Blocks Type I Interferon Production by Exploiting the Host SUMO Modification Machinery. PLoS Pathog 2009; 5(6):e1000493.

214. Reid SP, Leung LW, Hartman AL*, et al.* Ebola virus VP24 binds karyopherin alpha1 and blocks STAT1 nuclear accumulation. J Virol 2006; 80(11):5156-67.

215. Park MS, Shaw ML, Munoz-Jordan J*, et al.* Newcastle disease virus (NDV)-based assay demonstrates interferon-antagonist activity for the NDV V protein and the Nipah virus V, W, and C proteins. J Virol 2003; 77(2):1501-11.

216. Yoneda M, Guillaume V, Sato H*, et al.* The Nonstructural Proteins of Nipah Virus Play a Key Role in Pathogenicity in Experimentally Infected Animals. PLoS One 2010; 5(9):e12709.

217. Shaw ML, Cardenas WB, Zamarin D, Palese P, Basler CF. Nuclear localization of the Nipah virus W protein allows for inhibition of both virus- and toll-like receptor 3-triggered signaling pathways. J Virol 2005; 79(10):6078-88.

218. Rodriguez JJ, Parisien JP, Horvath CM. Nipah virus V protein evades alpha and gamma interferons by preventing STAT1 and STAT2 activation and nuclear accumulation. J Virol 2002; 76(22):11476-83.

219. Rodriguez JJ, Cruz CD, Horvath CM. Identification of the nuclear export signal and STAT-binding domains of the Nipah virus V protein reveals mechanisms underlying interferon evasion. J Virol 2004; 78(10):5358-67.

220. Harcourt BH, Tamin A, Ksiazek TG, Rollin PE, Anderson LJ, Bellini WJ, Rota PA. Molecular characterization of Nipah virus, a newly emergent paramyxovirus. Virology 2000; 271(2):334-49.

221. Wang L, Harcourt BH, Yu M, Tamin A, Rota PA, Bellini WJ, Eaton BT. Molecular biology of Hendra and Nipah viruses. Microbes Infect 2001; 3(4):279-87.

222. Kulkarni S, Volchkova V, Basler CF, Palese P, Volchkov VE, Shaw ML. Nipah virus edits its P gene at high frequency to express the V and W proteins. J Virol 2009; 83(8):3982-7.

223. Lo MK, Harcourt BH, Mungall BA, Tamin A, Peeples ME, Bellini WJ, Rota PA. Determination of the henipavirus phosphoprotein gene mRNA editing frequencies and detection of the C, V and W proteins of Nipah virus in virus-infected cells. J Gen Virol 2009; 90(Pt 2):398-404.

224. Park C, Lecomte MJ, Schindler C. Murine Stat2 is uncharacteristically divergent. Nucleic Acids Res 1999; 27(21):4191-9.

225. Parisien JP, Lau JF, Horvath CM. STAT2 acts as a host range determinant for species-specific paramyxovirus interferon antagonism and simian virus 5 replication. J Virol 2002; 76(13):6435-41.

226. Qureshi SA, Leung S, Kerr IM, Stark GR, Darnell JE, Jr. Function of Stat2 protein in transcriptional activation by alpha interferon. Mol Cell Biol 1996; 16(1):288-93.

227. Ebihara H, Takada A, Kobasa D*, et al.* Molecular Determinants of Ebola Virus Virulence in Mice. PLoS Pathog 2006; 2(7):e73.

228. Bluyssen HA, Levy DE. Stat2 is a transcriptional activator that requires sequence-specific contacts provided by stat1 and p48 for stable interaction with DNA. J Biol Chem 1997; 272(7):4600-5.

229. Knight E, Jr., Fahey D. Human interferon-beta: effects of deglycosylation. J Interferon Res 1982; 2(3):421-9.

230. Runkel L, Meier W, Pepinsky RB*, et al.* Structural and functional differences between glycosylated and non-glycosylated forms of human interferon-beta (IFN-beta). Pharm Res 1998; 15(4):641-9.

231. Watanabe Y, Kawade Y. Properties of non-glycosylated human interferon-beta from MG63 cells. J Gen Virol 1983; 64 (Pt 6):1391-5.

232. Iwata A, Saito T, Mizukoshi-Iwata N, Fujino M, Katsumata A, Hamada K, Sokawa Y, Ueda S. Cloning and expression of the canine interferon-beta gene. J Interferon Cytokine Res 1996; 16(10):765-70.

233. Cherentaeva E, Logunov D, Verkhovskaya L, Mezentseva M, Shmarov M, Ershov F, Naroditskii B, Gintsburg A. Production of the human β-interferon recombinant protein in avian cell culture. Molecular Genetics, Microbiology and Virology 2008; 23(3):153-7.

234. Derynck R, Devos R, Remaut E*, et al.* Isolation and characterization of a human fibroblast interferon gene and its expression in Escherichia coli. Rev Infect Dis 1981; 3(6):1186-95.

235. Smith GE, Summers MD, Fraser MJ. Production of human beta interferon in insect cells infected with a baculovirus expression vector. Mol Cell Biol 1983; 3(12):2156-65.

236. McCormick F, Trahey M, Innis M, Dieckmann B, Ringold G. Inducible expression of amplified human beta interferon genes in CHO cells. Mol Cell Biol 1984; 4(1):166-72.

237. Runkel L, deDios C, Karpusas M*, et al.* Systematic mutational mapping of sites on human interferon-beta-1a that are important for receptor binding and functional activity. Biochemistry 2000; 39(10):2538-51.

238. Crameri G, Todd S, Grimley S*, et al.* Establishment, immortalisation and characterisation of pteropid bat cell lines. PLoS One 2009; 4(12):e8266.

239. PBL InterferonSource. Universal Type I Interferon. 2011.

240. Human Genome Sequencing Center. Megabat Genome Project.Baylor College of Medicine, 2008.

241. Mortazavi A, Williams BA, McCue K, Schaeffer L, Wold B. Mapping and quantifying mammalian transcriptomes by RNA-Seq. Nat Meth 2008; 5(7):621-8.

242. Sultan M, Schulz MH, Richard H*, et al.* A Global View of Gene Activity and Alternative Splicing by Deep Sequencing of the Human Transcriptome. Science 2008; 321(5891):956-60.

243. Lister R, Gregory BD, Ecker JR. Next is now: new technologies for sequencing of genomes, transcriptomes, and beyond. Current Opinion in Plant Biology 2009; 12(2):107-18.

244. Libault M, Farmer A, Brechenmacher L*, et al.* Complete Transcriptome of the Soybean Root Hair Cell, a Single-Cell Model, and Its Alteration in Response to Bradyrhizobium japonicum Infection. Plant Physiology 2010; 152(2):541-52.

245. Woodhouse SD, Narayan R, Latham S*, et al.* Transcriptome sequencing, microarray, and proteomic analyses reveal cellular and metabolic impact of hepatitis C virus infection in vitro. Hepatology 2010; 52(2):443-53.

246. Mane VP, Heuer MA, Hillyer P, Navarro MB, Rabin RL. Systematic method for determining an ideal housekeeping gene for real-time PCR analysis. Journal of biomolecular techniques : JBT 2008; 19(5):342-7.

247. Carthagena L, Bergamaschi A, Luna JM*, et al.* Human TRIM Gene Expression in Response to Interferons. PLoS One 2009; 4(3):e4894.

248. Hruz T, Wyss M, Docquier M*, et al.* RefGenes: identification of reliable and condition specific reference genes for RT-qPCR data normalization. BMC Genomics 2011; 12(1):156.

249. Schmeisser H, Mejido J, Balinsky CA, Morrow AN, Clark CR, Zhao T, Zoon KC. Identification of Alpha Interferon-Induced Genes Associated with Antiviral Activity in Daudi Cells and Characterization of IFIT3 as a Novel Antiviral Gene. J Virol 2010; 84(20):10671-80.

250. Holzinger D, Jorns C, Stertz S*, et al.* Induction of MxA Gene Expression by Influenza A Virus Requires Type I or Type III Interferon Signaling. J Virol 2007; 81(14):7776-85.

251. Hsiang T-Y, Zhao C, Krug RM. Interferon-Induced ISG15 Conjugation Inhibits Influenza A Virus Gene Expression and Replication in Human Cells. J Virol 2009; 83(12):5971-7.

252. Marié I, Svab J, Robert N, Galabru J, Hovanessian AG. Differential expression and distinct structure of 69- and 100-kDa forms of 2-5A synthetase in human cells treated with interferon. Journal of Biological Chemistry 1990; 265(30):18601-7.

253. Lietzén N, Öhman T, Rintahaka J, Julkunen I, Aittokallio T, Matikainen S, Nyman TA. Quantitative Subcellular Proteome and Secretome Profiling of Influenza A Virus-Infected Human Primary Macrophages. PLoS Pathog 2011; 7(5):e1001340.

254. Utsumi J, Yamazaki S, Kawaguchi K, Kimura S, Shimizu H. Stability of human interferon-beta 1: oligomeric human interferon-beta 1 is inactive but is reactivated by monomerization. Biochimica et biophysica acta 1989; 998(2):167-72.

255. Faul EJ, Wanjalla CN, McGettigan JP, Schnell MJ. Interferon-beta expressed by a rabies virus-based HIV-1 vaccine vector serves as a molecular adjuvant and decreases pathogenicity. Virology 2008; 382(2):226-38.

256. Faul EJ, Wanjalla CN, Suthar MS, Gale M, Jr., Wirblich C, Schnell MJ. Rabies Virus Infection Induces Type I Interferon Production in an IPS-1 Dependent Manner While Dendritic Cell Activation Relies on IFNAR Signaling. PLoS Pathog 2010; 6(7):e1001016.

257. Emeny JM, Morgan MJ. Regulation of the interferon system: evidence that Vero cells have a genetic defect in interferon production. J Gen Virol 1979; 43(1):247-52.

258. Barchet W, Cella M, Odermatt B, Asselin-Paturel C, Colonna M, Kalinke U. Virus-induced Interferon α Production by a Dendritic Cell Subset in the Absence of Feedback Signaling In Vivo. The Journal of Experimental Medicine 2002; 195(4):507-16.

259. Lee HK, Lund JM, Ramanathan B, Mizushima N, Iwasaki A. Autophagy-Dependent Viral Recognition by Plasmacytoid Dendritic Cells. Science 2007; 315(5817):1398-401.

260. Marcus PI, Sekellick MJ. Interferon induction by viruses. III. Vesicular stomatitis virus: interferon-inducing particle activity requires partial transcription of gene N. J Gen Virol 1980; 47(1):89-96.

261. Paladino P, Cummings DT, Noyce RS, Mossman KL. The IFN-Independent Response to Virus Particle Entry Provides a First Line of Antiviral Defense That Is Independent of TLRs and Retinoic Acid-Inducible Gene I. The Journal of Immunology 2006; 177(11):8008-16.

262. Nagai Y, Ito Y, Hamaguchi M, Yoshida T, Matsumoto T. Relation of Interferon Production to the Limited Replication of Newcastle Disease Virus in L Cells. Journal of General Virology 1981; 55(1):109-16.

263. Andzhaparidze OG, Bogomolova NN, Boriskin YS, Bektemirova MS, Drynov ID. Comparative study of rabies virus persistence in human and hamster cell lines. J Virol 1981; 37(1):1-6.

264. Buckwold VE, Wei J, Huang Z*, et al.* Antiviral activity of CHO-SS cell-derived human omega interferon and other human interferons against HCV RNA replicons and related viruses. Antiviral Research 2007; 73(2):118-25.

265. Bullard J, Purdom E, Hansen K, Dudoit S. Evaluation of statistical methods for normalization and differential expression in mRNA-Seq experiments. BMC Bioinformatics 2010; 11(1):94.

266. Xiao S, Jia J, Mo D*, et al.* Understanding PRRSV Infection in Porcine Lung Based on Genome-Wide Transcriptome Response Identified by Deep Sequencing. PLoS One 2010; 5(6):e11377.

267. Maher CA, Kumar-Sinha C, Cao X*, et al.* Transcriptome sequencing to detect gene fusions in cancer. Nature 2009; 458(7234):97-101.

268. Rosenkranz R, Borodina T, Lehrach H, Himmelbauer H. Characterizing the mouse ES cell transcriptome with Illumina sequencing. Genomics 2008; 92(4):187-94.

269. Payvandi F, Amrute S, Fitzgerald-Bocarsly P. Exogenous and Endogenous IL-10 Regulate IFN-α Production by Peripheral Blood Mononuclear Cells in Response to Viral Stimulation. The Journal of Immunology 1998; 160(12):5861-8.

270. Wuyts A, Struyf S, Gijsbers K*, et al.* The CXC Chemokine GCP-2/CXCL6 Is Predominantly Induced in Mesenchymal Cells by Interleukin-1β and Is Down-Regulated by Interferon-γ: Comparison with Interleukin-8/CXCL8. Lab Invest 2003; 83(1):23-34.

271. Feldman SB, Ferraro M, Zheng HM, Patel N, Gould-Fogerite S, Fitzgerald-Bocarsly P. Viral Induction of Low Frequency Interferon-α Producing Cells. Virology 1994; 204(1):1-7.

272. Bartee E, Mohamed MR, Lopez MC, Baker HV, McFadden G. The Addition of Tumor Necrosis Factor plus Beta Interferon Induces a Novel Synergistic Antiviral State against Poxviruses in Primary Human Fibroblasts. J Virol 2009; 83(2):498-511.

273. Gouwy M, Struyf S, Proost P, Van Damme J. Synergy in cytokine and chemokine networks amplifies the inflammatory response. Cytokine & Growth Factor Reviews 2005; 16(6):561-80.

274. Mathieu C, Pohl C, Szecsi J*, et al.* Nipah Virus Uses Leukocytes for Efficient Dissemination within a Host. J Virol 2011; 85(15):7863-71.

275. Lo MK, Miller D, Aljofan M, Mungall BA, Rollin PE, Bellini WJ, Rota PA. Characterization of the antiviral and inflammatory responses against Nipah virus in endothelial cells and neurons. Virology 2010; 404(1):78-88.

276. Orzechowska B, Antoszków Z, Siemieniec I, Lorenc M, Jatczak B, Błach-Olszewska Z. Cytokine production by human leukocytes with different expressions of natural antiviral immunity and the effect of antibodies against interferons and TNF-α. Archivum Immunologiae et Therapiae Experimentalis 2007; 55(2):111-7.

277. Bußfeld D, Nain M, Hofmann P, Gemsa D, Sprenger H. Selective Induction of the Monocyte-Attracting Chemokines MCP-1 and IP-10 in Vesicular Stomatitis Virus-Infected Human Monocytes. Journal of Interferon & Cytokine Research 2000; 20(7):615-21.

278. Dhamija S, Kuehne N, Winzen R, Doerrie A, Dittrich-Breiholz O, Thakur BK, Kracht M, Holtmann H. Interleukin-1 Activates Synthesis of Interleukin-6 by Interfering with a KH-type Splicing Regulatory Protein (KSRP)-dependent Translational Silencing Mechanism. Journal of Biological Chemistry 2011; 286(38):33279-88.

279. Virtue ER, Marsh GA, Wang L-F. Interferon Signaling Remains Functional during Henipavirus Infection of Human Cell Lines. J Virol 2011; 85(8):4031-4.

280. Virtue ER, Marsh GA, Baker ML, Wang L-F. Interferon Production and Signaling Pathways Are Antagonized during Henipavirus Infection of Fruit Bat Cell Lines. PLoS One 2011; 6(7):e22488.

281. Huber JP, David Farrar J. Regulation of effector and memory T-cell functions by type I interferon. Immunology 2011; 132(4):466-74.

282. Rep MHG, Hintzen RQ, Polman CH, van Lier RW. Recombinant Interferon-β blocks proliferation but enhances interleukin-10 secretion by activated human T-cells. Journal of Neuroimmunology 1996; 67(2):111-8.

283. Garcia-Sastre A, Durbin RK, Zheng H, Palese P, Gertner R, Levy DE, Durbin JE. The Role of Interferon in Influenza Virus Tissue Tropism. J Virol 1998; 72(11):8550-8.

284. Kohlmeier JE, Cookenham T, Roberts AD, Miller SC, Woodland DL. Type I Interferons Regulate Cytolytic Activity of Memory CD8+ T Cells in the Lung Airways during Respiratory Virus Challenge. Immunity 2010; 33(1):96-105.